34th Annual Condensed Matter and Materials Meeting

2010

Waiheke Island Resort, Waiheke,
Auckland, New Zealand
2 - 5 February 2010

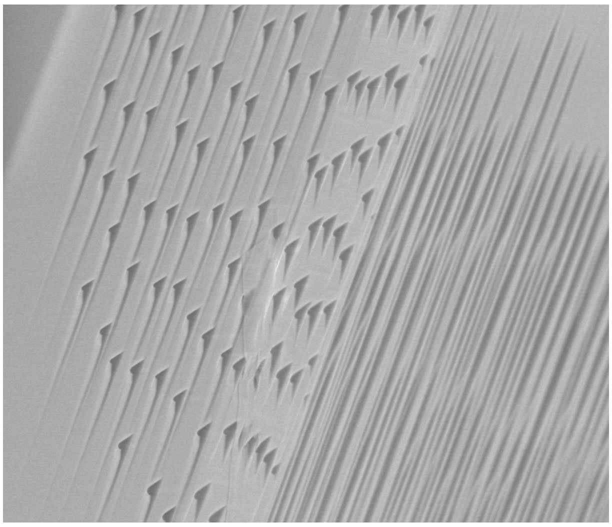

Australian Institute of Physics

34th Annual Condensed Matter and Materials Meeting

Waiheke Island Resort, Auckland,
New Zealand

2nd - 5th of February 2010

CONFERENCE HANDBOOK

Organising Committee

University of Auckland

Dr Tilo Söhnel (chair)

Prof Graham Bowmaker

A/Prof Jadranka Travas-Sejdic

Dr Kathrin Wichmann

Contents

General Information

Scientific program:

The conference will take place at the Waiheke Island Resort. All lectures will be held in the Waiheke Suite. Chairpersons and speakers are asked to adhere closely to the schedule for the oral program. A laptop, data projector, laser pointer and microphone will be available. Please check as early as possible the compatibility with the computer facilities provided. Posters should be mounted on Tuesday evening or Wednesday morning in the Bay Room and Palm Room (please refer to the number of your poster). Please remove all posters by Thursday night or Friday morning.

Administration:

Please wear your name tag at all times. Registration desk will be open from 3 pm - 6 pm on Tuesday for delegate registration and other matters regarding the conference. Questions or problems about the accommodation, please contact the Resort reception.
Wireless internet access is available in and around the conference facilities/main house. Please make sure to pay for any additional costs charged by you on your room number before your departure.

Meals, refreshments and recreational facilities:

Breakfast, lunch and dinner will be served in the Resort Restaurant ‘The Lookout’. Welcome drinks will be available on Tuesday, 2nd Feb. at ‘The Lookout’ Bar from 5.30 pm onwards. Breakfast will be served from 7 am - 9 am. Lunch will be served according to the program on Wednesday and Thursday between 12.50 pm and 1.50 pm. On Tuesday dinner (buffet) will be served at ‘The Lookout’ from 6.30 pm onwards. On Wednesday dinner will be a BBQ at ‘The Lookout’. The conference dinner will take place at ‘The Dunes’ at Onetangi Bay at 7.30 pm on Thursday. Shuttle busses will depart from the main entrance at 7 pm. Shuttle busses back to the Resort will depart every 30 min from 10 pm onwards. Morning and afternoon tea will be available outside the conference room. Refreshments will be available at ‘The Lookout’ Bar til late. You are welcome to enjoy the on-site facilities which include an outdoor swimming pool, tennis court, and petanque-pit.

Contact Details:

Waiheke Island Resort
4 Bay Road
Palm Beach
Waiheke Island

Phone 0064 - 9 - 372 0011

Organising committee:

Tilo Söhnel 0064 - 21 - 1719387 or

Kathrin Wichmann 0064 - 21 - 1794456

Sponsors

THE UNIVERSITY
OF AUCKLAND
NEW ZEALAND
Te Whare Wānanga o Tāmaki Makaurau

Faculty of Science
The University of Auckland
www.science.auckland.ac.nz/uoa

Department of Chemistry
The University of Auckland
www.che.auckland.ac.nz

Wine Science Programme
Department of Chemistry
The University of Auckland
www.winescience.auckland.ac.nz

rakon

Rakon Limited

justin.maloney@rakon.com

www.rakon.com

PEARSON

Pearson

chris.wakim@pearsoned.co.nz

www.pearsoned.co.nz

Exhibitors

AVT Services Pty Ltd

adamjee@avtservices.com.au

www.avt.net.au

Alphatech Systems Limited

evan.sales@alphatech.co.nz

www.alphatech.co.nz

PARTICIPANTS

Adamjee, Adil	adamjee@avtservices.com.au	AVT Services
Alario-Franco, Miguel	maaf@quim.ucm.es	Universidad Complutense, Madrid, Spain
Andrae, Dirk	andrae@uni-bielefeld.de	Freie Universität Berlin, Germany
Ashcroft, Neil	nwa@ccmr.cornell.edu	Cornell University, Ithaca, N.Y, USA
Assadollahzadeh, Behnam	b.assadollahzadeh@massey.ac.nz	Massey University, Albany
Bastow, Tim	Tim.Bastow@csiro.au	CSIRO
Bennett, Daniel	Daniel.Bennett@csiro.au	CSIRO
Bhatia, Vijay	Vijay.Bhatia@student.uts.edu.au	University of Technology Sydney
Biering, Susan	s.b.biering@massey.ac.nz	Massey University, Albany
Bowmaker, Graham	g.bowmaker@auckland.ac.nz	University of Auckland
Brown, Simon	simon.brown@canterbury.ac.nz	MacDiarmid Institute & University of Canterbury
Campbell, Stewart	S.Campbell@adfa.edu.au	University of NSW ADFA
Chen, Wei	wchen@phys.unsw.edu.au	University of NSW
Clements, Richard	rcs@ansto.gov.au	ANSTO & University of Sydney
Colligon, John	J.Colligon@mmu.ac.uk	Manchester Metropolitan University, UK
Danilikin, Sergey	sdz@ansto.gov.au	ANSTO
Das, Mukunda	mpd105@physics.anu.edu.au	ANU
Finlayson, Trevor	trevorf@unimelb.edu.au	University of Melbourne
Gao, Yongxiang	yongxiang@rsc.anu.edu.au,	ANU
Gaston, Nicola	n.gaston@irl.cri.nz	IRL
Geise, Geoffrey	ggeise@che.utexas.edu	The University of Texas, Austin, TX, USA
Gray, Malcolm	Malcolm.Gray@measurement.gov.au	National Measurement Institute
Greentree, Andrew	andrewg@unimelb.edu.au	University of Melbourne
Hamer, Chris	cjh@phys.unsw.edu.au	University of NSW
Hendy, Shaun	s.hendy@irl.cri.nz	IRL
Hermann, Andreas	A.H.Hermann@gmail.com	Massey University, Albany & University of Auckland
Hill, Anita	Anita.Hill@csiro.au	CSIRO
Hodgkiss, Justin	Justin.Hodgkiss@vuw.ac.nz	MacDiarmid & Victoria University Wellington
Holt, Michael	mholt@phys.unsw.edu.au	University of NSW
Hutchison, Wayne	W.Hutchison@adfa.edu.au	University of NSW ADFA
Hyndman, Adam	a.hyndman@irl.cri.nz	IRL
Ingham, Bridget	b.ingham@irl.cri.nz	IRL
Janssens, Stefaan	s.janssens@irl.cri.nz	IRL & Victoria University Wellington
Kaiser, Alan	alan.kaiser@vuw.ac.nz	Victoria University Wellington
Kennedy, Brendan	b.kennedy@chem.usyd.edu.au	University of Sydney
Lang, Sidney	lang@bgu.ac.il	Ben-Gurion University of the Negev, Israel
Leveneur, Jerome	J.Leveneur@gns.cri.nz	National Isotope Centre & University of Wellington
Ling, Chris	c.ling@chem.usyd.edu.au	University of Sydney
Liss, Klaus-Dieter	kdl@ansto.gov.au	ANSTO
Malik, Anwaar	a.malik@adfa.edu.au	University of NSW ADFA
Miller, David	djm@phys.unsw.edu.au	University of Sydney
Morgan, Scott	s.morgan@irl.cri.nz	IRL
Nelson, Andrew	andrew.nelson@ansto.gov.au	ANSTO
Pahl, Elke	E.Pahl@massey.ac.nz	Massey University, Albany
Plank, Natalie	Natalie.Plank@vuw.ac.nz	MacDiarmid & Victoria University Wellington
Puscasu, Ruslan	RPuscasu@groupwise.swin.edu.au	Swinburne University of Technology
Raymond, Sebastiampillai	s.raymond@irl.cri.nz	IRL

Read, Marlene	mnr@phys.unsw.edu.au	University of NSW
Richter, Jan	jan.richter@vuw.ac.nz	IRL & Victoria University Wellington
Riley, Daniel	driley@unimelb.edu.au	University Melbourne
Rohrmann, Urban	Urban_Rohrmann@gmx.net	Massey University, Albany & TU Darmstadt
Ruck, Ben	Ben.Ruck@vuw.ac.nz	MacDiarmid & Victoria University Wellington
Saengkae, Saowalak	ssaengkae@students.latrobe.edu.au	La Trobe University
Saerbeck, Thomas	tsk@ansto.gov.au	ANSTO & University of Western Australia
Salama, Hazar	h.salama@adfa.edu.au,	University of NSW ADFA
Schmid, Siegbert	s.schmid@chem.usyd.edu.au	University of Sydney
Schnyder, Thierry	t.schnyder@irl.cri.nz	Swiss Federal Institute of Technology & IRL
Schwerdtfeger, Peter	p.a.schwerdtfeger@massey.ac.nz	Massey University, Albany
Scott, Morgan	msco001@aucklanduni.ac.nz	University of Auckland
Sears, Kallista	Kallista.Sears@csiro.au	CSIRO
Sevick, Edie	sevick@rsc.anu.edu.au	ANU
Snyder, Evan	evan.sales@alphatech.co.nz	AlphaTech
Soehnel, Tilo	t.soehnel@auckland.ac.nz	University of Auckland
Spoljaric, Steven	s.spoljaric@student.rmit.edu.au	RMIT University
Stephen, Jibu	j.stephen@irl.cri.nz	IRL & MacDiarmid Institute
Stevens, Kevin	K.Stevens@questintegrity.com	Quest Reliability Ltd & MacDiarmid Institute
Stewart, Glen	G.Stewart@adfa.edu.au	University of NSW ADFA
Studer, Andrew	ajs@ansto.gov.au	ANSTO
Styles, Mark	m.styles2@pgrad.unimelb.edu.au	University of Melbourne
Talantsev, Evgeny	E.Talantsev@irl.cri.nz	IRL
Tallon, Jeffery	J.Tallon@irl.cri.nz	MacDiarmid Institute & IRL
Tilley, Richard	Richard.Tilley@vuw.ac.nz	Victoria University Wellington
Timmers, Heiko	H.Timmers@adfa.edu.au	University of NSW ADFA
Tonner, Ralf	r.e.tonner@massey.ac.nz	Massey University, Albany
Travas-Sejdic, Jadranka	j.travas-sejdic@auckland.ac.nz	University of Auckland
Ulrich. Clemens	ulrich@phys.unsw.edu.au	University of NSW
Usher, Brian	B.Usher@latrobe.edu.au	La Trobe University
Varoy Chris	Chris.Varoy@vuw.ac.nz	University of Melbourne
Wang, Genmiao	gmw@rsc.anu.edu.au	University of NSW ADFA
Watanabe, Masaaki	watanabe@hiro.kindai.ac.jp	Kinki University, Higashi-Hiroshima, Japan
Weisshaupt, Klaus	info@WITec.de	WiTec
Went, Michael	michael.went@anu.edu.au	ANU
Williams, David	drw110@physics.anu.edu.au	ANU
Williams, David E	david.williams@auckland.ac.nz	University of Auckland
Winch, Nicola	Nicola.Winch@vuw.ac.nz	University of Melbourne
Xia, James	J.Xia@irl.cri.nz	IRL
Zuelicke, Ulrich	U.Zuelicke@massey.ac.nz	Massey University

Tuesday, 2nd February

15:00 – 18:00 **Registration**

17:30 **Welcome Drinks** at “The Lookout”

18:30 **Dinner** at “The Lookout”

Wednesday, 3rd February

08:50 – 09:00 **Opening:** *Tilo Söhnel, University of Auckland*

09:00 – 10:30 **Chairperson:** Trevor Finlayson

09:00 – 09:30 1 High Pressure Simulations – Squeezing the Hell out of Atoms
Peter Schwerdtfeger, Massey University, NZ ***INVITED***

09:30 – 09:50 2 Specific heat of a Ferroelectric PZT Ceramic at the Morphotropic Phase Boundary
Sidney Lang, Ben-Gurion University, Israel

09:50 – 10:10 3 Electronic structure and magnetism in rare-earth nitrides
Ben Ruck, Mac Diarmid Institute/University of Wellington, New Zealand

10:10 – 10:30 4 Thermodynamics and the prospects for room-temperature superconductivity
Jeff Tallon, MacDiarmid Institute/IRL, New Zealand

10:30 – 10:50 Morning tea

10:50 – 12:50		**Chairperson:** Alan Kaiser
10:50 – 11:20	5	Surface treatment: new methods, new applications *John S. Colligon, Manchester Metropolitan University, UK* ***INVITED***
11:20 – 11:40	6	NMR detection of dilute defect phases in solids *Tim J. Bastow, CSIRO, South Clayton, Australia*
11:40 – 12:00	7	Wavefunction-based correlation calculations for the potential energy surface of zinc and cadmium: understanding the hcp anisotropy *Nicola Gaston, IRL and MacDiarmid Institute, New Zealand*
12:00 – 12:20	8	Solid state calculations of ice from an incremental coupled cluster approach *Andreas Hermann, Massey University Auckland, New Zealand*
12:20 – 12:50	9	The World of Wombat: a review of high speed neutron diffraction at the OPAL research reactor *Andrew J. Studer, The Bragg Institute, ANSTO, Sydney, Australia* ***INVITED***
12:50 – 13:50	Lunch	
14:00 – 16:40		**Chairperson:** Graham Bowmaker
14:00 – 14:30	10	Kohn Anomaly in Conventional Superconductors: A Surprise *Mukunda P. Das, The Australian National University, Australia* ***INVITED***
14:30 – 14:50	11	Spin-mediated strong coupling superconductivity in lightly doped cuprates *Wei Chen, University of New South Wales, Sydney, Australia*

14:50 – 15:10 12 Copper Selenide: Soft Photon Modes and Superionic Phase Transition
Sergey Danilkin, Bragg Institute, ANSTO, Sydney, Australia

15:10 – 15:30 13 ZnO solid state dye sensitized solar cells,
Natalie O. V. Plank, Victoria University, Wellington, New Zealand

15:30 – 15:50 14 The Crystal Structure of the Close-Packed Polymorphs of Ytterbium: A Quantum Chemical Study
Dirk Andrae, Freie Universität Berlin, Germany

15:50 – 16:10 Afternoon Tea

16:10 – 16:40 **Chairperson:** Jeff Tallon

16:10 – 16:40 15 Approaching metallic hydrogen through chemical stealth; the high hydrides
Neil Ashcroft, Cornell University, Ithaca, NY, USA
INVITED

16:45 – 17:00 **Business Meeting**
Chairperson: Tilo Söhnel

17:00 – 18:30 Poster Session

19:00 Dinner - *BBQ*

20:30 Wagga Trivia

Thursday, 4th February

09:00 – 10:30		**Chairperson**: Peter Schwerdtfeger
09:00 – 09:30	16	X-ray Photon Correlation Spectroscopy Applied to the Study of a Martensitic Transformation *Trevor R. Finlayson, University of Melbourne, Australia* ***INVITED***
09:30 – 09:50	17	Systematic trends in the structural phase transitions of the 4*d* transition-metal oxides $\mathrm{Sr}M\mathrm{O}_3$ (M = Zr, Nb, Mo, Tc, Ru and Rh) *Brendan Kennedy, The University of Sydney, Sydney, Australia*
09:50 – 10:10	18	Anomalous Spin Dynamics and Orbital Excitations in Mott-Insulating Titanates, *Clemens Ulrich, University of New South Wales, Sydney, Australia*
10:10 – 10:30	19	Single Polymer Golbules of Multiblock Copolymers: How to make a very Complicated Tennis Ball *David R. M. Williams, Australian National University, Canberra, Australia*
10:30 – 10:50	Morning tea	
10:50 – 12:50		**Chairperson:** Glen Stewart
10:50 – 11:20	20	Models and simulations of the growth of carbon nanotubes *Shaun C. Hendy, MacDiarmid Institute for Advanced Materials and Nanotechnology, Victoria University of Wellington, New Zealand* ***INVITED***

11:20 – 11:40	21	The coalescence of gold nanoparticles: an *in situ* synchrotron study *Bridget Ingham, Industrial Research Limited, Wellington, New Zealand*
11:40 – 12:00	22	Towards accurate melting temperatures from ab initio Monte Carlo simulations: from nano clusters to the bulk *E. Pahl, Massey University, NZ*
12:00 – 12:20	23	Junction effects and optical properties of RhPd/CeO_2 *Morgan Scott, University of Auckland, New Zealand*
12:20 – 12:50	24	Cluster-based Electronic Devices *Simon Brown, University of Canterbury, New Zealand* ***INVITED***
12:50 – 13:50	Lunch	
14:00 – 15:50		**Chairperson:** Jadranka Travas-Sedjic
14:00 – 14:30	25	Electrons in Carbon Flatland: Understanding Conduction in Graphene *Alan B. Kaiser, MacDiarmid Institute for Advanced Materials and Nanotechnology, Victoria University of Wellington, New Zealand* ***INVITED***
14:30 – 14:50	26	Time Reversal of a Pseudospin: General Properties and Applications to Graphene *Ulrich Zülicke, Massey University, Palmerston North, New Zealand*

14:50 – 15:10	27	Water and Ion Transport in a Novel Sulfonated Pentablock Copolymer *Geoffrey Geise, University of Texas, USA*
15:10 – 15:30	28	Characterisation and tracing of prosthesis debris – Can pathways of polymer particles be suppressed? *Heiko Timmers, University of New South Wales at ADFC, Canberra, Australia*
15:30 – 16:50		Afternoon Tea
15:50 – 16:50		**Chairperson:** Tilo Söhnel
15:50 – 16:10	29	Synthesis at High Pressure and High Temperature of M-1212 metalo-cuprates *Miguel Alario-Franco, Universidad Complutense, Spain*
16:10 – 16:30	30	The structures, phase transition and dynamics behind mixed ionic and electronic conduction in hydrated $Ba_4Nb_2O_9$ *Chris D. Ling, The University of Sydney, Sydney, Australia*
16:30 – 16:50	31	Modern Diffraction Methods for the Investigation of Thermo Mechanical Processes in Materials Physics *Klaus-Dieter Liss, ANSTO, Sydney, Australia*
17:00 – 18:00	**Poster Session**	

19:00 Departure to 'The Dunes'

19:30 Conference Dinner at 'The Dunes'

Friday 5th February

09:00 – 10:30		**Chairperson**: Shaun Hendy
09:00 – 09:30	32	Quantum Phase Transitions in Coupled Quantum Optical Cavities *Andrew D. Greentree, University of Melbourne, Australia* ***INVITED***
09:30 – 09:50	33	A new approach to the Creation of Magnetically Modulated Structures *Thomas Saebeck, ANSTO/University of Western Australia, Sydney/Perth, Australia*
09:50 – 10:10	34	Modulated Structures in the Fresnoite Family *Siegbert Schmid, The University of Sydney, Sydney, Australia*
10:10 – 10:30	35	Organic Solar Cells with Carbon Nanotube Sheet Electrodes *Kallista Sears, CSIRO, Clayton, Australia*
10:30 – 10:50	Morning Tea	
10:50 – 12:30		**Chairperson:** Simon Brown
10:50 – 11:20	36	Studying Electrical Double Layers in Ionic Liquids using Neutron and X-ray Reflectometry *Andrew Nelson, The Bragg Institute, ANSTO, Sydney, Australia* ***INVITED***

11:20 – 11:40	37	Hydrodynamic mobility of an optical trapped colloidal particle near fluid-fluid interfaces *Genmiao Wang, Australian National University, Canberra, Australia*
11:40 – 12:00	38	Pulsed ESR Measurement of Coherence Times in Si:P at Very Low Temperature *Wayne Hutchinson, The University of New South Wales, Sydney, Australia*
12:00 – 12:20	39	Synthesis and Applications of Nanoparticles *Richard D. Tilley, Victoria University, Wellington, New Zealand*
12:20 – 12:30	**Presentations and Closing:** *Tilo Söhnel, University of Auckland*	
12:30 – 13:30	Lunch	
13:30 and 14:30	**Shuttle bus departure to Waiheke Wharf**	

POSTER PRESENTATIONS

Poster #	Authors	Title
40	B. Assadollahzadeh and P. Schwerdtfeger	From Clusters to the Solid State: A Systematic Search for Global Minimum Structures for Cs, Sn and Au Clusters
41	J.A. Xia, N.M. Strickland, E.F. Talantsev, N.J. Long, M.W. Rupich, S. Sathyamurthy, X. Li, and J. Kennedy	Investigation of columnar defects in MOD YBCO films by TEM
42	V.K. Bhatia, C.S. Kealley, G.J. Thorogood, A. Dowd and M.B. Cortie	AuCuAl Shape Memory Alloys for Use in Nano-Actuators
43	S. Biering and P. Schwerdtfeger	The influence of relativistic effects on the structure of the group 12 chalcogenides: A density functional study
44	R. Clements, B. Kennedy, C. Ling, A.P.J. Stampfl	A Neutron and Synchrotron Investigation Of The Electronic Structure Of Lanthanide Zirconates
45	Y.X. Gao, G.M. Wang and E.M. Sevick	Under what experimental conditions are Fluctuation Theorems necessary?
46	M.B. Gray, W. Giardini, P. Manson, R.B. Warrington and M. Wouters	The Avogadro Project and it's role in the redefinition of the kilogram
47	C. Hamer, O. Rojas and J. Oitmaa	Spin-wave Approach to the Spin-1 Heisenberg Anitiferromagnet with Uniaxial Anisotropy in a Field

48	P. Falcaro, C. Doherty, K. Nairn, A. Thornton, S. Pas, C. Elvin and A. Hill	Adaptive materials
49	J.M. Hodgkiss, G. Tu, S. Albert-Seifried, W.T.S. Huck and R.H. Friend	Coupling ionic and electronic charge transport in organic semiconductors: A new paradigm for enhanced functionality in molecular electronics
50	M. Holt, D. Stanek, O.P. Sushkov and G.S. Uhrig	Pnictides as frustrated three dimensional quantum antiferromagnets close to a quantum phase transition
51	W.D. Hutchison, P.G. Spizzirri and M.S. Brandt	Electrically Detected Magnetic Resonance Applied to the Study of Near Surface Electron Donors in Silicon
52	A.R. Hyndman, G.V.M. Williams, and J. Stephen	Magnetization and Magnetotransport Study of $SrFeO_x$
53	S. Janssens, D. Clarke, G.V.M. Williams, and A. Edgar	Spectroscopic properties of sensitized $LaF_3:Eu^{3+}$ nanoparticles
54	J. Leveneur, S. Kupke, J. Kennedy, G.V.M. Williams, A. Markwitz and J. Metson	Fabrication of Fe nanoclusters using ion implantation and electron beam annealin
55	A.E. Malik, K. Belay, D. Llewellyn, W.D. Hutchison, K. Nishmura and R.G. Elliman	Ferromagnetic Nanoparticles Formed in Silica by Ion Implantation
56	A. Markwitz, F. Fang and P.B. Johnson	Electron beam annealing of (100) Si following dual ion implantation of Pb/N
57	D.J. Miller	Advantages of measuring average spin using condensed matter methods

58	S.W. Morgan, G.V.M. Williams, A.R. Hyndman and J. Stephen	Temperature Resolved Cathodoluminescence Spectroscopy and Magnetic Properties of Cobalt Doped Titanium Dioxide Thin Films
59	D. Bennett, D. Miljak, B. Schwitter and J. Khachan	Zero field NMR and NQR measurements of natural copper minerals
60	N.O.V. Plank, F. Natali, B.M. Ludbrook, J. Richter, B.J. Ruck, H.J. Trodahl and J.V. Kennedy	Epitaxial growth and electrical properties of thick SmSi$_2$ layers on (001) silicon.
61	R.M. Puscasu, B.D. Todd, P.J. Daivis, and J.S. Hansen	Nanoscale Modeling of Polymer Glasses – Dynamics of Viscous Kernel
62	S.G. Raymond, G.V.M. Williams, C. Varoy, C. Dotzler, and D. Clarke	New Materials for Optically stimulated Luminescence Dosimetry
63	M.N. Read	Momentum-dependent inelastic mean-free-path and high-energy electronic structure of Aluminium
64	J.H. Richter, B.J. Ruck, B.M. Ludbrook, I.L. Farrel, F. Natali, N.O.V. Plank, H.J. Trodahl	Properties of EuN thin films
65	U. Rohrmann, S. Schäfer and R. Schäfer	Magnetic Response of Molecular Cage Clusters: Mn@Sn$_{12}$ and Mn@Sn$_{13}$
66	S. Saengkae, M. Binder, B.F. Usher and J. Petrolito	Efficient Surface Stress Cancelling Algorithms
67	T. Saerbeck, N. Loh, M. Ali, B.J. Hickey, D. Lott, B.P. Toperverg, A. Mulders, A.P. J. Stampfl, F. Klose, R.L. Stamps	Temperature Dependent Biquadratic Exchange Coupling in Co/Cu$_{(0.94)}$Mn$_{(0.06)}$ Multilayers
68	H.A. Salama, G.A. Stewart, K. Nishimura, W.D. Hutchison, D. Scott, H.O'Neill, C.J. Voyer and D.H. Ryan	Hysteresis effects in o-YbMnO3?

69	W. R. Brant and S. Schmid	Defect Perovskites in the $Sr_{1-x}M_{1-2x}Nb_{2x}O_3$ (M = Ti, Zr) Family
70	X.-F. Song and L. Yin	Surface Fracture in Diamond Adjusting of a Leucite-Reinforced Glass Ceramic Using a Clinical Dental Handpiece
71	T. Schnyder, G. Williams and J. Tallon	Evidence of Ionic Effect ("Chemical Pressure") in $Bi_2Sr_{1.6}Ln_{0.4}CuO_{6+\delta}$ (Ln = Ba, La, Eu, Gd, Y) studied by Susceptibility and Raman Measurements
72	E.M. Sevick and D.R.M. Williams	A piston-rotaxane as a molecular shock absorber
73	T. Söhnel, W. Reichelt and K.Teske	Solid State Coulometric Investigations in the System Ir/Sn/O - Determination of the thermodynamical data of $Ir_{10}Sn_{45}O_{44}$, $IrSn_4O_{4-x}$, $Ir_3Sn_8O_4$, Ir_5Sn_7 and $IrSn_2$
74	S. Spoljaric, T. Köpplmayr, A. Genovese, T.K. Goh, A. Blencowe, G.G. Qiao and R.A. Shanks	Nano-composites with physical crosslinks introduced by core crosslinked star polymers into a like-polymer
75	S. Spoljaric, A. Genovese, T. Köpplmayr and R.A. Shanks	Long term structural integrity of high density polyethylene blends investigated by static force thermomechanometry
76	J. Stephen, G.V.M. Williams and B. Ruck	Magnetic and electronic study of the colossal magnetoresistance compound, Sr_2FeMoO_6
77	K.J. Stevens, B. Ingham, M. Ryan, J.A. Kimpton, K.S. Wallwork, V. Luzin and K. Cheong.	Carbide Composition and Stress Measurement in Ethylene Pyrolysis Tubes
78	B. Saensunon, G. Stewart, P.C.M. Gubbens, M. Russina and E. Kemner	The Crystal Field Schemes for Er^{3+} in $ErCr_2Si_2$ and $ErMn_2Si_2$

79	M.J. Styles, D.P. Riley and I.C. Madsen	Parametric Rietveld refinement applied to in-situ diffraction studies
80	E.F. Talantsev, N.M. Strickland, J.A. Xia, N.J. Long, M.W. Rupich, X. Li and S. Sathyamurthy	In-field performance and microstructure of metal-organic deposited YBCO films doped with $BaZrO_3$
81	P. Kessler, Th. Geruschke, H. Timmers, A.P. Byrne, R. Vianden	^{100}Pd/Rh gamma-ray perturbed angular correlations in GaN and ZnO – Are these semiconductors suitable for spintronics?
82	Y. Liu, L.G. Gladkis, H. Timmers	Micro-scratching of UHMW polyethylene surfaces
83	R. Tonner, V.A. Soloshonok and P. Schwerdtfeger	Optical purification via sublimation – DFT results on lactic acid derivatives
84	C. Roux, D. Williams, J. Travas-Sejdic	Comb-like coploymers based on polythiophene
85	A. Edgar, J. Zimmermann, H. von Seggern and C.R. Varoy	X-ray phosphor properties of Eu^{2+} - doped lanthanum-stabilised cubic barium chloride
86	J.L. Wang, S.J. Campbell, J.M. Cadogan, A.J. Studer, R. Zeng and S.X. Dou	Magnetic Phase Transitions in Layered $NdMn_2Ge_{2-x}Si_x$
87	M. Watanabe	The Angled Crack Problems in Compression and Tension
88	M. Went, J. Roberts, R. Weed, S. Buckman and J. Sullivan	A Variable Energy Positron Beamline for PALS experiments
89	N.M. Winch and A. Edgar	$CsBr:Eu^{2+}$ X-Ray Storage Phosphor Imaging Plates

ABSTRACTS

1

High Pressure Simulations – Squeezing the Hell out of Atoms

P. Schwerdtfeger, A. Hermann and J. Cox

Centre for Theoretical Chemistry and Physics, The New Zealand Institute for Advanced Study, Massey University (Albany Campus), Auckland, New Zealand.

The pressure range accessible to laboratory experiments exceeds now a remarkable 20 orders of magnitude, from ultra-high vacuum (< 1 nPa) to ulta-high pressures (> 100 GPa). With the development of high-pressure diamond-anvil cells we are now able to study materials at pressures equivalent to the pressure at the centre of our earth (350 GPa). In other planets and stars pressures beyond the TPa range are reached, which can only be explored by thermonuclear explosions or by theoretical methods. At high pressures unusual structures and materials properties are observed. It is currently a formidable task to obtain the equation-of-state for a solid up to high pressures and temperatures. Our research group has just achieved that recently for neon, where the isotherms are in excellent agreement with experimental data. Fundamental questions we are currently exploring is, for example, if we can already understand the simple density-pressure relationship of simple atomic crystals (like helium or neon) from squeezing atoms. We further present density functional results for the metallic phase transition of $CrCl_2$ (see picture below) currently investigated experimentally at the Max-Planck Institute in Stuttgart, and for optical properties

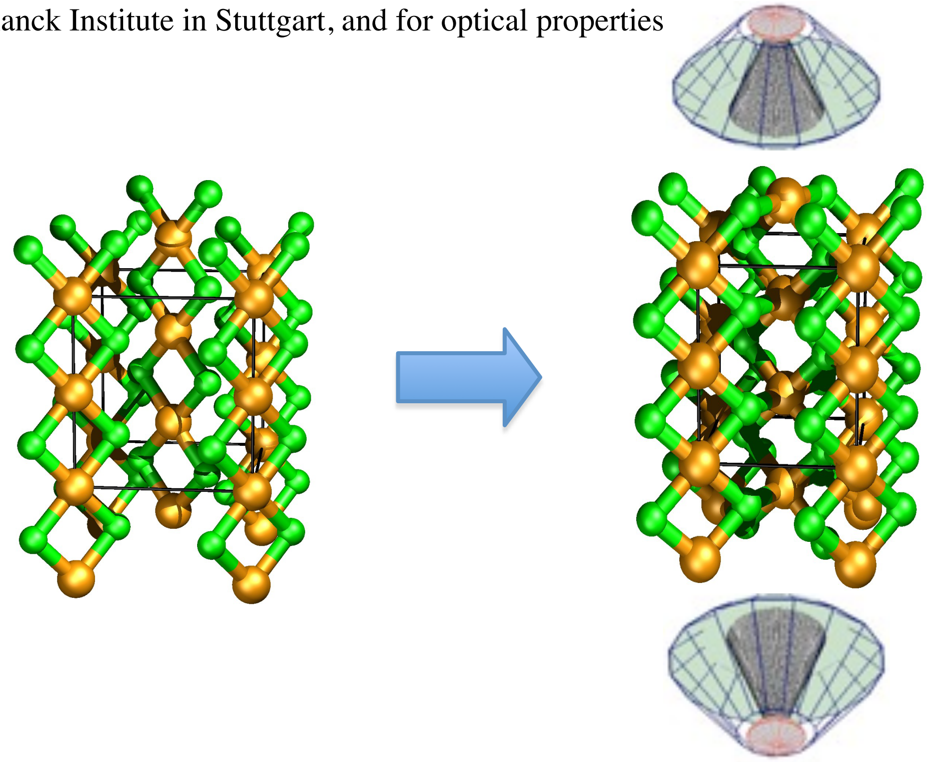

Specific heat of a Ferroelectric PZT Ceramic at the Morphotropic Phase Boundary

S.B. Lang[1], J.C. Lashley[2], K.A. Modic[2], R.A. Fisher[3], W.M. Zhu[4] and Z.G. Ye[4]

[1]*Department of Chemical Engineering, Ben-Gurion University of the Negev, Beer Sheva, Israel*

[2]*Los Alamos National Laboratory, Los Alamos, NM, USA*

[3]*Lawrence Berkeley National Laboratory, Berkeley, CA, USA*

[4]*Department of Chemistry & 4D Labs, Simon Fraser University, Burnaby, BC, Canada*

Ferroelectric ceramic materials have a wide range of applications because of their piezoelectric and pyroelectric properties. One of their most important physical properties is the specific heat. In this study, the specific heats of a series of lead-zirconate-titanate (PZT) compositions in the vicinity of the morphotropic phase boundary (MPB) were measured. The temperature range was from 1.8 to 300 K. It is believed that these are the lowest temperature measurements ever made on PZT. Differences between the specific heats of the different compositions were very small. However, the calculated Debye temperatures were slightly different. The results are useful in computing design parameters for technical devices.

Electronic structure and magnetism in rare-earth nitrides

B.J. Ruck[a,b], H.J. Trodahl[a,b], J. Richter[a,b], N.O.V. Planck[a,b], F. Natali[a,b], B.M. Ludbrook[a,b], A.R.H. Preston[a,b,f], S.M. Durbin[a,c], R.J. Reeves[a,d], I.L. Farrell[a,d], W.R.L Lambrecht[e], and K.E. Smith[f]

[a] *MacDiarmid Institute for Advanced Materials and Nanotechnology, New Zealand.*

[b] *School of Chemical and Physical Sciences, Victoria University of Wellington, PO Box 600, Wellington, New Zealand.*

[c] *Department of Electrical and Computer Engineering, University of Canterbury, Christchurch 8140, New Zealand.*

[d] *Department of Physics and Astronomy, University of Canterbury, Christchurch 8140, New Zealand.*

e *Case Western Reserve University, Cleveland, Ohio, USA.*

[f] *Boston University, Boston, Massachusetts, USA.*

The rare-earth nitrides (RE-N) represent a class of materials displaying especially strong coupling between their electronic and magnetic properties. They lie on the boundary between metals and insulators, and treating the strongly correlated 4*f* electrons within band theory is a challenge for the developing theoretical methods. Various treatments disagree about such fundamental issues as whether the members of the RE-N series are metals or insulators, and of equal interest to the possibility of half-metals are predictions that some are intrinsic ferromagnetic semiconductors, with the same spin polarisation in both the valence and conduction bands.

Experimental studies addressing the theoretical predictions have been limited, due largely to the lack of quality samples, and the propensity of the RE-Ns to react with atmosphere. We have recently made advances in the growth and passivation of thin RE-N films, and using a combination of optical and synchrotron-based x-ray spectroscopy, along with magnetic and transport measurements, we have begun to elucidate their electronic and magnetic structure. We have found that GdN, SmN, and DyN are semiconducting, with GdN in particular showing very strong coupling between magnetic and transport properties. By contrast, EuN is metallic, and quite likely half-metallic, with mobile electrons of only one spin orientation. The results suggest that interesting spintronics devices could be made based on these materials.

Thermodynamics and the prospects for room-temperature superconductivity

J.L. Tallon

MacDiarmid Institute for Advanced Materials and Nanotechnology and
Industrial Research Ltd, P.O. Box 31310, Lower Hutt, New Zealand.

There is as yet no agreed theory of high-T_c superconductivity in the cuprates. That need not hold us back from understanding many of their properties.. Thermodynamics presents a powerful theoretical tool to predict physical properties even in the absence of a detailed microscopic theory. Here we focus on two features: (i) the temperature and doping dependence of the relevant energy scales and (ii) the role of thermodynamic fluctuations.

We will firstly reconcile the apparently disparate spectroscopic data and show from many different spectroscopic techniques that there are two distinct energy scales to the problem, namely the superconducting energy gap, Δ_0, and the pseudogap which coexists with superconductivity and persists into the normal state. We deduce the temperature, doping and momentum dependence of these energy gaps [1].

We then turn to the role of fluctuations and show that they are a billion-fold stronger than in e.g. aluminium. An important outcome is that T_c is depressed well below its mean-field value, T_c^{mf}. A simple entropy construction allows the computation of T_c^{mf} from experimental data and the values are surprisingly high [2]. In the light of this we then consider again the energy gaps and show that, surprisingly, $2\Delta_0/k_BT_c^{mf}$ takes the conventional BCS value, as does the condensation energy suggesting that the cuprates are perhaps more conventional than we previously thought.

The stage is now set to consider the prospects for superconductivity at room temperature. Here we can make some very clear predictions...

[1] J. L. Tallon and J. G. Storey, *Nature Physics* (submitted); http://arxiv.org/abs/0908.4430.

[2] J. L. Tallon, J. G. Storey, and J. W. Loram, *Phys. Rev. Lett.* (submitted); http://arxiv.org/abs/0908.4428

Surface treatment: new methods, new applications

J.S. Colligon

Dalton Research Institute, Manchester Metropolitan University, Chester Street,
Manchester M1 5GD, UK.

The ability to provide a wide range of surface coatings on materials, or, to modify the surface in other ways, gives the design engineer considerable freedom since a material can be selected for its ideal bulk properties and the surface tailored to provide protection, or, to generate special features. The glass and cutting tool industry has already taken advantage of such coatings with glass coating itself now worth USD65 billion p.a. and hard/wear-resistant coatings some USD10 billion p.a. However there are continuing developments in coating techniques and many new applications of such coatings are proving to be viable. The present Highlights talk will describe some of these many developments.

The presentation will include a discussion of some recent vapour deposition and ion bombardment methods which provide special surface treatments and coatings. Examples will be given of techniques which, depending on chosen parameters, produce dense coatings, open-structured coatings, corrosion-resistant layers, nanocomposite hard coatings, low friction surfaces, coatings promoting bio-activity and the new MAX-phase multilayers which can, like ceramics, withstand extremely high temperatures (order 1400°C) but are easy to machine. It will be shown that the presence of even low levels of impurities can change the properties of certain types of coating.

NMR detection of dilute defect phases in solids

T.J. Bastow

CSIRO Private Bag 33 South Clayton, Victoria 3169, Australia.

The capability of NMR to observe defect structures in solids, to detect substitutional sites or atom interchange (antisites), and to infer the presence of vacancies, is demonstrated for a number of intermetallic and geological specimens.

Carefully prepared $A_{1-x}B_{1+x}$ binaries (AlFe, CuZn, CoZr) where $-0.02< x <0.02$ were examined. The probe nuclei ^{27}Al, ^{63}Cu and ^{91}Zr were used to detect and quantify defect sites [1]. In different preparations of the stoichiometric compound La_2Cu_2Mg, ^{25}Mg is used to detect atomic interchange in a structure for which X-ray diffraction indicated excellent lattice ordering and all sites fully occupied within two standard deviations [2]. Finally several naturally occuring minerals into which impurity elements such as Al or F have diffused over geological time have been shown to exhibit sharply defined ^{27}Al and ^{19}F resonances, indicating substitution of these elements in the host lattice [3].

In such materials the presence of vacancies and atomic interchange can go undetected by powder X-ray diffraction which is very sensitive to long range lattice ordering but considerably less sensitive to short range or localised disorder. NMR provides a good complement to XRD in that only nearest or next nearest neighbours to the atom of the probe nucleus make any substantial contribution to the chemical shifts and hyperfine interactions that determine the resonance line(shape) and characterise the site.

[1] T. J. Bastow and C. J. Rossouw, *Phil. Mag. Letters*, **78**, 461 (1998).
[2] R. Mishra, R.-D. Hoffmann and R. Pöttgen, *Z. Naturforsch.*, **56b**, 239 (2001).
T. J. Bastow and S. Celotto, *Solid State Magnetic Resonance,* **35**, 217 (2009).
[3] I. Grey et al, MSs in preparation.

Wavefunction-based correlation calculations for the potential energy surface of zinc and cadmium: understanding the hcp anisotropy

N. Gaston[a,b], B. Paulus[c], D. Andrae[c], U. Wedig[d], and M. Jansen[d]
[a] *Industrial Research Limited, PO Box 31-310, Lower Hutt, New Zealand.*
[b] *MacDiarmid Institute for Advanced Materials and Nanotechnology,*
Victoria University of Wellington, P.O. Box 600, Wellington, New Zealand.
[c] *Physical and Theoretical Chemistry, Free University Berlin,*
Takustrasse 3, D-14195 Berlin, Germany
[d] *Max Planck Institute for Solid State Research,*
Heisenbergstrasse 1, D-70569 Stuttgart, Germany

Cadmium crystallises in the hcp structure, but with an anomalously large *c/a* ratio, indicating a strong distortion away from ideal packing. Coupled cluster calculations within the framework of the method of increments with an embedding scheme for metals were performed to explore the potential energy surface of cadmium with respect to the hexagonal lattice parameters. This potential energy surface is compared to density functional theory based surfaces, as calculated with various functionals. The overall flatness of the potential energy surface over a wide range of values of the lattice parameter *c* is analogous for both treatments, however only within the method of increments do we quantitatively describe the cohesion. The overall behaviour of the method of increments for cadmium is consistent with previous results for zinc [1], emphasising the dominant role of electronic correlation in achieving a sufficiently accurate description of bonding properties for the two elements; however, a detailed analysis shows differences [2].

[1] N. Gaston, B. Paulus, U. Wedig, and M. Jansen, *Phys. Rev. Lett.* **100**, 226404 (2008).
[2] N. Gaston, B. Paulus, D. Andrae, U. Wedig, and M. Jansen, *Phys. Chem. Chem. Phys. accepted* (2009).

Solid state calculations of ice from an incremental coupled cluster approach

A. Hermann[a,b], and P. Schwerdtfeger[b]

[a] *Department of Chemistry, The University of Auckland, New Zealand.*

[b] *Centre for Theoretical Chemistry and Physics, NZ Institute for Advanced Study, Massey University, New Zealand.*

Water and ice attract a huge amount of interest in the physical and biological sciences, because of their abundance on Earth and in interstellar space, and their role in a multitude of biological, chemical and physical processes. Many of their properties are related to the unique characteristics of the hydrogen bond between water molecules. Understanding and, in theoretical studies, correctly describing the hydrogen bond network in water and ice is crucial to their understanding.

Here, we present ground state calculations of crystalline ice, from a combination of periodic Hartree-Fock and localized correlation calculations on coupled-cluster level of theory. We show that the method of increments [1] used here is applicable to aqueous systems and can be truncated after the two-body term. We obtain ground state properties in very good agreement with experimental results, beating the accuracy of density functional theory results by about an order of magnitude [2]. The pair-wise character of the hydrogen bond interaction suggests the possibility to accurately simulate liquid water by using periodic Hartree-Fock calculations together with a parameterized two-body correlation potential.

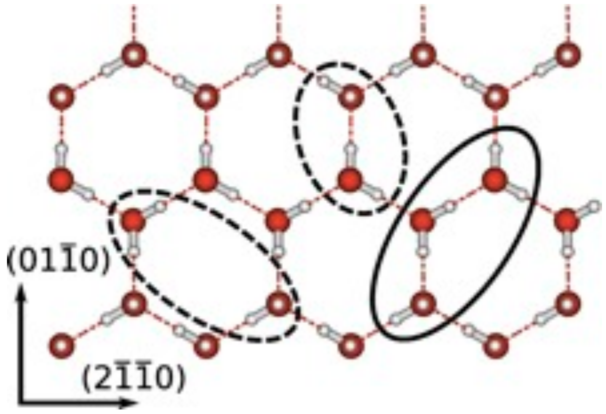

Figure 1: Hexagonal ice I*h*, with typical two- and three-body interactions used in the incremental calculation of the solid's correlation energy.

[1] H. Stoll. *Phys. Rev. B* **46**, 6700 (1992).

[2] A. Hermann and P. Schwerdtfeger. *Phys. Rev. Lett.* **101**, 183005 (2008).

The World of Wombat: a review of high speed neutron diffraction at the OPAL research reactor.

A.J. Studer

The Bragg Institute, ANSTO, Menai NSW 2234, Australia.

Wombat is one of a suite of neutron beam instruments at the OPAL reactor at the ANSTO site at Lucas Heights, just south of Sydney. In its original conception, Wombat was intended to be used for high speed powder diffraction. One key aim of the instrument was to be able to follow structural change in real time, in timeframes down to less than a second. For example, Wombat has been used to follow the progress of industrial processes such as sintering of steels *in situ*.

In cyclic systems, Wombat is able to acquire data stroboscopically. This means that the instrument can measure a rapidly changing system (easily up to a kilohertz) with time resolutions down to tens of microseconds, provided the system repeats itself enough to acquire sufficient statistics. For example, Wombat has been used to measure real time structural change in piezoelectric materials due to electric field cycling.

Wombat is routinely used for parametric studies, for example in mapping the response of a material to temperature or magnetic field. Wombat is capable of measuring single crystal samples too, and is complementary to the dedicated Koala single crystal instrument at OPAL. For example, the instrument has been used to measure magnetic structure transitions in single crystal samples as a result of applied magnetic field.

Wombat is an exciting instrument with a broad, exciting range of applications, and the aim of this talk is to illustrate the diversity of possibilities of the instrument by describing a range of recent experiments performed on it.

Kohn Anomaly in Conventional Superconductors: A Surprise

M.P. Das
Department of Theoretical Physics, Research School of Physics and Engineering
The Australian National University, Canberra, ACT 0200, Australia.

Kohn anomaly occurs in metals as a weak but discernible kink in the phonon spectrum around $2k_F$ arising out of screened Coulombic interaction. The implication of the Kohn anomaly has to provide the direct information about the shape of the Fermi surface. In the early sixties Brockhouse and coworkers made the first observation of Kohn anomaly in Pb and over the years this has been observed in a number of normal metallic systems. Recently as a major surprise, neutron spin-echo experiments on elemental (conventional) superconductors Pb and Nb (Keimer and coworkers 2008) reveal a very important and striking relation that Kohn (anomaly) energy, ω_{KA} equals twice the energy of the superconducting gap, $\Delta(0)$. From the theoretical perspective the Kohn anomaly and the BCS pairing theory do not seem to belong to a common platform. In this talk we explore the microscopic origin of this novel phenomenon and discuss its implication to the standard model BCS theory.

Spin-mediated strong coupling superconductivity in lightly doped cuprates

W. Chen[a] and O. P. Sushkov[a]

[a] *School of Physics, University of New South Wales, Sydney 2052, Australia.*

We show that in the lightly doped regime of cuprates, where magnetic spiral order is present, the interaction between holes and magnetic spirals can lead to superconductivity. Formulated within strong coupling Eliashberg equations, we found that holes excite both in-plane and out-of-plane distortion of magnetic spirals, which effectively causes a retarded attractive interaction between holes, similar to the pairing mechanism in phonon-mediated strong coupling superconductors. The d-wave symmetry of pairing amplitude is well reproduced, and the comparison with experiments in the relevant doping regime will be discussed.

Copper Selenide: Soft Phonon Modes and Superionic Phase Transition

S.A. Danilkin, M. Yethiraj, G.J. Kearley

Bragg Institute, ANSTO, New Illawarra Road, Lucas Heights NSW, Australia

This paper reports lattice dynamical measurements of $Cu_{1.8}Se$ superionic conductor having structure of the superionic α-phase at ambient temperature. $Cu_{2\delta}Se$ is a mixed ionic-electronic conductor with a superionic transition at 414K in stoichiometric compound Cu_2Se. At room temperature the superionic α-phase exists in the composition range from $\delta = 0.15$ to 0.25. The important features of the $Cu_{1.8}Se$ compound is the ordering of Cu atoms observed at ambient temperature [1] which is described as "disordered" α - phase in the literature and presence of low-energy transverse acoustic (TA) modes [2]. Measurements of phonon dispersion curves were performed with the new triple-axis spectrometer, TAIPAN, at the OPAL reactor [3]. We found that TA [100], TA [111] and TA_1 [110] phonon branches demonstrate a decrease in frequency at wavevectors $q/q_m > 0.5$ rather than the flattening observed previously. Results are compared with calculated density functional theoretical calculations showing the presence of unstable soft mode related to ordering of Cu atoms in $Cu_{1.8}Se$ at room temperature followed by α - β phase transition at a lower temperature. Superstructure arising from the ordering causes effects similar to the folding of the Brillouin zone, although phonon intensities at new Brillouin zone centres are weak. The coupling of low-energy phonon modes with displacement of mobile ions can explain the strong damping of phonons at $q/q_m > 0.5$.

[1] S.A. Danilkin, *Solid State Ionics*, **180**, 483 (2009).
[2] S.A. Danilkin, A.N. Skomorokhov, A. Hoser, H. Fuess, V. Rajevac, N.N. Bickulova, *J. Alloys and Compounds,* **361**, 57 (2003).
[3] S. Danilkin, G. Horton, R. Moore, G. Braoudakis, M. Hagen: *J. Neutron Research*, **15**, 55 (2007).

ZnO solid state dye sensitized solar cells

N.O.V. Plank[a,b], M.E. Welland[b] and H.J. Snaith[c]

[a]*The MacDiarmid Institute for Advanced Materials and Nanotechnology, School of Chemical and Physical Sciences, Victoria University, PO Box 600, Wellington 6140, New Zealand.*

[b]*The Nanoscience centre, 11 JJ Thomson Avenue. Cambridge, U.K.*

[c]*Condensed Matter Physics, Department of Physics,Clarendon Laboratory, Parks Road,OxfordU.K.*

Solid-state dye-sensitised solar cells (SDSCs) are a promising technology for energy applications due to their low cost fabrication methods and the use of low toxicity materials. [1-4] One of the key advantages of SDSCs is that the resulting devices are lightweight, can be "flexible" and transparent in certain wavelength ranges, making solar cells useful for a wide-range of applications. Here work is presented on the facile synthesis of ZnO nanowires for SDSCs. In general the power conversion efficiency for ZnO solar cells has been routinely lower than the TiO_2 nanoparticle counter parts [1-4], however, the two materials are similar and ZnO should show improved conduction performance. We have applied an MgO and a ZrO_2 shell deposition method to control the interface between two indolene based organic dyes, in SDSCs. The shell deposition was carried out at less than 100°C and shell thickness was shown to be 2nm for the ZrO_2 and 6-10nm for the MgO by transmission electron microscopy (TEM) [5,6]. X-ray photoelectron spectroscopy (XPS) has shown the ZnO NWs and core-shell structures have little water contamination. The use of dyes, D102 and D149 has lead to power conversion efficiency for ZnO NW based hybrid solar cells of 0.71%.

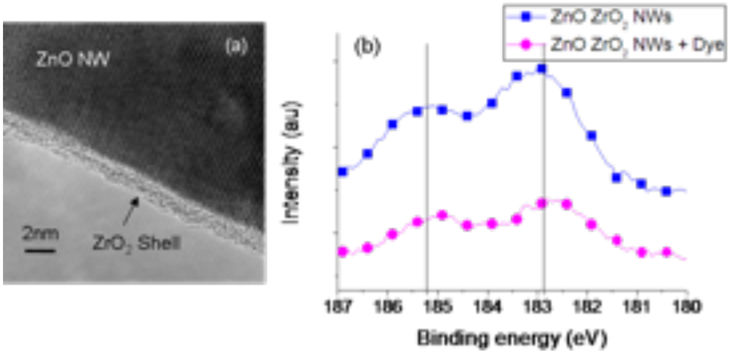

Figure 1 (a) TEM image of ZrO_2 on ZnO NWs and (b) resulting XPS spectra indicating ZrO_2.

[1] Brian O'Regan, Frank Lenzmann, Ruud Muis, and Jeannette Wienke, Chem. Mat., 2002 14, 5023

[2] Henry J. Snaith, Shaik M. Zakeeruddin, Qing Wang, Péter Péchy, and Michael Grätzel. Nano Lett., 2006, 6, 2000

[3] Henry J Snaith, Robin Humphry-Baker, Peter Chen, Ilkay Cesar, Shaik M Zakeeruddin and Michael Grätzel, Nanotech., 2008, **19,** 424003

[4] Jun-Ho Yum, Dr., Peter Chen, Michael Grätzel, Prof. Dr., Mohammad K. Nazeeruddin, ChemSusChem, 2008, 1, 699

The Crystal Structure of the Close-Packed Polymorphs of Ytterbium: A Quantum Chemical Study

D. Andrae and B. Paulus

Institute of Chemistry and Biochemistry, Physical and Theoretical Chemistry,
Freie Universität Berlin, Takustr. 3, D-14195 Berlin, Germany.

The rare earth element ytterbium ($_{70}$Yb) is known to exist in three allotropic forms at ambient pressure. The α-phase with hcp structure is reported as being the most stable polymorph at temperatures below 260 K, the β-phase with fcc structure is the most stable form at room temperature, and the γ-phase with bcc structure is the preferred form in a small temperature range below the melting point (1097 K). Furthermore, the β-phase is known to become a semiconductor at higher pressure (1.6 GPa).

The present theoretical study aims to improve the understanding of electronic structure in the α- and β-phases of ytterbium, in particular with respect to the role of electron correlation contributions from different atomic shells. We apply quantum chemical methods, based either on wave functions or on density functionals, in order to elucidate differences and / or similarities in the electronic and crystal structures of the close-packed polymorphs of ytterbium. This work extends our previous studies on crystal structures of metals from group 2 [1] and group 12 [2,3] which are also formed from atoms with closed-shell ground states (the ground state of the ytterbium atom is [$_{54}$Xe] $4f^{14}$ $6s^2$ ^1S).

[1] E. Voloshina and B. Paulus, *Phys. Rev. B* **75**, 245117 (2007).
[2] N. Gaston, B. Paulus, U. Wedig and M. Jansen, *Phys. Rev. Lett.* **100**, 226404 (2008).
[3] N. Gaston, D. Andrae, B. Paulus, U. Wedig and M. Jansen, *Phys. Chem. Chem. Phys.*, 2009, in print (DOI: 10.1039/b915967c)

Approaching metallic hydrogen through chemical stealth

N. W. Ashcroft

Laboratory of Atomic and Solid State Physics,

Cornell University, Ithaca, N.Y 14853-2501, USA.

Isolated atoms later classified as metals possess high linear dipole polarizabilities, sufficiently high that large assemblies of them undergo polarization catastrophes en route to condensed states. Except for hydrogen whose polarizability is relatively low, this is the case for the Group I elements, with or without intervention of any dimerization. The dimer in hydrogen is robustly preserved in the condensed state even under the action of mutual invasion by neighbors impelled by high pressure. Static densification of solid hydrogen, by as much as a factor of 13, has not yet led to a metallic state. Were such a state to exist, recent superconducting density functional theories are confirming earlier estimates of superconducting transition temperatures of over 200K. Might, therefore, an approximant to a metallic phase of hydrogen, even as a hydrogen-rich eutectic alloy, be approached through indirect chemical pathways by exploiting hydrogen's willingness to engage in the formation of some very high hydrides? The crucial involvement of what may be termed “chemical pre-compression” in influencing formation of hydrogen’s metallic state will be explored, starting with the hydrogen problem itself, along with some of the emerging consequences as manifested in recent experiments and analyses.

X-ray Photon Correlation Spectroscopy Applied to the Study of a Martensitic Transformation

L. Müller[a], M. Waldorf[a], C. Gutt[b], A. Madsen[c], G. Grübel[b], T.R. Finlayson[d] and U. Klemradt[a]
[a] *II Physikalisches Institute, RWTH Aachen University, D-52056 Aachen, Germany.*
[b] *HASYLAB at DESY, D-22603 Hamburg, Germany.*
[c] *European Synchrotron Research Facility, 38043 Grenoble Cedex, France.*
[d] *School of Physics, University of Melbourne, Victoria 3010, Australia.*

Photon correlation spectroscopy (PCS) which had its origins in the study of the dynamics of concentration fluctuations in bulk polymers, particularly in the vicinity of the glass transition [1], will be briefly reviewed. In the current research this spectroscopy has been extended to the X-ray wavelength range in order to examine aging dynamics in the vicinity of the martensitic transformation. Such aging dynamics have been a topic of considerable discussion in the martensite literature during the last two decades and some of this literature will also be reviewed. Indeed, while the most successful explanation for the aging phenomenon of martensites is defect-related diffusion diffusion processes in the low-temperature (martensitic) phase [2], no previous experiments have specifically addressed the time scales associated with the nanoscopic structural changes.

Using a $Au_{50.5}Cd_{49.5}$, single crystal, X-ray photon correlation spectroscopy (XPCS) measurements in diffraction geometry were carried out at the ESRF beamline, ID10A. High, temperature resolution (0.1 K) and stability (± 4 mK) were employed to resolve potentially slow dynamics in the vicinity of the phase transformation. Two-dimensional scattering data were recorded close to the (001) Bragg reflection. From an analysis of correlation functions at each temperature, characteristic timescales have been determined as a function of aging time, which reveal time constants ranging from about 400 s to over 6000 s at the largest aging times.

[1] G.D. Patterson in *Light Scattering from Polymers* (Springer-Verlag, 1983) pp125-159.
[2] X. Ren and K. Otsuka, *Nature* **389**, 579-582 (1997).

Systematic trends in the structural phase transitions of the 4*d* transition-metal oxides Sr*M*O3 (*M* = Zr, Nb, Mo, Tc, Ru and Rh)

B.J. Kennedy

[a] *School of Chemistry, The University of Sydney, Sydney, NSW 2042, Australia.*

The technological demand for materials with new or novel properties drives much of the current research of perovskite-type oxides. The 4*d* transition metal oxides (TMO) are currently attracting considerable attention because of the intriguing properties these display including phenomena such as superconductivity, metal-insulator transitions and colossal magneto-resistivity. These phenomena suggest that, contrary to the traditional view that the 4d orbitals are diffuse, strong correlation effects are present in some 4d TMO. By comparison with the 3*d* TMO there are relatively few systematic studies of the 4d TMO.

In this presentation I will review our work on the structural phase transition of the series $SrMO_3$, including presenting the results of our recent synchrotron X-ray and neutron diffraction studies of the early 4d oxides $SrNbO_3$; $SrMoO_3$ and $SrTcO_3$. In all cases the $SrMO_3$ oxides form a perovskite-type structure however the nature and magnitude of the cooperative tilting of the MO_6 octahedra is found to depend on both the electronic configuration and ionic radii of the 4d metal. Two other remarkable observations emerge from this work, namely the robust magnetic structure of $SrTcO_3$ and the presence of an unusual class of tilted perovskite in $SrNbO_3$

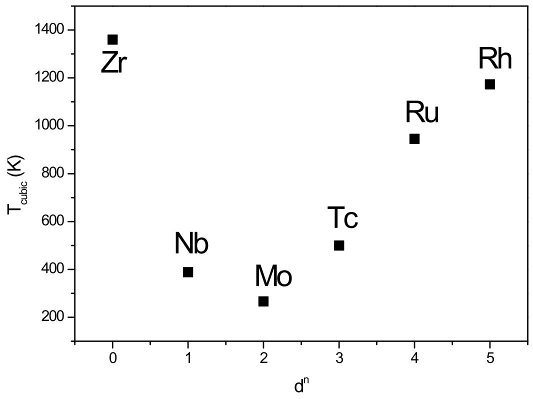

.

Figure 1. Temperature dependence of the cubic transition temperature for the series of 4*d* $SrMO_3$ perovskites.

Anomalous Spin Dynamics and Orbital Excitations in Mott-Insulating Titanates

C. Ulrich[a,b,c], G. Khaliullin[c], L.J.P. Ament[d], G. Ghiringhelli[e], L. Braicovich[e], T. Lorenz[f],
Y. Tokura[g], J. van den Brink[d], and B. Keimer[c]

[a] *School of Physics, University of New South Wales, NSW 2052, Australia.*
[b] *The Bragg Institute, ANSTO, NSW 2234, Australia.*
[c] *Max-Planck Institute for solid state research, 70567 Stuttgart, Germany.*
[d] *Institute-Lorentz for Theoretical Physics, Universiteit Leiden, The Netherlands.*
[e] *Dipartimento di Fisica, Politecnico di Milano, 20133 Milano, Italy.*
[f] *II. Physikalisches Institut, Universität zu Köln, 50937 Köln, Germany.*
[g] *Department of Applied Physics, University of Tokyo, 113 Tokyo, Japan.*

Spin and orbital degrees of freedom play an important role in the various phenomena of strongly correlated electron systems like unconventional high-temperature superconductivity in cuprates or colossal magnetoresistance in manganates. Our extensive neutron scattering experiments on the cubic perovskite titanates $LaTiO_3$ and $YTiO_3$ lead to the discovery of a highly unusual magnetic ground state which is in contradiction to the standard Goodenough-Kanamori rules, but indicates the presence of strong orbital fluctuations [1-4].

Raman light scattering spectra of $LaTiO_3$ and $YTiO_3$ exhibit unexpected features in the high energy range well above the phonon spectrum [5]. Using momentum dependent resonant inelastic x-ray scattering (RIXS) experiments in combination with theoretical calculations, we were able to identify these excitations as collective orbital excitations (orbital waves termed ‘orbitons’) [6-7].

[1] B. Keimer *et al.*, *Phys. Rev. Lett.* **85**, 3946 (2000).
[2] G. Khaliulin and S. Maekawa, *Phys. Rev. Lett.* **85**, 3950 (2000).
[3] C. Ulrich *et al.*, *Phys. Rev. Lett.* **89**, 167202 (2002).
[4] G. Khaliullin and S. Okamoto, *Phys. Rev. Lett.* **89**, 167201 (2002).
[5] C. Ulrich *et al.*, *Phys. Rev. Lett.* **97**, 157401 (2006).
[6] C. Ulrich *et al.*, *Phys. Rev. B* **77**, 113102 (2008).
[7] C. Ulrich *et al.*, *Phys. Rev. Lett.* **103**, 107205 (2009).

Single Polymer Globules of Multiblock Copolymers: How to make a very Complicated Tennis Ball.

M.B. Pinson, R. Holmes and D.R.M. Williams
Research School of Physical Sciences, IAS, Australian National University,
Canberra ACT 0200, Australia.

We present a study of the conformations of a single multiblock copolymer chain in a poor solvent. The chain has blocks ABAB.... with the A and B blocks of equal length and with identical interactions with a solvent. The system is thus as symmetrical as possible. Using numerical self-consistent field theory we study this system across the entire range of experimentally accessible parameters, from the homogenous phase through to the strongly-segregated state. The phase separated states are characterised by the interfacial area between the A and B sections. In particular we show that the usual phase-separated structure consists of two cylindrical-like regions wrapped around each other to form a sphere. This study allows us to map out the whole phase diagram for this system. Moreover, we present a very simple free energy analysis which allows the the phase boundaries to be predicted.

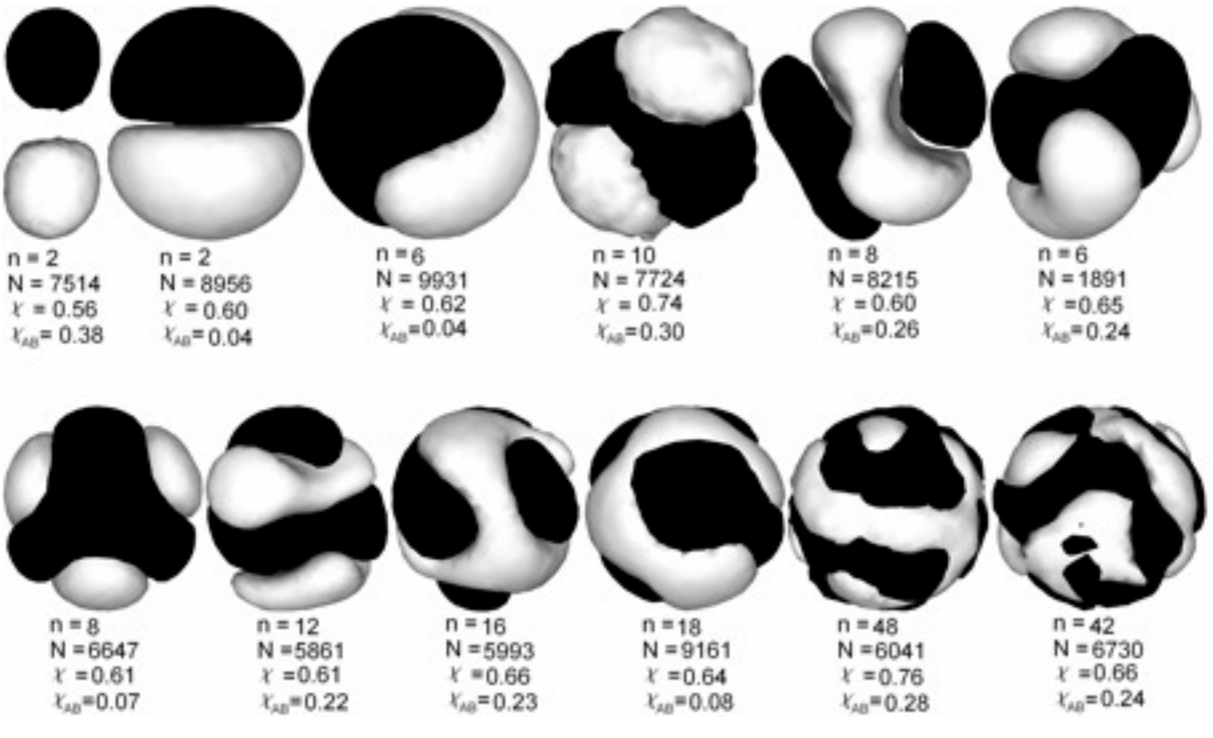

Models and simulations of the growth of carbon nanotubes

D. Schebarchov[a], S.C. Hendy[a,b], A. Awasthi[b] and B. Cox[c]

[a] *MacDiarmid Institute for Advanced Materials and Nanotechnology, Victoria University of Wellington, Wellington 6140, New Zealand.*

[b] *Industrial Research Ltd, Lower Hutt 5040, New Zealand.*

[c] *University of Wollongong, Wollongong NSW 2522, Australia.*

Despite almost twenty years of endeavour, it is still not possible to grow single-walled carbon nanotubes with selected chirality. Unfortunately, there are few clues from theory to guide experiments in this area, which have largely relied on a trial and error approach. The growth process is difficult to simulate computationally, due to the complex chemistry and thermodynamics involved, and the long timescales associated with growth. Furthermore, there have been few attempts to develop quantitative models that provide insight into chiral selectivity. Here we report on the development of a model that focuses on the lift-off of the carbon nanotube cap after nucleation. We test the model using atomistic molecular dynamics simulations and discuss the implications of the model for understanding growth processes that may control chirality.

The coalescence of gold nanoparticles: an *in situ* synchrotron study

B. Ingham[a], T.H. Lim[b*] and R.D. Tilley[b]

[a] *Industrial Research Limited, Lower Hutt, New Zealand.*

[b] *School of Chemical and Physical Sciences, Victoria University of Wellington, Wellington, New Zealand.*

The coalescence of metallic nanoparticles is of interest as a method for bottom-up fabrication of nanoelectronic components. Coalescence is observed to occur at temperatures significantly lower than the bulk melting temperature: in the case of gold nanoparticles, for temperatures as low as 200°C (T_m = 1064°C).

We have used *in situ* synchrotron small-angle x-ray scattering (SAXS) and x-ray diffraction (XRD) to observe the particle/agglomerate size and the crystallographic grain size, respectively, as a function of time at different temperatures. For each process there is a threshold temperature below which no size increase is observed (200°C for agglommeration and 220°C for grain ripening). The kinetics of each process at comparable temperatures are different. The overall picture is that the initial coalescence is rapid, followed by grain ripening to a maximum size determined by the temperature. This is also supported by computer modelling work [1].

[1] T. Lim, D. McCarthy, S. Hendy, K. Stevens, S. Brown and R. Tilley, *ACS Nano* (2009) in press.

We acknowledge funding from the Marsden Fund (IRL0602). Portions of this work were carried out at the Stanford Synchrotron Radiation Lightsource, a national U.S. user facility operated by Stanford University on behalf of the U.S. Department of Energy, Office of Basic Energy Sciences.

* Current address: Department of Materials, Oxford University, Oxford, U.K.

Towards accurate melting temperatures from ab initio Monte Carlo simulations: from nano clusters to the bulk

E. Pahl[a], F. Calvo[b] and P. Schwerdtfeger[a]

a) Centre of Theoretical Chemistry and Physics, The New Zealand Institute for
Advanced Study, Bldg.44, Massey University, Private Bag 102904,
North Shore City 0745 Auckland, New Zealand
b) LASIM, Universite Claude Bernard Lyon I, Bat. A. Kastler,
43 Bd du novembre 1918, 69622 Villeurbanne, France

We pursue the idea of obtaining information about the melting transition by studying finite clusters and extrapolating the results to infinitely large systems. In a first step, extended Lennard-Jones (ELJ) potentials are generated by a fit to *ab initio* dimer data. These pair potentials describe the most important two-body interactions in the clusters very accurately but are at the same time computationally very efficient (as efficient as the widely used Lennard-Jones potential). The melting behaviour of the nano clusters is then simulated by making use of the so-called parallel tempering Monte Carlo method. In order to extrapolate the results to the bulk we look at magic number clusters which possess prominent stabilities due to several completed shells of atoms around the central atom.

Very promising results on rare gas clusters RG_N (N=13-923) are presented from which we could extract melting temperatures with a deviation of only about 5 per cent of the experimental values (see Fig.1). Quantum effects and three-body effects have been included where necessary. The next goal is to study mercury Hg, for which very accurate dimer data have already been computed and fitted to the ELJ form.

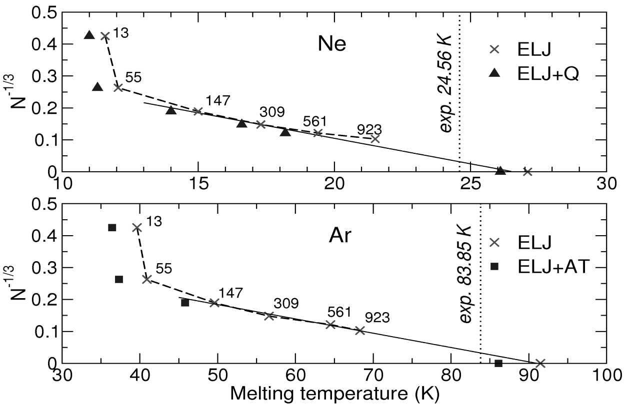

Figure 1: Dependence of melting temperatures on cluster size for neon and argon obtained using classical two-body ELJ interactions (crosses). For neon, quantum-corrected values are shown as triangles; for argon, three-body corrected values are shown as squares. The experimental bulk melting lines are indicated as vertical dotted lines.

[1] E. Pahl, F. Calvo, L. Koci, and P. Schwerdtfeger, *Angew. Chem. Int. Ed.,* **47**, 8207 (2008).

[2] E. Pahl, F. Calvo, and P. Schwerdtfeger, *Int. J. of Quant. Chem.,* **109**, 1812 (2009).

Junction effects and optical properties of RhPd/CeO_2

M. Scott[a], T. Söhnel[a], H. Idriss[b], J. Llorca[c], S.D. Senanayake[d]
[a] *Department of Chemistry, University of Auckland, N.Z.*
[b] *Energy Futures, University of Aberdeen, Scotland, U.K.*
[c]*Institute of Energy Technology, Technical University of Catalonia, Spain.*
[d]*Oak Ridge National Laboratory, Oak Ridge, Tennessee, U.S.A.*

Rh,Pd bimetallic nanoclusters supported on ceria show an active interface for steam reforming of ethanol [1]. These studies implement the VASP code to elucidate the dispersion of the active metal by modeling the metal support interaction and investigate manipulation of the nanostructure by applied field [2]. Phenomenonology of the Metal-Semiconductor junction and enhancement of the activity and selectivity for Hydrogen by amplification of the image force induced dipole is presented. A model of the electronic structure of the junction is developed which includes electron tunnelling in interfacial oxygen abstraction [3] and contribution from the f states of cerium.

The studies are complemented by Synchrotron characterisation techniques; XAFS in determination of the fine structure of the active metal clusters and XANES in identifying the interfacial cationic active metal centers. An overview of the Synchrotron techniques is given.

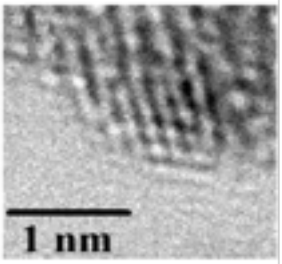

Figure 1: HRTEM of bimetallic cluster supported on ceria, estimated atomic size 35 (courtesy Jordi Llorca).

Figure 2 : Optimised Pd_{10} cluster.

[1] H. Idriss, M. Scott, J. Llorca, S. C. Chan, W. Chiu, P.-Y. Sheng, A. Yee, M. A. Blackford, S. J. Pas, A. J. Hill, F. M. Alamgir, R. Rettew, C. Petersburg, S. D. Senanayake, M. A. Barteau, *ChemSusChem*, **1**, 905-910 (2008).

[2] B. Yoon, U. Landman, *Physical Review Letters*, **100**, 1-4 (2008).

[3] J. C. Frost, *Nature*, **334**, 577 (1988).

Cluster-based Electronic Devices

S.A. Brown

MacDiarmid Institute of Advanced Materials and Nanotechnology

Department of Physics and Astronomy, University of Canterbury, Christchurch, New Zealand.

Over the past few decades studies of atomic clusters have largely focussed on fundamental science issues. While some effort has previously been devoted to the production of new materials based on clusters, the possibility that clusters could be used as nanoscale building blocks for construction of nanoscale electronic devices has been little explored.

Since nanowires have been previously demonstrated by many groups to be effective components in devices ranging from chemical sensors to transistors, we have focussed our programme on the formation of contacted cluster chains / nanowires. We have demonstrated nanowire formation by percolation, templating, and stencilling, as well as through novel no-lift-off lithography techniques. We have also demonstrated prototype hydrogen sensors based on Pd clusters, H_2 and NH_3 gas sensors based on oxidised Sn clusters, filling of high aspect ratio trenches with Cu clusters for interconnect applications, and working transistor structures based on semiconductor cluster structures. In addition, we have observed many interesting and striking physical effects during cluster deposition, such as bouncing of the clusters, and we have developed a detailed of understanding of many of these processes, for example electrical signatures of cluster coalescence and oxidation.

Electrons in Carbon Flatland: Understanding Conduction in Graphene

A.B. Kaiser[a] and V. Skákalová[b]

[a] *MacDiarmid Institute for Advanced Materials and Nanotechnology,*
SCPS, Victoria University of Wellington, P O Box 600, Wellington, New Zealand.
[b] *Max Planck Institute for Solid State Research, 70569 Stuttgart, Germany.*

It was widely believed that layers of atoms only a single atom thick (i.e. monolayers) could not exist in the free state. It was therefore a surprise when Andre Geim and his group recently demonstrated that they had succeeded in separating free-standing monolayers of carbon atoms ("graphene") from graphite. We give a brief overview of the unique properties and possible applications of these graphene sheets [1,2]. The conductivity of samples with larger carrier densities appears to be limited by relatively conventional scattering of charge carriers by lattice vibrations at higher temperatures, but high-purity graphene can have electron mobilities higher than that of any conventional semiconductor.

We have found the origin of the low-temperature resistance anomaly observed in graphene samples for all carrier densities, showing [3] that it is caused by the decay of mesoscopic resistance fluctuations that play a much greater role than in conventional 2D semiconductors; however, some of the features observed provide a challenge for current theory. We shall discuss the relation of the properties of graphene to those of carbon nanotubes [4] (which can be regarded as thin graphene sheets rolled up). We have also analyzed conduction in samples of graphene made by chemical reduction of sheets of graphene oxide. We propose an inhomogeneous model involving different conduction mechanisms that provides a very good account of the measured conductivity data for this type of sample [5].

[1] A.K. Geim and K.S. Novoselov, *Nature Mater.* **6**, 183 (2007).
[2] A.K. Geim, *Science* **324**, 1530 (2009).
[3] V. Skákalová, A.B. Kaiser, J.S. Yoo, D. Obergfell and S. Roth, *Phys. Rev. B* **74**, 153404 (2009).
[4] V. Skákalová, A.B. Kaiser, Y.-S. Woo and S. Roth, *Phys. Rev. B* **74**, 085403 (2006).
[5] A.B. Kaiser, C. Gómez-Navarro, R.S. Sunderam, M. Burghard and K. Kern, *Nano Lett.* **9**, 1787 (2009).

Time Reversal of a Pseudospin: General Properties and Application to Graphene

R. Winkler[a,b,c] and U. Zuelicke[a,d]

[a] *Institute of Fundamental Sciences & MacDiarmid Institute for Advanced Materials & Nano-technology, Massey University (Manawatu Campus), Palmerston North 4442, New Zealand.*

[b] *Materials Science Division, Argonne National Laboratory, Argonne, IL 60439, USA.*

[c] *Department of Physics, Northern Illinois University, DeKalb, IL 60115, USA.*

[d] *Centre for Theoretical Chemistry and Physics, Massey University (Albany Campus), Auckland 0745, New Zealand.*

Two-level systems are routinely represented in terms of pseudo-spin-1/2 degrees of freedom, and such pseudo-spins are usually considered to be entirely analogous to the real spin angular momentum. Here we consider time reversal (TR) of pseudo-spins from a completely general perspective and find that there exist two different types. One type behaves like ordinary spin, for which all of its three Cartesian components are odd under TR. In addition, a second type of pseudo-spin exists, behaving counter-intuitively in that only one Cartesian component is odd and the other two are even under TR. The second type is not merely of academic interest, as it is realised, eg, by the pseudo-spin representation of the 2D isotropic harmonic oscillator (Schwinger model of spin-1/2) [1]. We show that the sublattice-related pseudospin of quasi-relativistic charge carriers in graphene [2] also belongs to the second type. Our results imply that, in the absence of true spin-orbit coupling, the quantum correction to the electric resistance of single-layer graphene will be positive (weak localization). This provides a natural explanation for the hitherto puzzling absence of the proposed [3,4] weak-anti-localisation behaviour of graphene, as observed in recent experiments [5–7].

[1] J.J. Sakurai, *Modern Quantum Mechanics* (Addison-Wesley, 1994) revised ed.
[2] A.H. Castro Neto et al, *Rev. Mod. Phys.* **81**, 109 (2009).
[3] H. Suzuura and T. Ando, *Phys. Rev. Lett.* **89**, 266603 (2002).
[4] E. McCann et al, *Phys. Rev. Lett.* **97**, 146805 (2006).
[5] S.V. Morozov et al., *Phys. Rev. Lett.* **97**, 016801 (2006).
[6] X. Wu et al., *Phys. Rev. Lett.* **98**, 136801 (2007).
[7] F.V. Tikhonenko et al., *Phys. Rev. Lett.* **100**, 056802 (2008).

Water and Ion Transport in a Novel Sulfonated Pentablock Copolymer

G.M. Geise, B.D. Freeman and D.R. Paul

Department of Chemical Engineering, The University of Texas at Austin, Austin, TX, USA.

Understanding water and ion transport in polymeric materials is critical for development of new and improved desalination membrane materials. Currently, the materials used to produce desalination membranes are generally polyamide or cellulose acetate based. However, cellulose acetate materials are only applicable under restricted conditions and polyamide materials suffer from low resistance to oxidation by chemicals such as the chlorine used to disinfect water. Therefore, interest exists for developing new and improved materials for desalination membranes. One such approach involves sulfonation of a hydrocarbon polymer. Sulfonation increases the hydrophilic character of the polymer and, at high levels of sulfonation, a polymer can have very high water permeability. However, as the degree of sulfonation increases, the material can become water soluble. To avoid this, a block copolymer architecture can be used. Here, a symmetric pentablock copolymer containing *t*-butyl styrene end blocks, a selectively sulfonated middle block, and hydrogenated isoprene blocks to connect the end blocks to the middle block has been studied. Water transport in these materials has been studied as a function of degree of sulfonation and hydrophobicity of the block copolymer. Ion transport behavior of highly charged materials, such as sulfonated polymers, differs from that observed in hydrophilic and/or weakly charged polymer materials due to ion exclusion, or Donnan exclusion, effects. Here, theory and experimental data for ion transport in a sulfonated pentablock copolymer is presented and discussed. By increasing the density of sulfonate groups in the hydrated micro-domains of the polymer, transport properties can be tuned and the selectivity of water permeability to salt permeability can be improved.

Characterisation and tracing of prosthesis debris - Can pathways of polymer particles be suppressed?

H. Timmers[a] , J.A. Warner[a], L.G. Gladkis[a,b],

[a] *School of Physical, Environmental and Mathematical Sciences, University of New South Wales at the Australian Defence Force Academy, Canberra, Australia*

[b] *Trauma and Orthopaedic Research Unit, The Canberra Hospital, PO BOX 11, Woden, ACT 2606, Australia*

Ultra-high molecular weight polyethylene polymer is the established bearing material in knee prostheses due to its favourable wear properties. The large and persistent dynamic forces in an artificial knee joint create however an immense number of polymer wear debris particles ranging from submicron to visible size. These particles trigger the biochemical reactions which in many patients result in early clinical failure of the prosthesis. The wear mechanisms creating the particles are uncertain. The particle pathways in and near the prosthesis are not clear. The relevance of particle size and shape on the bioactivity of particles is debated.

In a new experimental approach using radioisotope implantation, the pathways of polymer wear particles have been traced from dislodgement to dispersion. In particular, during the wear-in phase the formation of a polymer film on the actuating surface has been identified as the result of a two-way transfer process of debris particles between actuator and polymer. Similar experiments on actual prostheses using a realistic knee motion simulator are planned. Dislodgement mechanisms of polymer debris are being studied with micro-scratching. Debris particle sizes and shapes have been fully characterized in three-dimensions using scanning probe microscopy. The dependence of bioactivity on particle size has been tested and compared with results from other authors. A better understanding of the complex tribological and transport processes which initiate prosthesis failure may emerge. Ultimately, adverse debris particles and their pathways in the prosthesis may be suppressed.

Synthesis at High Pressure and High Temperature of M-1212 metalo-cuprates

M.Á. Alario-Franco

Laboratorio Complutense de Altas Presiones,

Facultad de Química, Universidad Complutense, Madrid, Spain.

In this talk, after an overview of the influence that the combined use of High Pressure and High temperature have in solids, we will describe our recent work in the synthesis of an interesting family of *metalocuprates.*

We have been working for sometime on the synthesis at high pressure (*P* up to 12.5 Gpa) and high temperature (*T up to* 1400ºC) of new materials of the type $MSr_2RECu_2O_8$ (RE Rare Earth; M <> Ru, Cr or Ir), which formally derive from the celebrated High Temperature Superconductor YBCO (*i.e.*,$CuBa_2YCu_2O_7$) by replacing the [Cu-O_4] squares in the basal plane of the structure by [M-O_6] octahedra.

We have then observed that the adequate formation of these cuprates as majority phases, can only be performed in a particular and relatively narrow window of *P* and *T*, outside which they cannot be obtained pure or even obtained at all.

On the other hand, these "optimum conditions" bear a remarkable Gaussian correlation with the rare earth ion size, and they do not follow the classic *lanthanide contraction* so often observed in the chemistry of these elements.

After describing this family of materials in some detail, including the structure, microstructure and some properties, we will give an interpretation of the origin of such discrepancy which can be attributed to *interelectronic repulsion* in the lanthanide ions

The structures, phase transitions and dynamics behind mixed ionic and electronic conduction in hydrated $Ba_4Nb_2O_9$

C.D. Ling[a,b], M. Avdeev[b], and M.R. Johnson[c]

[a] *School of Chemistry, The University of Sydney, Sydney 2006, Australia.*

[b] *Bragg Institute, ANSTO, PMB 1, Menai 2234, Australia.*

[c] *Institut Laue-Langevin, 6, rue Jules Horowitz, 38042 Grenoble Cedex 9, France.*

Although $Ba_4Nb_2O_9$ was first synthesised in 1965, [1] its structure remained unsolved until a recent study [2] in which we showed that $Ba_4Nb_2O_9$ has two basic polymorphs: a high-temperature γ phase, which represents an entirely new structure type; and a low-temperature α phase, which has the rare $Sr_4Ru_2O_9$ structure type. The phases are separated by a reconstructive transition at ~1370 K, the kinetics of which are sufficiently slow that the γ phase can easily be quenched to room temperature. Below ~950 K, both α and γ absorb significant amounts of water. In the γ phase, protons occupy ordered positions, giving rise to a stoichiometric phase γ-III-$Ba_4Nb_2O_9.1/3H_2O$ at room temperature. γ-III-$Ba_4Nb_2O_9.1/3H_2O$ partially dehydrates at ~760 K to γ-II-$Ba_4Nb_2O_9.1/6H_2O$, then completely dehydrates at ~950 K to γ-I-$Ba_4Nb_2O_9$. The hydrated γ phases exhibit faster protonic and oxide ionic transport than the hydrated α phases, due to the presence in the gamma phases of 2D layers containing Nb^{5+} cations with unusually low oxygen coordination numbers (4 or 5) separated by discrete OH groups. In this paper, we will discuss the structures and mechanisms of hydration – and, therefore, of ionic conduction – in the various phases of $Ba_4Nb_2O_9$ on the basis of neutron diffraction experiments and *ab initio* (density functional theory) dynamics simulations.

[1] G. Blasse, *Journal of Inorganic & Nuclear Chemistry* **27**, 993-1003 (1965).

[2] C.D. Ling, M. Avdeev, R. Kutteh, V.V. Kharton, A.A. Yaremchenko, S. Fialkova, N. Sharma, R.B. Macquart, M. Hoelzel and M.J. Gutmann, *Chemistry of Materials* **21**, 3853-3864 (2009).

Modern Diffraction Methods for the Investigation of Thermo Mechanical Processes In Materials Physics

K.-D. Liss

Australian Nuclear Science and Technology Organisation, Lucas Heights NSW 2234, Australia

Well collimated, high energy X-rays of 90 keV from synchrotron sources have been used to study metals undergoing plastic deformation in-situ, in real time and in the bulk of the materials. The spottiness of poorly illuminated Debye-Scherrer rings showing reflections from individual crystallites is analyzed to obtain grain statistics, mosaic spread and orientation. Upon cold deformation, coarse grained materials show fingerprints of sub-grain formation, grain rotation, grain refinement and the evolution from a single grain into the asymptotic texture. Heating of metals under continuous load drives the observation through the regimes of phase transformation and grain relationships therein, grain coarsening, dynamic recovery and dynamic recrystallization. The distinct kinetics and deformation mechanisms of co-existing phases can be distinguished in a dual-phase system. The paper points out these different phenomena which were observed without precedence.

Quantum Phase Transitions in Coupled Quantum Optical Cavities

A.D. Greentree

School of Physics, University of Melbourne, Victoria 3010, Australia.

Quantum phase transitions are amongst the most interesting features of condensed matter systems. Recent work has focused on ways to translate the physics embedded in toy models, for example, the Bose-Hubbard model, into physical systems that are highly amenable to control and readout. An excellent example is the realisation of quantum phase transitions in optical lattices [1]. More recently, it has been shown that coupled cavity systems in the photonic blockade regime provide an excellent realisation of a Hubbard model [2,3,4]. Hopping terms are affected via evanescent tunneling between the cavities, and the interaction via the photon-blockade mechanism. Interestingly, the system is not a realisation of either a Bose- or Fermi-Hubbard model, as the statistics of the polaritons (atom-photon 'molecules') are not well-defined. This shows that the photonic case is showing new physics. Since the 2006 proposals, there have been significant advancements in the theoretical treatment and in the push to realise such structures experimentally, including new cavity designs [5] and the creation of long, one-dimensional, coupled-cavity structures [6]. We will discuss some of the recent progress and highlight some of the possible new future directions in which these ideas may take us [7, 8, 9].

[1] M. Greiner, O. Mandel, T. Esslinger, T.W. Hansch and I. Bloch, *Nature* **415**, 39 (2002).
[2] D.G. Angelakis, M.F. Santos and S. Bose, *Phys. Rev. A* **76**, 031805(R) (2007).
[3] M.J. Hartmann, G.S. Fernando, G.S.L. Brandão and M.B. Plenio, *Nat. Phys*. **2**, 849 (2006).
[4] A.D. Greentree, C. Tahan, J.H. Cole and L.C.L Hollenberg, *Nat. Phys*. **2**, 856 (2006).
[5] S. Tomljenovic-Hanic, A.D. Greentree, C. Martijn de Sterke and S. Prawer, *Opt. Exp.* **17**, 6465 (2009).
[6] M. Notomi, E. Kuramochi and T. Tamabe, *Nat. Photonics* **2**, 741 (2008).
[7] M.I. Makin, J.H. Cole, C. Tahan, L.C.L. Hollenberg, and A.D. Greentree, *Phys. Rev. A* **77**, 053819 (2008).
[8] M.I. Makin, J.H. Cole, C.D. Hill, A.D. Greentree, L.C.L. Hollenberg, *Phys. Rev. A* (in press), arXiv:0907.0539.
[9] J. Quach, M.I. Makin, C.-H. Su, A.D. Greentree, and L.C.L. Hollenberg, arXiv: 0909.2723.

A New Approach to the Creation of Magnetically Modulated Structures

T. Saerbeck[1,2], F. Klose[1], D. Lott[3], G.J. Mankey[4], Z. Lu[4], P.R. LeClair[4],
A.P.J. Stampfl[1], S. Danilkin[1], M. Yethiraj[1], A. Schreyer[3]
[1]*Australian Nuclear Science and Technology Organisation, Menai, NSW 2234, Australia*
[2] *University of Western Australia, School of Physics, 35 Stirling Highway, Crawley, WA 6009, Australia*
[3]*GKSS Research Center, Max-Planck-Str. 1, 21502 Geesthacht, Germany*
[4]*MINT Center, University of Alabama, Tuscaloosa, AL 35487, USA*
[5]*Institute Laue Langevin, 6 rue Jules Horowitz, 38042 Grenoble, France*

The plethora of structural and magnetic properties observed in many transition metal alloys has attracted a great deal of interest in both the pure and applied sciences [1]. One key attribute of these alloys is that their electronic and magnetic properties are extremely sensitive to not only stoichiometry but order as well. In this paper we report on a new approach of creating a magnetically modulated structure, without changing composition or lattice structure, namely by artificially controlling the degree of chemical order in the material.

The compound $FePt_3$, as it is well known from bulk crystals, has the extraordinary property to evolve ferromagnetic (FM) or antiferromagnetic (AFM) phases determined by the degree of chemical ordering [2]. We succeeded in preparing epitaxial FePt3 superlattices of homogeneous composition consisting of an artificially modulated ferro/antiferromagnetic layering sequence simply by alternating the growth temperature. A direct effect of such an exotic FM/AFM interface is the observation of a high exchange bias upon field cooling through the Nèel temperature. In order to quantify the degree of antiferromagnetic ordering, high angle neutron diffraction has been performed using the triple axis spectrometer IN12 (Institute Laue Langevin, Grenoble) and TAIPAN (Australian Nuclear Science and Technology Organisation). Similar to chemically ordered bulk $FePt_3$ the superlattice exhibits the onset of a (½ ½ 0) AFM Bragg peak below a temperature of T_N=140 K (Bulk T_N=160 K [2]). Using the polarized neutron reflectometry technique at the German research facility GKSS, Geesthacht, a detailed layer resolved magnetic characterization of the superlattice was carried out.

[1] Farrow, R.F.C., Weller, D., Marks, R.F., Toney, M.F., Hom, S., Harp, G.R., Cebollada, A., *Appl. Phys. Lett.* 69, 1166 (1996).
[2] Bacon, G.E. and Crangle, J., *Proc. R. Soc. London, Ser. A*. 272, 387 (1962).

Modulated Structures in the Fresnoite Family

P. K. K. Allen and S. Schmid

School of Chemistry, The University of Sydney, NSW 2006, Australia.

Strong demand for lead-free electronic materials, particularly piezoelectrics, has been created in response to recent European Union and Japanese legislation that introduced severe restrictions on the use of hazardous substances in electronic equipment [1, 2]. A comprehensive understanding of the relationship between the structural chemistry and physical properties is vital for the design and development of new, environmentally friendly electronic materials.

The fresnoite family of modulated structures, $A_2TiM_2O_8$ (A = Ba, Sr; M = Si, Ge), has been shown to exhibit excellent piezoelectric properties [3], making them one of several possible alternatives to replace lead-based electroceramic materials. We have synthesised $Ba_{22x}Sr_{2x}TiSi_2O_8$ in the composition range $0 \leq x \leq 1$ and investigated the structural behaviour of selected members. Temperature and composition dependent phase transitions have been probed using a wide range of techniques including synchrotron X-ray powder diffraction, neutron powder diffraction, electron diffraction, and differential scanning calorimetry.

This contribution will discuss the non-trivial synthesis of the $Ba_{2-2x}Sr_{2x}TiSi_2O_8$ series, the use of a modulated structure approach to characterise powder diffraction data using Jana2006, and new evidence of the phase transition that removes the structural modulation in $Ba_2TiSi_2O_8$. In addition, recent indications for the coexistence of two incommensurately modulated $Sr_2TiSi_2O_8$ phases at room temperature and results from variable temperature X-ray powder diffraction will also be presented.

.

[1] Y. Li, K. S. Moon and C. P. Wong, *Science*, **2005**, 308, (5727), 1419-1420.

[2] Y. Saito, H. Takao, T. Tani, T. Nonoyama, K. Takatori, T. Homma, T. Nagaya, M. Nakamura, *Nature*, **2004**, 432, (7013), 84-87.

[3] T. Asahi, T. Osaka, J. Kobayashi, S. C. Abrahams, S. Nanamatsu, M. Kimura, *Phys. Rev. B*, 63, **2001**, (9), 1-13.

Organic Solar Cells with Carbon Nanotube Sheet Electrodes

K. Sears[a], G. Fanchini[b], S. Watkins[b], L. Rozanski[c], K. Mielzcharek[d], A. Zakhidov[d]

[a]*CSIRO Materials Science and Engineering, Clayton VIC, 3168, Australia*

[b]*CSIRO Molecular Health and Technology, Clayton VIC, 3168, Australia*

[c]*CSIRO Energy Technology, Newcastle, Australia*

[d]*NanoTech Institute, The University of Texas at Dallas, TX 75083, USA.*

Organic solar cells are attractive for flexible devices due to their compatibility with plastic substrates and high throughput processing techniques such as ink jet printing. However, to achieve fully flexible organic solar cells, new materials are needed to replace Indium Tin Oxide (ITO) which serves as the transparent electrode for hole collection. ITO is expensive, cannot be solution processed and is brittle. Flexible, conductive films fabricated from carbon nanotubes (CNTs) are a promising alternative to ITO and have attracted considerable interest [1,2].

In this work P3HT:PCBM bulk heterojunction solar cells are fabricated with the ITO electrode replaced by a sheet of CNTs (Figure 1). The sheets are drawn from a forest of CNTs and deposited directly onto the substrate, avoiding the need to disperse CNTs in a solution-based method. This study extends on previous work [2] by exploring the trade-off between transparency and conductivity of the CNT sheets. Devices were fabricated with either one or two layers of CNT sheets, and their performance compared to that of devices using ITO. Despite their lower transparency, the best performance was observed for devices fabricated with two layers of CNT sheet, giving an excellent fill factor of 0.47. This presentation will discuss this study in greater detail and also present preliminary results on flexible devices.

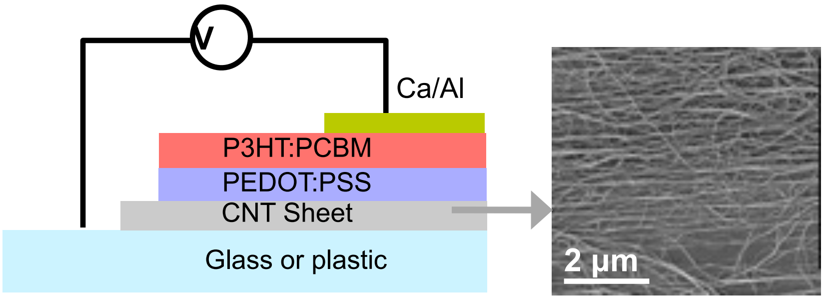

Figure 1 Schematic of device structure and scanning electron microscopy image of a CNT web.

[1] G. Grüner, *Scientific American* **296** (5), 76 (2007)

[2] R. Ulbricht, S. B. Lee, X. Jiang, K. Inoue, M. Zhang, S. Fang, R. H. Baughman, A. A. Zakhidov, *Solar Energy Materials and Solar Cells*, **91**, 416 (2007).

Studying Electrical Double Layers in Ionic Liquids using Neutron and X-ray Reflectometry

Y. Lauw[a,b], A. Nelson[a], M. Horne[b], T. Rodopoulos[b], B. Minoofar[c], N. Webster[b], W. Hamilton[a]
[a] *Australian Nuclear Science and Technology Organisation, Sydney, NSW 2234.*
[b] *CSIRO Minerals, Bayview Avenue, Clayton South, VIC 3169.*
[c]*University of South Bohemia, Nove Hrady, Czech Republic.*

Ionic liquids are typically defined as salts that exist in a liquid state at, or near, room temperature. Due to their favourable properties (e.g., good thermal stability, low volatility, and wide electrochemical window), ionic liquids have potential use in many industrial applications, such as catalysis, lubrication, batteries, and metal electrodeposition. Despite recent advances in the field, ionic liquid research is still in its infancy. Additional fundamental studies are needed to explore the properties of ionic liquids and to allow the full potential of these properties in particular applications to be exploited.

Electrical double layers (EDL) are well known in aqueous colloidal systems where the potential field from a charged surface affects many properties of the particle. The structure of the EDL at a conductive surface is of prime importance to electrochemistry because it strongly affects the transport of reactants and products within the region where electrochemical reactions take place. The understanding of the EDL in ionic liquids is not nearly as advanced as aqueous systems and even a description of how it responds to changes in the conductor potential is yet to be agreed. Here we present some recent results from simulation and Neutron/X-ray reflectometry measurements that explore the electrical double layer in ionic liquids at the air-liquid and solid-liquid interfaces. The effect of water impurities within the (EDL) of an ionic liquid is of particular interest since they are known to reduce the electrochemical window of ionic liquids, decrease their density and viscosity, and anomalously decrease their surface tension.

Hydrodynamic mobility of an optically trapped colloidal particle near fluid-fluid interfaces

G.M. Wang, R. Prabhakar, and E.M. Sevick
Research School of Chemistry, The Australian National University, Canberra 0200,
Department of Mechanical & Aerospace Engineering, Monash University Clayton VIC 3800

The aim of microfluidics is to miniaturise reaction vessels and their connecting conduits to “lab on a chip" dimensions. However, this magnifies the influence of bounding walls on the microflow. The drag force on a particle entrained in these microfluidic flows is larger than the particle's drag in a bulk fluid. This is due to the hydrodynamic interactions between colloid and surrounding solvent molecules being altered by the nearby solid surface. These micro-vessel boundaries need not be solid surfaces, but can also be soft surfaces, such as in vesicle membranes, or an immiscible fluid that forms impenetrable boundaries. Fluid mechanicists have derived theoretical predictions of how the particle friction becomes anisotropic and dependent upon distance from a surface that is governed by various boundary conditions [1-5]. However experimental measures of particle friction near a single surface are comparatively few and exist only near solid surfaces.

Using Optical Tweezers, we measure the anisotropic hydrodynamic mobility or friction of a colloidal particle as a function of distance from fluid-fluid interfaces, namely a liquid-vapor interface and a liquid-liquid interface [6]. The measurement is based on the thermal motion of a Brownian particle which is localised near the interface, and the method is uniquely capable of detailing the anisotropic, distance-dependent mobility/friction near fluid-fluid interfaces. It is a quiescient method, requiring no controlled fluid flow, is independent of distance-dependent conservative interactions (e.g. electrostatic interactions) between particle and interface, and resolves distance-dependence in friction to within a fraction of the particle radius. Near the liquid-vapor interface, the friction decreases below the value of friction in bulk fluid, corresponding to the hydrodynamic predictions of a “perfect-slip" surface which does not support stresses.

[1] H. Brenner, *Chem. Eng. Sci.* **16**, 242 (1961).
[2] H. Faxen, *Arkiv. Mat. Astron. Fys*., **17,** 27 (1923).
[3] S.H. Lee, R.S. Chadwick and L.G. Leal, *J. Fluid Mech*. **93**, 705 (1979); S.H. Lee and L.G. Leal, *J. Fluid Mech*, **98**, 193 (1980).
[4] E. Lauga and T.M. Squires, *Phys. Fluids* **17**, 103102 (2005).
[5] T. Bickel, *Phys. Rev. E* **75**, 041403 (2007) .
[6] G.M. Wang, R. Prabhakar, and E.M. Sevick, under review *Phys.Rev. Lett.*

Pulsed ESR Measurement of Coherence Times in Si:P at Very Low Temperatures

W.D. Hutchison[a,b], L. Alexander[a,b], N. Suwuntanasarn[a,b] and G.N. Milford[a,c]

[a] *ARC Centre for Quantum Computer Technology.*

[b] *School of Physical, Environmental and Mathematical Sciences, The University of New South Wales, ADFA, Canberra, ACT 2600, Australia.*

[c] *School of Engineering and Information Technology, The University of New South Wales, ADFA, Canberra, ACT 2600, Australia.*

Phosphorus donors placed in silicon (Si:P) are expected to have very long (both nuclear and electron) spin relaxation times, and in addition, the compatibility of silicon with existing device fabrication technology, makes this system of interest as a potential basis for quantum computing (QC) devices [1]. In Si:P, the dephasing of the donor electron spin represents the decoherence time of the device (single qubit decoherence). Pulsed electron spin resonance (ESR) offers a convenient and most effective way to study this dephasing. The original pulsed ESR studies of Si:P were conducted a long time ago. However, since the interest in Si:P for QC, further work has been done. For example in [2], a projected isolated spin decoherence time (T_2) of 60 ms at 7 K was reported. Here we describe a millikelvin X-band pulsed ESR system that has been set up to provide the most optimal conditions for the Si:P decoherence time measurements. Using this set-up we have measured isolated spin T_2 for phosphorous donor electron spins in isotopically purified silicon in excess of 100 ms.

[1] B.E. Kane, *Nature* **393**, 133, (1998).

[2] A.M. Tyryshkin, S.A. Lyon, A.V. Astashkin, A.M. Raitsimring, *Phy. Rev. B* **68**, 193207, (2003).

Synthesis and Applications of Nanoparticles

R.D. Tilley

[a] *School of Chemical and Physical Sciences and MacDiarmid Institute, Victoria University of Wellington, New Zealand.*

Liquid phase synthesis is a powerful method for the formation of uniform sized nanoparticles and nanoparticles with a faceted morphology. General strategies for the formation of nanoparticles and quantum dots through chemical synthesis will be outlined. The results presented will include the formation of noble metal such as platinum and palladium and group IV quantum dots. The growth mechanism of how the particles form will also be presented along with in-situ synchrotron data and HRTEM observations.

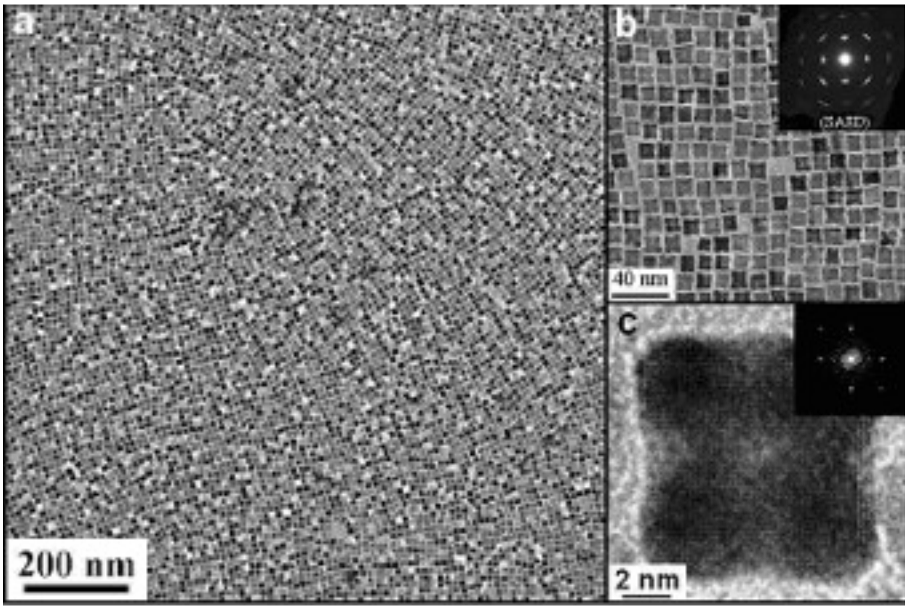

Fig. 1. TEM image of self-assembled highly monodispersed platinum nanocubes.

[1] J. Watt, N. Young, S. Haigh, A.I. Kirkland and R.D. Tilley, *Advanced Materials*, **21**, 2288 (2009).
[2] S. Cheong, J. Watt, B. Ingham, M. F. Toney and R. D. Tilley, *Journal of the American Chemical Society*, available online (2009).
[3]R. D. Tilley and K. Yamamoto, *Advanced Materials*, **18**, 2053 (2006).

From Clusters to the Solid State: A Systematic Search for Global Minimum Structures for Cs, Sn and Au Clusters

B. Assadollahzadeh and P. Schwerdtfeger

Massey University Albany,

Centre for Theoretical Chemistry and Physics,

The New Zealand Institute for Advanced Study,

Auckland, New Zealand.

A prerequisite for developing new nano-materials is the prior knowledge of the geometrical structures of nano-clusters. Laser vaporization sources produce gas-phase cluster, but give no insight into cluster geometries. Subsequent beam deflection experiments, induced via a static, inhomogeneous electric field, can be used to observe cluster polarizabilities, which in turn give good indication for electronic and geometrical structures [1]. Theoretical studies are of utmost importance in this respect, as they complement experimental findings and furthermore can be used to determine global minimum structures of nano-clusters. Such structures, of given size, correspond to the geometrical arrangement which are thermodynamically most stable.

For this purpose, we developed and used a density functional based genetic algorithm code to systematically search for global minimum structures of Au, Sn and Cs clusters. [1-5] We compare our calculated electronic properties such as dipole moments and dipole polarizabilities with those observed via experiments and extrapolate our results to the solid state. Finally, we discuss current shortcomings and problems on both the experimental and theoretical side.

[1] S. Schafer, B. Assadollahzadeh, M. Mehring, P. Schwerdtfeger, R. Schafer *J. Phys. Chem. A* **112,** 12312 (2008).

[2] B. Assadollahzadeh, P.R. Bunker, P. Schwerdtfeger *Chem. Phys. Lett.* **451**, 262 (2008).

[3] B. Assadollahzadeh, S. Schafer, P. Schwerdtfeger *J. Comput. Chem.* in press, available online (2009).

[4] B. Assadollahzadeh, P. Schwerdtfeger *J. Chem. Phys.* **131**, 064306 (2009).

[5] B. Assadollahzadeh, C. Thierfelder, P. Schwerdtfeger *Phys. Rev. B* **78**, 245423 (2008).

Investigation of columnar defects in MOD YBCO films by TEM

J.A. Xia[a], N.M. Strickland[a], E.F. Talantsev[a], N.J. Long[a], M.W. Rupich[b], S. Sathyamurthy[b],
X. Li[b], and J. Kennedy[c]

[a] *Industrial Research Ltd, PO Box 31-310, Lower Hutt, New Zealand*
[b] *American Superconductor Corporation, 64 Jackson Rd, Devens, MA 01434, USA*
[c] *GNS Science, PO Box 31-312, Lower Hutt, New Zealand*

Defects in $YBa_2Cu_3O_7$ (YBCO) films play a significant role in determining the critical current density of superconducting wires through pinning of magnetic flux lines. Tailoring the size, concentration, and shape of these defects to optimize the critical current density is one of the principal goals of materials research on YBCO films. YBCO has a distorted perovskite structure; for thin-film growth by metal-organic deposition, planar defects parallel to the a-b plane and the film surface are commonly observed. These planar defects enhance the critical current when the magnetic field is parallel to the film. Point-like nanoparticle defects can also be introduced, giving an isotropic enhancement. To enhance critical currents particularly when the magnetic field is perpendicular to the film, columnar defects would be desirable. We have reported ion irradiation on YBCO films resulting in columnar ion tracks which provide strong flux pinning for magnetic fields aligned close to the irradiation direction [1]. Columnar defects have also been observed in uniradiated YBCO films doped with Dy and Sn, however these defects do not provide such a significant flux pinning benefit. In this work, we use Transmission Electron Microscopy (TEM) to observe these defects and explore their relationship with the critical current anisotropy.

[1] N.M. Strickland et al. *Physica C*, (2009, in press).

AuCuAl Shape Memory Alloys for Use in Nano-Actuators

V.K. Bhatia[a], C.S. Kealley[a], G.J. Thorogood[b], A. Dowd[a] and M.B. Cortie[a]

[a]*University of Technology Sydney, PO Box 123, Broadway NSW 2007, Australia*

[b]*Australain Nuclear Science and Technology Organisation, PMB 1, Menai NSW 2234, Australia*

Although Al, Au and Cu each has the face centered cubic structure in elemental solid form, they do not readily alloy with one another, and instead form a series of binary and ternary intermetallic compounds. The ternary system is very interesting and contains, amongst other features, an 18-carat shape memory electron compound sometimes called ‘Spangold’ [1] (Figure 1).

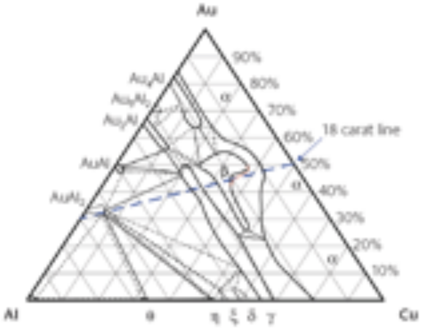

Figure 1. Au Al Cu ternary diagram at 500°C [2].

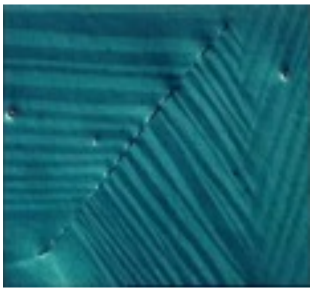

Figure 2. Martensite laths, imaged under Nomarski interference contrast.

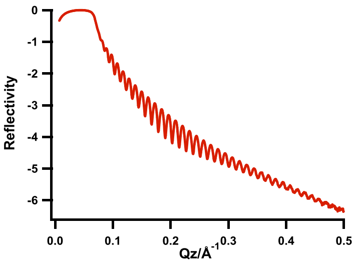

Figure 3. Reflectometry data for AuCuAl thin film.

Shape memory alloys are remarkable in that they have the ability to return to their initial state and shape after being deformed. This ability arises from a martensitic (displacive) phase transformation (see Figure 2), which is strongly influenced by temperature, crystal structure and degree of ordering. It is already known that the parent phase of ‘Spangold’ must contain at least a minimum degree of ternary ordering before the reversible displacive transformation needed for the shape memory effect can take place [3]. Furthermore, the parent phase has been found to have the $L2_1$ ordered body-centered cubic packing arrangement [4], while it has been reported that the martensite can be described using a monoclinic unit cell [5]. Here we examine the possibility of using this compound as a nano-actuator. Magnetron sputtering was used to deposit the Au, Cu and Al. The films were then characterized using x-ray reflectometry (see figure 3), grazing incidence X-ray diffraction, scanning electron microscopy and atomic force microscopy. The properties of these films are compared with that of bulk samples.

[1] I.M. Wolff and M.B. Cortie, *Gold Bulletin*, **27**(2), 44 (1994).
[2] V.K. Bhatia, F.C.Levey., C.S. Kealley, A. Dowd and M.B. Cortie, *Gold Bull.*, **42**(3), 201, 2009.
[3] F.C. Levey, M.B. Cortie and L.A. Cornish, *Metall. Mater. Trans. A.*, **31A**, 1917 (2000).
[4] M.B. Cortie and F.C. Levey, *Intermetallics*, **8**(7), 793 (2000).
[5] L. Battezzati, G. Fiore, M. Massazza, *J. Alloys and Compounds*, **434–435**, 264 (2007).

The influence of relativistic effects on the structure of the group 12 chalcogenides: A density functional study

S. Biering, P. Schwerdtfeger

Centre for Theoretical Chemistry and Physics, The New Zealand Institute for Advanced Study, Massey University (Auckland Campus), Private Bag 102904, North Shore City, 0745 Auckland , New Zealand.

Even though relativistic effects in atoms and molecules are well-known and understood, little attention has been given to their influence on the solid state. Motivated by a recent study concerning the group 11 halides [1], this work aims to investigate relativistic changes in the crystal structure of the group 12 chalcogenides [2].

Bulk HgO crystallizes in a rather unusual structure, whereby two different polymorphs exist at ambient pressure. Hereby the low temperature form adopts an orthorhombic structure with the spacegroup *Pmna* and is built from planar O-Hg-O zigzag chains running parallel to the x-axis, whereas the high temperature cinnabar form consists of spiral chains parallel to the z-axis. Those equilibrium phases are in stark contrast to the lighter group 12 chalcogenides, which under ambient conditions are known to crystallize in rather simple hexagonal wurtzite and cubic rocksalt or zinc blende structures. Following the periodic table, mercury sulfide as well crystallizes in the cinnabar structure, but cinnabar disappears as a equilibrium phase for HgSe and HgTe, where the zinc blende form is found to be more stable. However, the transition to cinnabar occurs at very low 'high pressures', compared to ZnTe and CdTe, where the structures exists too, even though only as a hidden intermediate phase.

Considering this behavior of the mercury chalcogenides: What causes the occurrence of the unusual structure in the mercury chalcogenides? The objective of this study therefore is to show that indeed the unusual structure of the mercury chalcogenides is a result of relativistic effects. Comparative relativistic and nonrelativistic density functional studies of equilibrium and high pressure phases of ZnX, CdX and HgX (X=O, S, Se, Te) are carried out to investigate the problem.

[1] T. Söhnel, H.L. Hermann and P. Schwerdtfeger, *Angew. Chem., Int. Ed.* **40**, 4382 (2001).
[2] S. Biering, A. Hermann and P. Schwerdtfeger, *J. Phys. Chem. A* in press (2009).

A Neutron and Synchrotron Investigation Of The Electronic Structure Of Lanthanide Zirconates

R. Clements[a,b], B. Kennedy[a], C. Ling[a,b], A.P.J. Stampfl[b]
[a]*School of Chemistry, The University of Sydney, New South Wales, 2006, Australia;* [b]*Bragg Institute, Australian Nuclear Science and Technology Organisation, PMB 1, Menai, New South Wales, 2234, Australia.*

The lanthanide zirconates are of interest for use in inert matrix fuels and nuclear wasteforms. For use in these applications, the material's structure must be resistant to radiation damage and its thermal, thermodynamic and mechanical properties must be known. The structure's ability to incorporate an actinide host into the lattice vacancy must also be known. These properties may be better understood by investigating the *f*-electronic structure, which has historically proved difficult to model.

We have undertaken a synthesis of the full range of lanthanide zirconate series using solid state techniques. We have performed neutron powder diffraction on a selection of the series in conjunction with the following measurements using synchrotron radiation: powder X-ray diffraction, VUV photoluminescence spectra, X-ray photoemission spectroscopy (XPS) and X-ray absorption near edge spectroscopy (XANES). These results will be presented, along with details of the analysis and synthetic techniques used.

Under what experimental conditions are Fluctuation Theorems necessary?

Y.X. Gao, G.M. Wang and E.M. Sevick

Research School of Chemistry, Australian National University, Canberra ACT 0200, Australia.

The recently developed Fluctuation Theorems of Evans & Searles and Crooks make it possible for the first time to determine the free energy difference between equilibrium states by experimentally measuring the work along paths, traversed at arbitrary rates, between the states. This has gained significant attention in the field of single molecule force spectroscopy where, for example one can measure the work required to unravel a single RNA hairpin or to disrupt protein-DNA interactions. Despite these potentially important applications of the theorems, there remains a lack of unambiguous experimental demonstrations – this is one reason for the current debate on the theorems' validity and universality. Here, we demonstrate the range of applicability of the theorems using a colloidal particle fluctuating in an optical trap whose strength is varied. We drive the colloidal particle between two equilibrium states along paths that are (i) quasistatic, (ii) near-equilibrium and (iii) far-from-equilibrium. Our results provide a useful guide to researchers, demonstrating the conditions under which the Fluctuations Theorems are necessary, and the conditions where the simpler classical results are sufficient to determine free energy differences.

The Avogadro Project and it’s role in the redefinition of the kilogram

M.B. Gray, W. Giardini, P. Manson, R.B. Warrington, and M. Wouters

[a] *Physical Metrology Branch, National Measurement Institute, PO Box 264, Lindfield, NSW 2070, Australia.*

The Avogadro project is an international consortium of five national metrology institutes, one of which is Australia. It’s aim is to redefine the SI unit for mass, the kilogram, in terms of the number of Silicon 28 atoms in a near perfect silicon sphere. This would remove the last artifact from the SI system and base the kilogram entirely on fundamental atomic constants.

In this talk I will outline the importance of mass to the entire SI system of units and the issues that have motivated the Avogadro project. I will outline the wide variety of physical measurements necessary to enable the redefinition of the kilogram, the current status of the Avogadro project and the prospects for successful redefinition of the kilogram. I will focus on volume measurements using advanced interferometric techniques and present data from our latest series of measurements. In addition, I will present a candid view of the current issues we face and our plans to address these issues.

Spin-wave Approach to the Spin-1 Heisenberg Anitiferromagnet with Uniaxial Anisotropy in a Field

C. Hamer, O. Rojas and J. Oitmaa[a]

[a] *School of Physics, University of New South Wales, Sydney NSW 2052, Australia.*

Spin-1 magnetic materials with uniaxial anisotropy in a magnetic field at zero temperature may display a number of interesting phenomena, including quadrupolar paramagnetic phases, magnetization plateaus, and a magnetic analogue of "supersolid" behaviour [1,2,3]. We discuss a spin-wave approach to the problem in the 'spin-flop' phase [4]. A proof is given that the Goldstone theorem is observed order-by-order in a 1/S expansion, up to second order, and some numerical results are presented. No indication of the onset of the quadrupolar phase is seen in the formulation to this order.

[1] P. Sengupta and C.D. Batista, *Phys. Rev. Lett.* **98**, 227201 (2007); *J. Appl. Phys.* **103**, 07C709 (2008).

[2] M. Holtschneider and W. Selke, *Eur. Phys. J. B* **62**, 147 (2008).

[3] S.A. Zvyagin et al, *Phys. Rev. Lett.* **98**, 047205 (2007); *Physica B* **403**, 1497 (2008).

[4] M.E. Zhitomirsky and T. Nikuni, *Phys. Rev. B* **57**, 5013 (1998); M.E. Zhitomirsky and A.L. Chernyshev, *Phys. Rev. Lett.* **82**, 4536 (1999).

Adaptive materials

P. Falcaro, C. Doherty, K. Nairn, A. Thornton, S. Pas, C. Elvin and A. Hill

CSIRO Private Bag 33 South Clayton, Victoria 3169, Australia.

Nature's materials are functionally adaptive with structure-property features including molecular recognition, hybrid organic inorganic structures, self organisation, templating, non-equilibrium and equilibrium structures, hierarchical structuring, and functionally gradient materials. We are developing a synthetic design strategy for adaptive materials that takes into account those structure property features utilised by nature.

Our work focuses on the measurement and manipulation of the space in materials with pore dimensions on the atomic and molecular scale. Nature uses such tailored pores to control the selective movement of molecules in and out of cells for the purposes of filtration, catalysis, toxin removal, and to deliver healing agents. Recently we have demonstrated that the design rules from biology can be used in synthetic materials to control and tune the pores [1], giving the materials a degree of autonomous function [2]. We employed approaches from nature - hybrid organic inorganic structures, self organisation, hourglass channels, and pore gating - to design the pore complexes and tune their accessibility to produce synthetic materials that can be incorporated in membranes, coatings, and thin films that can function as filters or delivery platforms.

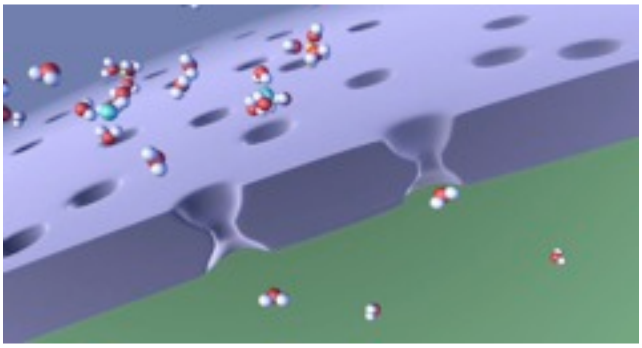

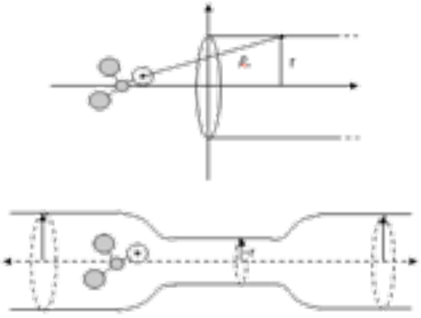

Robert Kerton CSIRO

We are developing synthetic analogues of ion channels and aquaporins to give highly permeable but highly selective membranes [1]. We have developed a new model that allows us to predict the optimum size, shape, and chemistry of the pore for a particular separation [3]. We have coupled our skills in porous materials synthesis with micro- and nano-fabrication methods to make responsive thin films with molecular recognition properties. We are combining bottom-up sol-gel assembly of functional porous materials with micro- and nano-fabrication to offer a simple and fast route to multifunctional integrated platforms, from microfluidics to microarrays, tailoring the chemistry and geometry to the application [4].

[1] H. B. Park, C. H. Jung, Y. M. Lee, A. J. Hill, S. J. Pas, S. T. Mudie, E. Van Wagner, B. D. Freeman, D. J. Cookson, Science, 2007, 318, 254.

[2] A. Bögerhausen, S. J. Pas, A. J. Hill, H. Koller, Chem Mater, 2006, 18, 664.

[3] A. W. Thornton, T. Hilder, A. J. Hill, J. M. Hill, J. Membr. Sci., 2009, 336, 101.

[4] P. Falcaro, L. Malfatti, L. Vaccari, H. Amenitsch, B. Marmioli, G. Grenci, P. Innocenzi, Adv. Mater., 2009 DOI: 10.1002/adma.200901561

Coupling ionic and electronic charge transport in organic semiconductors: A new paradigm for enhanced functionality in molecular electronics

J.M. Hodgkiss[a], G. Tu[b], S. Albert-Seifried[c], W.T.S. Huck[b] and R.H. Friend[c]

[a] *MacDiarmid Institute for Advanced Materials and Nanotechnology, and School of Chemical and Physical Sciences, Victoria University of Wellington, New Zealand.*

[b] *Melville Laboratory for Polymer Synthesis, Dept. of Chemistry, University of Cambridge, U.K.*

[c] *Optoelectronics Group, Dept. of Physics, University of Cambridge, Cambridge, U.K.*

Organic semiconductors such as conjugated polymers make remarkably effective substitutes for their inorganic counterparts in a range of functional devices including light-emitting diodes, solar cells and transistors. The material advantages that conjugated polymers offer (chemically tunable optoelectronic properties and low-temperature, solution-based processing) have received considerably more attention than their functional advantages - including the capacity to employ both electronic and ionic charge carriers in device operation. We use time-resolved optical spectroscopy to demonstrate that in films of conjugated polyelectrolytes, the Coulomb field of ions interacts with electronic excitations to stabilize electronic charge-transfer (CT) states [1]. Our investigation is focused on a conjugated polyelectrolyte derived from F8BT (poly(9,9′-dioctylfluorene-*alt*-benzothiadiazole)). The photoluminescence quantum efficiency (~6%) is considerably lower for the polyelectrolyte compared with F8BT (~60%) in thin films. Time-resolved photoluminescence spectroscopy reveals that the primary exciton lifetime is shortened in the polyelectrolyte and a red-shifted CT emission peak with a longer lifetime emerges. Transient absorption spectroscopy of thin films enables us to detect CT states that persist beyond the primary decay and are found to be immobile. Temperature dependent photoluminescence measurements reveal thermally activated exciton hopping ($E_{\mathrm{act}} = 28$ meV) prior to formation of CT states at ionic regions. We suggest that ionic stabilization of CT states is a general phenomenon in conjugated polyelectrolytes, raising the possibility that ions could direct the flow of excitons towards charge-separating interfaces in polymer solar cells.

[1] J. M. Hodgkiss, G. Tu, S. Albert-Seifried, W. T. S. Huck and R. H. Friend *J. Am. Chem. Soc.* **131**, 8913-8921 (2009).

Pnictides as frustrated three dimensional quantum antiferromagnets close to a quantum phase transition

M. Holt[a], D. Stanek O.P. Sushkov[a] and G.S. Uhrig[a,b]

[a] *School of Physics, University of New South Wales, Sydney 2052, Australia.*

[b] *Lehrstuhl für Theoretische Physik I, Technische Universität Dortmund, Germany.*

Magnetism in the pnictides has been widely discussed in terms of a two dimensional frustrated Heisenberg model, in a similar way to the cuprate parent compounds. Does the quasi-two dimensional frustrated nature of the parent compounds suggest that a two dimensional model captures the essential physics, or is a three dimensional model more appropriate? [1]. Continuing on from previous work [2-3], we present the results of our study of the role of the interlayer coupling on the sublattice magnetization and magnetic excitations using self-consistent spin wave theory on a tetragonal lattice for at . We found that the introduction of suppresses the strong quantum fluctuations and strengthens the long range ordering. Comparing our model with various neutron scattering studies we conclude that the pnictides can be classed as frustrated three dimensional quantum antiferromagnets close to a quantum phase transition.

1. A. Smerald and N. Shannon, arXiv:0909.2207v1 (2009).
2. G. S. Uhrig, M. Holt, J. Oitmaa, O. P. Sushkov and R. R. P. Singh, Phys. Rev. B 79, 092416 (2009).
3. A. Ong, G. S. Uhrig and O. P. Sushkov, Phys. Rev. B 80, 014514 (2009).

Electrically Detected Magnetic Resonance Applied to the Study of Near Surface Electron Donors in Silicon

W.D. Hutchison[a], P.G. Spizzirri[b] and M.S. Brandt[c]

[a] *Centre for Quantum Computer Technology, School of PEMS, The University of New South Wales, ADFA, Canberra, ACT 2600, Australia.*

[b] *Centre for Quantum Computer Technology, School of Physics, The University of Melbourne, Parkville, Victoria 3010, Australia.*

[c] *Walter Schottky Institute, Technical University of Munich, D-85748 Garching, Germany*

Magnetic resonance of donors in semiconductors via electron spin resonance (ESR) is well established. However, the sensitivity of conventional ESR is limited, requiring samples with 10^{10} donors or more. This problem can be overcome by detecting magnetic resonance via the effects of spin selection rules on other observables, such as charge transport.

Electrically detected magnetic resonance (EDMR), is where a change of the dc conductivity due to donor resonance is observed. EDMR was first demonstrated on Si:P by Schmidt and Solomon [1]. More recently, McCamey et. al. [2] showed that EDMR could be used to detect as few as 50 spins in a submicron size silicon device into which the phosphorus donors had been implanted. EDMR is also particular useful in the study of surface defects on semiconductors and their influence on donors placed near to the surface. In this paper we describe the development of robust multimicron EDMR devices in silicon optimal for detailed comparisons of surface preparations as well as variations in donor profiles. Preliminary results using bulk doped substrates with native oxide and thermal oxide, as well as H- and D-terminated surfaces are presented and discussed.

[1] J. Schmidt and I. Solomon, *Compt. Rend. Paris* **263**, 169 (1966) .

[2] D.R. McCamey, H. Huebl, M.S. Brandt, W.D. Hutchison, J.C. McCallum, R.G. Clark and A.R. Hamilton, *Applied Physics Letters* **89,** 182115-1 (2006).

Magnetization and Magnetotransport Study of $SrFeO_x$

A.R. Hyndman, G.V.M. Williams, and J. Stephen

Industrial Research, PO Box 31310, Lower Hutt, New Zealand

The antiferromagnetic compound, $SrFeO_x$ is known to show a rich magnetic and electronic phase diagram. It exists as a homogeneous oxygen ordered compound for x=3 ($SrFeO_3$), x=2.875 ($Sr_8Fe_8O_{23}$), x=2.75 ($Sr_4Fe_4O_{11}$), and x=2.5 ($Sr_2Fe_2O_5$). All other oxygen concentrations of $SrFeO_x$ are believed to be made from inhomogeneous fractions of these four phases [1]. The fully oxygenated compound, $SrFeO_3$ is metallic and the Fe moments have helical antiferromagnetic ordering below ~140K. The $Sr_8Fe_8O_{23}$ (x=2.875) phase displays partial charge ordering and a large magneto-resistance [2], while the $Sr_4Fe_4O_{11}$ (x=2.75) phase is believed to be a G-type antiferromagnetic insulator where one of the Fe moments is geometrically spin-frustrated [2,3].

In this talk we present the results from magnetotransport and magnetization measurements on sintered $SrFeO_x$ samples and well as from $SrFeO_x$ thin films. We show that there is an anomalously large change in the $Sr_8Fe_8O_{23}$ thermopower at the antiferromagnetic ordering temperature [4], which we attribute to partial charge ordering. There is evidence of a spin-glass in the $Sr_4Fe_4O_{11}$ phase that possibly arises from spin-frustration and we find an exchange bias-like effect as well as a colossal magnetoresistance [5].

[1] J. P. Hodges, S. Short, J. D. Jorgensen, X. Xiong, B. Dabrowski, S. M. Mini, and C. W. Kimball, *J. Solid State Chem*. **151**, 190 (2000).
[2] A. Lebon, P. Adler, C. Bernhard, A. V. Boris, A. V. Pimenov, A. Maljuk, C. T. Lin, C. Ulrich, and B. Keimer, *Phys. Rev. Lett.* **92**, 037202 (2004).
[3] R. Vidya, P. Ravindran, H. Fjellvag, and A. Kjekshus, *Phys. Rev. B* **74**, 054422 (2006).
[4] E. K. Hemery, G. V. M. Williams, and H. J. Trodahl, *Phys. Rev. B* **75**, 092403 (2007).
[5] G. V. M. Williams, E. K. Hemery, and D. McCann, P*hys. Rev. B* **79**, 024412 (2009).

Spectroscopic properties of sensitized $LaF_3:Eu^{3+}$ nanoparticles

S. Janssens [a,b], D. Clarke [a], G.V.M. Williams [a] , and A. Edgar[b]

[a]*Industrial Research Limited, 5040 Lower Hutt, New Zealand.*

[b]*School of Chemical and Physical Sciences, Victoria University of Wellington, box 600, Wellington, New Zealand.*

Rare earth doped nanocrystals are promising materials for a wide variety of applications ranging from amplifiers for fiber optic communication [1], upconversion, and bioimaging [2]. LaF_3 is an ideal host for lanthanide ions, because of the low vibrational energies it exhibits. Nanocrystals can be prepared using low temperature chemical methods [3] or through controlled crystallization of glasses [4], which results in a glass-ceramic. Lanthanides typically have a low absorption cross section because of the forbidden character of the 4f transitions. The cross section can be increased by surface functionalizing the nanocrystals with a sensitizing ligand.

In this report we focus on the optical properties of europium doped into low vibrational energy nanoparticles. Organic soluble LaF_3 nanocrystals capped with oleic acid were synthesized according to a modification of a procedure described in the literature [3]. The ability to sensitize these nanocrystals with β−diketonates will be demonstrated. Furthermore, the effect of concentration on the emission spectra and energy transfer from the sensitizing ligand to the dopants will be discussed. We also report the results from measurements on a glass-ceramic containing rare earth doped LaF_3 nanocrystals. The spectroscopic properties of nanocrystals fabricated with the coprecipitation method will be compared with those in the glass-ceramic.

[1] R. Dekker, D.J. Klunder, A. Borreman, M.B.J. Diemeer, K.Wörhoff, A. Driessen, J.W. Stouwdam, F.C.J.M. van Veggel, *Applied Physics Letters* **85**, 25 (2004).

[2] G.-S. Yi and G.-M. Chow, *J.Mater. Chem.* **15**, 4460 (2005).

[3] J. Wang, J. Hu, D. Tang, X. Liu, Z. Zhen, *J.Mater. Chem.* **17**, 1597 (2007).

[4] M.J. Dejneka, *Journal of Non-Crystalline Solids* **239**, 149 (1998).

Fabrication of Fe nanoclusters using ion implantation and electron beam annealing

J. Leveneur [a,c], S. Kupke [a], J. Kennedy [a], G.V.M. Williams [b], A. Markwitz[a] and J. Metson [c]

[a] *National Isotope Centre, GNS Science, 30 Gracefield Road, Lower Hutt, New Zealand*

[b] *The MacDiarmid Institute, Industrial Research, PO Box 31310, Lower Hutt, New Zealand*

[c] *Department of Chemistry, The University of Auckland, Private Bag 92019 , Auckland, New Zealand*

Metallic nanoclusters embedded in an insulator/dielectric matrix show unique properties associated with quantum-size effects, with possible applications such as enhanced magnetic refrigerants, high density magnetic recording media and magnetic resistance devices [1-3]. The aims of the present study are: 1) to develop a protocol to fabricate metallic nanoclusters of specific size and spacing using low-energy ion implantation and subsequent electron beam annealing, 2) to investigate the magnetic behaviour of these nanoclusters, and 3) to optimise the fabrication protocol regarding given magnetic sensor applications.

We have implanted 15 keV $^{56}Fe^{+}$ ions, with fluences from $5x10^{15}$ to $5x10^{16}$ ions cm^{-2}, into a 500 nm thick SiO_2 film on a Si (100) substrate. Dynamic-TRIM predicts the maximum depth of the implantation as 25 nm. The implanted samples were annealed under an electron beam for seconds to hours at 1000 °C. RBS analysis indicates that the implanted Fe atoms reside at the near-surface region for the samples annealed for a few seconds and start to migrate after that time. AFM and TEM images show that 5-10 nm diameter Fe-rich spherical clusters are present in the samples after annealing for 15 s at 1000 °C. The magnetic properties of Fe nanoclusters were investigated using PPMS and SQUID magnetometer. The observed magnetic moments at 5 K per atom were slightly higher than in bulk Fe which is in accordance with the literature [4]. The measurements also revealed different magnetic behavior due to the different protocols. Detailed results regarding the fabrication protocols and the results obtained from the various characterization techniques will be presented.

[1] R.P.Cowburn, *Nature* **448**, 2 (2007)
[2] S. Sun, C.B. Murray, D. Weller, L. Folks and A. Moser, *Science* **287**, 1989 (2006)
[3] G.G. Hadjipanays, *J. Magn. Magn. Mater.* **200**, 273 (1999)
[4] P. Lobotka, J. Dérer and I. Vávra, *Phys. Rev. B* **75**, 024423 (2007)

Ferromagnetic Nanoparticles Formed in Silica by Ion Implantation

A.E. Malik[a] , K. Belay[b], D. Llewellyn[b], W.D. Hutchison[a], K. Nishmura[c] and R.G. Elliman[b]

[a] *School of Physical, Environmental and Mathematical Sciences, The University of NSW, ADFA, Canberra, ACT 2600, Australia.*

[b] *Electronic Materials Engineering Department, Research School of Physics and Engineering, Australian National University, Canberra, ACT 0200, Australia.*

[c] *Graduate School of Science and Engineering, University of Toyama, Toyama, Japan.*

Magnetic nanoparticles, typically composed of Fe, Ni, Co and their alloys or compounds, are of great scientific and technological interest becausetheir properties can differ from those of bulk materials as a direct consequence of their small physical dimensions and/or quantum confinement effects [1]. Such nanoparticles have many potential applications in areas as diverse as biotechnology, magnetic fluids, catalysis, magnetic resonance imaging and data storage. The latter application, which is the focus of the present study, typically requires a high density of small magnetic nanoparticles located in the near-surface region of protective matrix or thin-film.

At Wagga 2009, we outlined preliminary studies of synthesis of Ni and Co nanoparticles, embedded in silica layers, by the combination of ion implantation and post implantation annealing. Here we document refinements of the production techniques, and expand the study to include nanoparticles of Co, Ni, Pt and their respective alloys. Nanoparticle size distributions and structure have been ascertained with transmission electron microscopy. The depth- and size-distributions are found to depend on the particular metallic species, the implant fluence and the anneal conditions. SQUID magnetometry has also been applied to reveal ferromagnetic behaviour in a number of the nanoparticle types. The strength of magnetisation and the coercivity of the various nanoparticles correlate strongly with the particle sizes and metal/alloy types.

[1] L.G. Jacobsohn, M.E. Hawley, D.W. Cooke, M.F. Hundley, J.D. Thompson, R.K. Schulze and M. Nastasi, *Journal of Applied Physics* **96(8),** 4444 (2004).

[2] A. Malik, K. Belay, D. Llwellyn, W.D. Hutchison and R. Elliman, **WP19,** *Proceedings of the 33rd Annual ANZIP Condensed Matter and Materials Meeting, Wagga Wagga 2009.*

Electron beam annealing of (100) Si following dual ion implantation of Pb/N

A. Markwitz, F. Fang and P.B. Johnson

National Isotope Centre, GNS Science, Lower Hutt, New Zealand

Low-energy high-fluence ion implantation combined with an annealing process is a promising method for producing novel precipitates or layers of compounds residing in the near-surface region of the implanted material. Over the past 10 years, our research has shown that electron beam annealing (EBA) in high vacuum can produce novel structures that cannot be produced by any other annealing technique. In this project, (100) Si was dual-implanted with 7 keV Pb^+ and 24 keV $^{14}N^+$ ions to peak concentrations of typically 10 at.%. The implanted samples were annealed at 900 ºC for 30 s with precisely defined temperature gradients under ultra high vacuum EBA.

Channelled RBS measurements performed with 1.5 MeV $^4He^+$ ions showed that annealing of the dual implanted samples resulted in the most unexpected Pb diffusion away from the surface to be trapped in a deep diffusion sink provided by the implanted N. XRD analyses exhibited Pb (111) and Pb (220) reflections suggesting that Pb nanoclusters have grown in the understoichiometric silicon nitride layer. These results offer an interesting opportunity for producing ferroelectric and anti-ferroelectric materials for nanoelectronic and piezoelectric devices.

Advantages of measuring average spin using condensed matter methods

D.J. Miller
Centre for Time, University of Sydney, NSW 2006, Australia and
School of Physics, University of NSW, NSW 2052, Australia.

Traditional forms of quantum measurement have significant limitations. For example, information about the original state of a quantum system is obtained only from the *probabilities* of the measurement outcomes. That is because the measured quantum system and the measuring apparatus are left in states which are independent of their states before the measurement. One way of avoiding the traditional form of measurement is to weaken the interaction between the quantum system and the measuring apparatus [1]. Since the interaction is weaker, one then needs to measure an ensemble of systems or to measure collective effects. Condensed matter systems can involve collective effects and so they provide a means of implementing non-traditional measurements.

The present work investigates two different scenarios. In the first, it is shown that a spin state can be measured via a weak interaction with a large number of other spins. The most significant conclusion is that for this type of weak measurement, the quantum system is left in a state which *does* depend on its initial state. The second scenario that is investigated addresses the problem that, in a traditional measurement, the measurement basis is set by the measurement apparatus. It would be advantageous in some cases, for example in the measurement of entangled states, for the quantum system itself to determine the measurement basis. It is shown that can be realized, at least in principle, in a condensed matter system by taking advantage of the Einstein-de Haas effect. The practicalities of implementing such a scheme using superparamagnetism in small particles is investigated

[1] Y. Aharonov and A. Botero, *Phys. Rev. A* **72**, 052111 (2005).

Temperature Resolved Cathodoluminescence Spectroscopy and Magnetic Properties of Cobalt Doped Titanium Dioxide Thin Films

S.W. Morgan, G.V.M. Williams, A.R. Hyndman and J. Stephen

HTS Conductors & Devices, Industrial Research Limited, Lower Hutt 5040, New Zealand.

Dilute magnetic semiconducting cobalt doped titanium dioxide (Co:TiO_2) has received widespread attention since it was recently discovered to exhibit room temperature ferromagnetism [1, 2]. As a consequence, Co:TiO_2 is an ideal candidate for a multitude of spin transport electronics (spintronics) applications such as optoelectronic devices, spin quantum devices, spin pumping and quantum computing [3].

We present temperature resolved (77 K to 300 K) cathodoluminescence (CL) spectra and magnetic properties of Co:TiO_2 thin films. Highly orientated rutile and anatase films of 70-150 nm thickness were grown on high purity silicon (Si (111)), sapphire (Al_2O_3) and strontium titanate ($SrTiO_3$) substrates using e-beam evaporation and pulsed laser deposition (PLD). SQUID magnetization measurements confirmed that the films produced exhibit ferromagnetic behavior up to room temperature, as previously demonstrated [4]. X-ray diffraction (XRD), CL, magnetization and transport measurements demonstrated that the properties of the films such as crystal structure, defect structure, saturation magnetic moment, and resistivity can be optimized by varying the cobalt concentration, growth conditions, and substrate material.

[1] Y. Matsumoto, M. Murakami, T. Shono, T. Hasegawa, T. Fukumura, M. Kawasaki, P. Ahmet, T. Chikyow, S. Koshihara and H. Koinuma, *Science* **291**, 854 (2001).
[2] J.Y. Kim, J.H. Park, B.G. Park, H.J. Noh, S.J. Oh, J.S. Yang, D.H. Kim, S.D. Bu, T.W. Noh, H.J. Lin, H.H. Hsieh and C.T. Chen, *Phys. Rev. Lett.* **90**, 017401 (2003).
[3] S.A. Wolf, D.D. Awschalom, R.A. Buhrman, J.M. Daughton, S. von Molnar, M.L. Roukes, A.Y. Chtchelkanova and D.M. Treger, *Science* **294**, 1488 (2001).
[4] A.R. Hyndman, G.V.M. Williams, R.J. Reeves and D.M. McCann, *AIP Conference Proceedings* **1151**, 137 (2009).

Zero field NMR and NQR measurements of natural copper minerals

D. Bennett[a], D. Miljak[a], B. Schwitter[a] and J. Khachan[b]

[a] *CSIRO Division of Process Science and Engineering, Lucas Heights 2234, New South Wales Australia.*

[b] *School of Physics, University of Sydney, Australia.*

Zero field nuclear magnetic and nuclear quadrupole resonance are interesting methods for use in on-line instrumentation, as they provide the opportunity to perform bulk mineral characterisation within timeframes useful for process control. Using this technique, CSIRO has developed an instrument to probe the $^{63,\ 65}$Cu nuclei in naturally occurring copper oxide and sulfide minerals. The performance has been demonstrated by measurements on natural mineral concentrate powders, ore fragments and slurries containing chalcopyrite $CuFeS_2$. These measurements have demonstrated accuracies as low as 0.08 wt% and detection limits of 0.2 wt% for acquisition periods of 1000 seconds.

Besides the investigation of the methods as on-line analysis tools, the magnetic resonance response of naturally occurring minerals has also been investigated to develop an understanding of variations observed in the magnetic resonance spectra for different samples. Nuclear magnetic resonance measurements on a suite of chalcopyrite samples show a range of inhomogeneous broadening, asymmetric line shape and shift in transition frequency at room temperature and at 77 K. This behaviour has been analysed with simulations, conductivity, x-ray diffraction and microprobe measurements. Other preliminary measurements on chalcocite Cu_2S and djurleite $Cu_{31}S_{16}$ performed at room temperature and at 77 K respectively have detected magnetic resonance transitions for the first time.

Epitaxial growth and electrical properties of thick SmSi2 layers on (001) silicon.

N.O.V. Plank[a], F. Natali[a], B.M. Ludbrook[a], J. Richter[a], B.J. Ruck[a], H.J. Trodahl[a] and J.V. Kennedy[b]

[a]*The MacDiarmid Institute for Advanced Materials and Nanotechnology, School of Chemical and Physical Sciences, Victoria University, PO Box 600, Wellington 6140, New Zealand.*

[b]*National Isotope Centre, GNS Science, 30 Gracefield Road, P.O. Box 31312, Lower Hutt, New Zealand*

The potential to form silicides, and especially epitaxial silicides, as an element of Si-based integrated circuitry has attracted attention for some decades. Chief among these are the transition-metal and rare-earth silicides (RESi), attractive for their metallic nature and, in the case of the latter, their very low Schottky barrier heights of 0.3-0.4eV (0.7-0.8eV) on n-type (p-type) silicon[1-3]. More recently their propensity to form nanostructures [4,5] and promise for a new generation of interconnects and contacts in very large scale Si-based integrated circuits [6] has sparked renewed interest in significant investigations of RESi films. We will present the growth of thick (up to 1.2μm) epitaxial samarium disilicide ($SmSi_2$) layers on (001) oriented silicon substrate. Evidence from reflection high-energy electron diffraction (RHEED) observations is given that (1) the in-plane lattice parameter agrees well with the bulk tetragonal $SmSi_2$ structure and (2) the epitaxial growth is achieved with a preferential orientation $SmSi_2$[110]//Si[100]. The electrical properties of these films are studied by Hall effect and resistivity measurements at room and low temperature. We observe $SmSi_2$ having metallic type conduction with a room temperature resistivity of 173.9 μΩcm decreasing to 85.11 μΩcm at 4K. Hall measurements have shown n-type carrier concentration of 1.3×10^{22} cm^{-3}. The conduction properties are reproducible for both thin layers at 300nm to very thick layers of 1.2 μm.

[1] J.A. Knapp, and S.T. Picraux, Appl. Phys. Lett. **48**, 466 (1986).
[2] F. Arnaud d’Avitaya, A. Piero, J.C. Oberlin, Y. Campidelli, and J.A. Chroboczek, Appl. Phys. Lett. **54,** 2198 (1989).
[3] J.Y. Duboz, P.A. Badoz, F. Arnaud d'Avitaya, and J.A. Chroboczek, Appl. Phys. Lett. **55**, 84 (1989).
[4] Tao Ding, Junquind Song, and Qun CAI, International Journal of Modern Physics B **21**, 1799 (2007),
[5] C. Preinesberger, S. K. Becker, S. Vandré, T. Kalka, and M. Dähne, J. Appl. Phys. **91**, 1695 (2002).
[6] Meikei IeongVijay Narayanan, Dinkar Singh, Anna Topol, Victor Chan and Zhibin Ren, Materialtoday **9**, 26 (2006).

Nanoscale Modeling of Polymer Glasses – Dynamics of Viscous Kernel

R.M. Puscasu[a], B.D. Todd[a], P.J. Daivis[b], and J.S. Hansen[a]

[a] *Centre for Molecular Simulation, Swinburne University of Technology,*
Melbourne, Victoria 3122, Australia

[b] *School of Applied Sciences, Applied Physics, RMIT University,*
GPO Box 2746V, Melbourne, 3001, Victoria, Australia

Once the confinement of polymers approaches molecular dimensions, classical theory must be generalized to allow for local position dependent coefficients. It has been recently shown that for fields with nonlinear gradients in the strain rate over the width of the real-space kernels nonlocality plays a significant role [1,2]. We extended the analysis of the exact nonlocal viscous kernel [3] for undercooled polymer melts modelled by freely jointed tangent chain and finitely extensible nonlinear elastic models. The analysis is based on molecular dynamics simulations which involve the evaluation of transverse momentum density and stress autocorrelation functions. The results show that the width of the kernel in reciprocal space reduces dramatically near the glass transition, being described by a delta like function near and below the glass transition leading to a slowly decaying function in physical space. Thus the non-locality turns out to play an important role in polymeric systems for temperatures ranging from well above and down to glass transition temperature which confirms our expectations that non-local constitutive relations are required for an adequate description of such systems.

[1] B. D. Todd, J. S. Hansen, and P. J. Daivis, *Phys. Rev. Lett.* **100**, 195901 (2008).
[2] B. D. Todd and J. S. Hansen, *Phys. Rev. E.* **78**, 051202 (2008).
[3] J. S. Hansen, P. J. Daivis, K. P. Travis and B. D. Todd, *Phys. Rev. E.* **76**, 041121 (2007).

New Materials for Optically stimulated Luminescence Dosimetry

S.G. Raymond[1], G.V.M. Williams[1], C. Varoy[2], C. Dotzler [1], and D. Clarke[1]
[1]*Industrial Research, PO Box 31310, Lower Hutt 5040, New Zealand*
[2]*School of Chemical and Physical Sciences, Victoria University, Wellington 6140, New Zealand*

Optically stimulated luminescence (OSL) arises from a recombination of charge that has been moved into meta-stable locations in semiconducting and insulating compounds. These are usually point defects, such as lattice imperfections or impurity ions in the host crystal, in which electrons and holes created by ionizing radiation are trapped. The trapped electrons and holes can be optically excited out of their traps and recombine, which can result in the emission of light. Fluoroperovskites are known to show optically stimulated luminescence (OSL) after exposure to ionizing radiation [1-3], which makes them good candidates for radiation dosimeter applications. We have recently been studying a range of fluoroperovskites and shown that they have potential as OSL dosimeters [4-6].

In this talk, we report the results from optical measurements on rare earth or transition metal ions doped fluoroperovskites (e.g. $RbCdF_3:Mn^{2+}$, $RbMgF_3:Mn^{2+}$, $RbMgF_3:Eu^{2+}$ and $NaMgF_3:Eu^{2+}$) after exposure to ionizing radiation. We discuss the possible point defects that lead to the optically stimulated luminescence and the feasibility of using these materials as radiation dosimeters. We will also discuss the progress towards the development of a fibre optic OSL dosimeter prototype using one of these materials.

[1] M.J.M. Le Masson, A.J.J. Bos, C.W.E. Van Eijk, C. Furetta and J.P. Chaminade, *Radiat. Prot. Dosim*. **100**, 229 (2002).
[2] M. Springis, A. Sharakovsky, I. Tale, and U. Rogulis, *Phys. Status Solidi* **C2**, 511 (2005).
[3] C. Dotzler, G.V.M. Williams, A. Edgar, S. Schweizer, B. Henke, M. Spaeth, A. Bittar, J. Hamlin, and C. Dunford, *J. Appl. Phys*. **100**, 033102 (2006).
[4] C. Dotzler, G.V.M. Williams, and A. Edgar, *Appl. Phys. Lett*. **91**, 181909 (2007).
[5] C. Dotzler, G.V.M. Williams, U. Rieser, and A. Edgar, *Appl. Phys. Lett.* **91**, 121910 (2007).
[6] C. Dotzler, G. Williams, U. Rieser, and J. Robinson, *J. Appl. Phys*. **105**, 023107 (2009).

Momentum-dependent inelastic mean-free-path and high-energy electronic structure of Aluminium

M.N. Read

School of Physics, University of New South Wales, NSW 2052, Australia.

For many spectroscopies that probe the semi-infinite crystal or semi-infinite layered materials, knowledge of the unoccupied bulk (and surface) electronic energy band structure is required. This energy region is complicated by significant variation in the inelastic mean-free-path λ and inelastic lifetime τ of the electron. At higher energies of 40 eV above the Fermi energy E_f, τ [illegible] reached a near constant minimum value and band structures become nearly free-electron-like. At lower energies τ is larger and energy E dependent and where there are more localized bands there is also a momentum $\boldsymbol{k}$ dependence. [1] The modification of calculated bulk bands for the case of no inelastic collisions to the realistic case is complicated for these lower energies.

Aluminium has 3*d* and 4*f* states in this critical range near 23 and 35 eV above E_f. We use a scheme to incorporate a momentum-dependence into τ (as well as an E dependence) to evaluate its importance in the calculation of the bulk band structure for Al. The 2D layer Green function method and transfer matrix method are used to calculate the bulk Bloch states for the unoccupied energy range 0 – 60 eV above E_f. The complex bulk band structure is plotted in the form $E(\boldsymbol{k}_\mathrm{P}, k_\perp)$ which is convenient for surface sensitive spectroscopies and $\boldsymbol{k}_\mathrm{P}, k_\perp$ are the parallel and perpendicular electron momentum components relative to a surface of the semi-infinite solid. For $\boldsymbol{k}_\mathrm{P}$ in the (111) surface plane, bulk bands for $\Gamma \rightarrow \mathrm{L} \rightarrow \mathrm{X}$ are produced. While there are a number of calculations of unoccupied bulk bands for Al in this energy range [2] they do not include any inelastic interactions and are hence not realistic. There are various experimental techniques that could confirm the accuracy of the present calculated band structure in this energy range.

[1] E. V. Chulkov et al, *Chem. Rev.* **106**, 4160 (2006).
[2] M. Levinson, J. L. Benton, and L. C. Kimerling, *Phys. Rev. B* **27**, 6216 (1983).

Properties of EuN thin films

J.H. Richter[1], B.J. Ruck[1], B.M. Ludbrook[1], I.L. Farrel[2], F. Natali[1], N.O.V. Plank[1],
H.J. Trodahl[1]

[1] MacDiarmid Institute for Advanced Materials and Nanotechnology, School of Chemical and Physical Sciences, Victoria University of Wellington, P.O. Box 600, Wellington, New Zealand

[2] The MacDiarmid Institute for Advanced Materials and Nanotechnology, University of Canterbury, Private Bag 4800, Christchurch 8140, New Zealand

The rare earth nitrides are interesting both from a theoretical as well as experimental point of view. They adopt a simple rocksalt structure, yet despite this simplicity the exchange interaction among their 4*f* shells has only recently been realistically described. These recent improvements in theoretical calculations have led to predictions of exotic electronic and magnetic states such as half-metallicity. Among the rare-earth nitrides europium nitride represents an especially interesting case [1,2] with its possible ground state of J=0. Major questions, such as whether it is metallic or semiconducting, about this material remain unanswered as its propensity to show mixed valence (2^+ or 3^+) makes band structure calculations especially difficult [1] and there is a distinct lack of high quality samples for experimental analysis.

Experimentally, EuN is also difficult to study, due to its quick oxidation and film degradation when exposed to atmosphere, particularly water vapours. We have successfully grown thin EuN films on various substrates employing two different methods. In Wellington we use physical vapour deposition of metallic Eu in the presence of a nitrogen gas partial pressure and in Christchurch we use pulsed laser deposition in the presence of a nitrogen plasma. In both cases the EuN films are provided with a capping layer to protect them for ex-situ study. We have characterized the structural, electronic, and magnetic properties of the films using x-ray diffraction, Raman spectroscopy, temperature dependent resistivity, SQUID magnetometry, and synchrotron-based x-ray spectroscopy.

Preliminary measurements show EuN to be ferromagnetic at low temperatures with a T_c of 30K and x-ray absorption shows clear evidence for a 3+ charge state. Temperature dependent conductivity measurements indicate metallic conductivity.

[1] P. Larson, W.R.L. Lambrecht, A. Chantis, and M. van Schilfgaarde, P*hys. Rev. B* **75,** 045114 (2007).

[2] M.D. Johannes and W.E. Pickett, *Phys. Rev. B* **72,** 195116 (2005).

Magnetic Response of Molecular Cage Clusters: $Mn@Sn_{12}$ and $Mn@Sn_{13}$

U. Rohrmann, S. Schäfer and R. Schäfer
Eduard-Zintl-Institut für Anorganische und Physikalische Chemie,
Technical University of Darmstadt, Germany.

To study the intrinsic magnetic properties of nanometer sized particles experimentally, isolated clusters in the gas phase are ideal model systems, as interactions with each other and a substrate are eliminated. In a Stern-Gerlach type experiment a supersonic molecular beam of doped tin clusters is deflected via an inhomogeneous magnetic field. The extend of such a deflection depends on the clusters' magnetic dipole moment and in general an ensemble of magnetic clusters can show two limiting kinds of behavior: either a symmetric broadening of the beam-profile resulting from a spin which is locked to the clusters' structure, or a single-sided deflection in the direction of higher field, resulting from a Langevin-like alignment of the spin in field direction.

The results of two manganese doped clusters-species are reported here, $Mn@Sn_{12}$ and $Mn@Sn_{13}$. Although the composition of the clusters differs only by one tin atom, the response to magnetic fields at low expansion nozzle temperatures is vastly different. $Mn@Sn_{12}$ shows symmetric deflection, indicating a locked-spin in a rigid structure, while $Mn@Sn_{13}$ shows a Langevin-like behavior, possibly due to a fluxional/floppy structure.
At elevated temperatures of the expansion nozzle, the response of $Mn@Sn_{12}$ continuously changes towards a full alignment of the magnetic moment, which confirms the idea that excited vibrational states might serve as a heat bath to the cluster and therefore lead to the Langevin-like behavior.

[1] U. Rohrmann, S. Schäfer and R. Schäfer, *J. Phys. Chem. A* **133**, 12115 (2009).

Efficient Surface Stress Cancelling Algorithms

S. Saengkae[a], M. Binder[b], B.F. Usher[a] and J. Petrolito[c]

[a] *School of Engineering and Mathematical Sciences, La Trobe University, Bundoora, Victoria 3086, Australia.*

[b] *Fachhochschule und Berufskollegs NTA Prof. Dr. Gruebler gGmbH, Seidentrasse 12-35 88316 Isny, Germany.*

[c] *School of Engineering and Mathematical Sciences, La Trobe University, Bendigo, Victoria 3010, Australia.*

Pre-existing threading dislocations experience forces due to the external stress-field during the growth of strained epitaxial layers on crystalline substrates. The threading dislocations themselves give rise to an additional self-stress field with associated forces acting along the length of the dislocation. In principle it is possible to account for the external and self-stresses and model evolution of a threading dislocation's configuration as a strained layer is grown. However, growth takes place at the surface of crystals, at which surface-stress boundary conditions require zero normal and shear stresses. This requires that any non-zero external and self-stresses arising at the surface must be cancelled. Any cancelling procedure will give rise to additional stresses which will modify a dislocation's configuration. The final configuration therefore reflects the summed effect of three sources of stress, the external (misfit) stress field, self-stresses due to the dislocation and stresses at the dislocation due to surface stress cancellation. Together these stresses may cause the creation of highly damaging interfacial misfit dislocations. The surface stress cancellation equations originally developed by Cerruti [1] and Boussinesq [2] can be integrated numerically across the surface in the vicinity of a dislocation's emergent point at the surface, however this approach is very time-consuming. We have investigated the functional form of the stress fields across large surface "tiles" for a variety of dislocation configurations. Based on these observations we have developed "pre-integrated" closed form solutions for parabolic, polynomial and hyperbolic stress field combinations for the orthogonal in-plane surface directions. This achieves orders-of-magnitude improvements in processing times while maintaining the accuracy required in such calculations.

[1] V. Cerruti, *Mem. Fis. Mat.* **45**, (1882).

[2] J. Boussinesq**,** *Application des potentiels à l'étude de l'équilibre et du mouvement des solides élastiques.* (Paris: Gauthier-Villars, 1885) p 45, 108**.**

Temperature Dependent Biquadratic Exchange Coupling in Co/Cu $_{(0.94)}$Mn$_{(0.06)}$ Multilayers

T. Saerbeck$^{(1,2)}$, N. Loh$^{(1,2)}$, M. Ali$^{(3)}$, B.J. Hickey$^{(3)}$, D.Lott$^{(4)}$, B.P. Toperverg$^{(5)}$, A. Mulders$^{(6)}$, A.P. J. Stampfl$^{(1,7)}$, F. Klose$^{(1)}$, R.L. Stamps$^{(2)}$
(1)Bragg Institute, Australian Nuclear science and Technology Organisation, PMB 1, Menai, NSW 2234, Australia
(2)School of Physics, University of Western Australia, Crawley, WA 6009, Australia
(3)School of Physics and Astronomy, University of Leeds, Leeds LS2 9JT, UK (4) GKSS Research Center, Geesthacht, 21502, Germany
(5)Department of Physics, Ruhr-University Bochum, 44780 Bochum
(6)Curtin University of Technology, Perth, WA 6845, Australia
(7)School of Chemistry, The University of Sydney, NSW, 2006, Australia

Magnetic interlayer coupling phenomena in systems consisting of ferromagnetic films separated by non-magnetic spacer layers, such as Co/Cu multilayers, are heavily dependent on the thickness and composition of the spacer layer. Usual Co/Cu multilayers exhibit the normal oscillatory RKKY exchange coupling resulting in alternating ferromagnetic/antiferromagnetic magnetic alignment of adjacent layers with increasing Cu thickness. We report on a crucial temperature dependence of this coupling introduced as the non-magnetic spacer layer is substituted by a spin-glass material, such as CuMn. Kobayashi et al. first discovered the extraordinary behaviour of a ferromagnetic exchange coupled Co/CuMn multilayer structure showing an increasing antiferromagnetic component as the system is cooled below a critical temperature. In order to investigate the magnetic rearrangement throughout the transition temperature in more detail we used polarized neutron reflectometry in specular and off-specular geometry to resolve the orientation of the magnetization in the Co layers. Co/Cu$_{(0.94)}$Mn$_{(0.06)}$ multilayer samples with a manganese concentration of 6at% in the spacer layer are grown using sputter deposition and quality checked with X-ray reflectivity and diffraction. The onset of a magnetic rearrangement into an antiferromagnetic constitution around 100K is confirmed by neutron reflectivity measurements, revealing the onset of biquadratic interlayer coupling. Simulations of the full two dimensional off-specular scattering points out each layer breaking into magnetic domains. Further magnetic characterisation of the sample using X-Ray magnetic circular dichroism and conventional magnetometry indicate the role of the Mn doping in the magnetic transition into a biquadratic coupling.

[1] Y. Kobayashi et al., *Phys. Rev. B* 59, 3734 (1999)

Hysteresis effects in o-$YbMnO_3$?

H.A. Salama[a], G.A. Stewart[a], K. Nishimura[b], W.D. Hutchison[a], D. Scott[c], H.O'Neill[c],
C.J. Voyer[d] and D.H. Ryan[d]
[a]*School of Physical, Environmental & Mathematical Sciences,*
University of New South Wales, ADFA, Canberra, ACT 2600, Australia.
[b]*Graduate School of Science & Engineering, University of Toyama,*
Toyama 930-8555, Japan.
[c]*Research School of Earth Sciences, Australian National University,*
Canberra, ACT 0200, Australia.
[d]*Centre for the Physics of Materials and Physics Department,*
McGill University, QC, H3A 2T8, Canada

The discovery of multiferroicity in orthorhombic phase o-$TbMnO_3$ and o-$DyMnO_3$ [1,2] rekindled researchers' interest in the perovskite $RMnO_3$ (R = rare earth) compounds. We report here on recent Mössbauer investigations of o-$YbMnO_3$ whose Mn sub-lattice orders antiferromagnetically at T_N(Mn) ≈ 40 K. The polycrystalline specimens were prepared by rapid quenching from a prolonged high pressure anneal (3.5 GPa, 1100 °C, 10h) of the hexagonal phase. ^{57}Fe-Mössbauer spectra were recorded for a specimen with 0.5 at. % enriched ^{57}Fe doped into the Mn sub-lattice and, as expected, a magnetically split sextet was observed below T_N(Mn). However, the paramagnetic doublet persisted as a second spectral component down to about 30 K and a curious magnetic hysteresis effect was observed at 36 K. Some time after these measurements, hysteresis effects were reported by Tachibana *et al.* [3] for their specific heat data and they attributed these to an incommensurate magnetic structure which locks into a commensurate *E-type* linear structure at the lower temperature of T_C ≈ 35 K. Similar specific heat data have since been recorded by us for undoped specimen material that was prepared for ^{170}Yb-Mössbauer measurements. Encouraged by the agreement of the specific heat results, we recently revisited the ^{57}Fe-Mössbauer measurements and recorded new spectra with improved statistics for the identical Mössbauer specimen, only to find that the magnetic hysteresis effect was no longer evident. These puzzling data and the ^{170}Yb-Mössbauer results will be presented and discussed.

[1] T. Kimura *et al.*, *Nature (London)* **426**, 55 (2003).
[2] T. Goto *et al.*, *Phys. Rev. Lett.* 92, 257201 (2004).
[3] M. Tachibana *et al.*, *Phys. Rev. B* **75**, 144425 (2007).

Defect Perovskites in the $Sr_{1-x}M_{1-2x}Nb_{2x}O_3$ (M = Ti, Zr) Family

W. R. Brant and S. Schmid

School of Chemistry, The University of Sydney, NSW 2006, Australia.

The development of new high capacity cathodes for Li ion batteries is becoming increasingly important as currently used materials reach their critical limit in terms of energy density. Defect perovskite structures such as $Li_{3x}La_{2/3-x}TiO_3$ have been shown to exhibit excellent lithium ion conductivities and structural stability leading to potential for additional perovskite structures to be developed as new cathode materials.

.

The $Sr_{1-x}NbO_3$, $0 \leq x \leq 0.3$, solid solution, with niobium in both oxidation states +IV and +V for $x > 0$, has been reported to adopt the ideal cubic perovskite structure across the whole solid solution field [1]. An investigation of the SrO-ZrO_2-Nb_2O_5 system was performed to see whether an analogous solid solution can be formed. X-ray and neutron powder diffraction patterns showed that while there was an underlying pseudo cubic perovskite sub-structure the symmetry for all investigated compositions was lowered to tetragonal or orthorhombic.

High resolution X-ray powder diffraction data have been collected recently on the powder diffraction beamline at the Australian Synchrotron for the analogous $Sr_{1-x}Ti_{1-x/2}Nb_{x/2}O_3$, $0 < x < 0.2$, solid solution. While it has a somewhat smaller composition range it stays cubic over that range and over the temperature range from 4.2 to 1273 K.

Selected members of both families underwent chemical and electrochemical lithium intercalation to investigate the amount of lithium that can be intercalated as well as the possible effects on the structure, including whether lithium is ordered or disordered on intercalation. The results of structural refinements using the JANA2006 [2] refinement package will be presented.

[1] Hessen B., Sunshine S.A., Siegrist T., Jimenez R. (1991). *Mat. Res. Bull.* 26, 85.

[2] Petricek, V., Dusek, M. & Palatinus, L. (2006). Jana2006. The crystallographic computing system. Institute of Physics, Praha, Czech Republic.

Surface Fracture in Diamond Adjusting of a Leucite-Reinforced Glass Ceramic Using a Clinical Dental Handpiece

X.-F. Song[a] and L. Yin[b]

[a] *School of Mechanical Engineering, Tianjin University, Tianjin 300072, China.*

[b] *School of Engineering & Physical Sciences, James Cook University, Townsville QLD 4811, Australia.*

Ceramic materials have been developed for dental restorations because of their outstanding esthetics and biocompatibility. Tooth colored ceramic restorations are applied for replacement of missing tooth structures to achieve an esthetic appearance. However, the possible applications for dental all-ceramic restorations are limited by the nature of ceramics. They are very brittle and weak under tensile stresses [1]. In dental restorations, these ceramic crowns are often intraorally adjusted by dentists using high-speed dental handpieces and diamond burs. In this process, the brittle nature of these materials results in fracture features on the adjusted surfaces. Leucite-reinforced glass ceramics have good stability and aesthetic properties. The bulk materials can be accurately milled and ground using dental CAD/CAM systems as a result of the small, uniform size of the leucite crystallites. We report on surface fracture occurring in a leucite-reinforced glass ceramic adjusted with a clinical dental hardpiece and coarse-grit diamond burs. We have found that brittle fracture is the dominant adjusting mechanism for the leucite-reinforced glass ceramic. Brittle fracture is attributed to the indentation and high-frequency impact of diamond abrasives in the ceramic material. Plastic deformation was also observed in the adjusted surface. There is a tendency for brittle-ductile transition when the depth of cut and feed rate decreased. Phase transformation of leucite crystals might have occurred in the adjusting process, which will be further examined using x-ray diffraction.

[1] Fisher H and Marx R 2001 *J. Dent. Res.* **80** 336.

Evidence of Ionic Effect ("Chemical Pressure") in $Bi_2Sr_{1.6}Ln_{0.4}CuO_{6+\delta}$ (Ln = Ba, La, Eu, Gd, Y) studied by Susceptibility and Raman Measurements

T. Schnyder[1,2], G. Williams[2] and J. Tallon[2]
[1]*Swiss Federal Institute of Technology (EPFL), Lausanne, Switzerland*
[2]*Industrial Research Ltd, P.O. Box 31310, Lower Hutt, New Zealand.*

Recently there has been much discussion on the $Bi_2Sr_{1.6}Ln_{0.4}CuO_{6+\delta}$ system where Ln=La, Nd, Sm, Eu, Gd, Dy... are lanthanide rare earths. T_c decreases quickly as the size of the lanthanide rare earth decreases. Most people argue in favor of an "out-of-plane disorder" (disorder in the layers outside the copper oxide planes) to explain the suppression of T_c in this system, for a fixed doping state. In this view the scattering from disorder breaks Cooper pairs. We are convinced that the change in T_c is more due to "chemical pressure"; the copper oxide bond length is decreased by reducing the size of the lanthanide rare earth Ln ions, which increases the effective pressure. Consequently, the orbital overlap is increased and therefore the exchange energy, J, also increases. This affects the magnetic correlations that compete with superconductivity

Firstly, this view was investigated by two-magnon Raman and micro-Raman scattering measurements on $Bi_2Sr_{1.6}Ln_{0.4}CuO_{6+\delta}$ samples with similar hole concentrations. This allows the shift in J (related to the two-magnon peak near 3000 cm^{-1}) and other interesting Raman shifts at lower frequencies (due to phonon modes) to be obtained as the ionic size of the Ln ions is reduced. The results are correlated with data from magnetization and specific heat measurements.

Secondly, we investigated the inverse effect of barium doping on the strontium site in $Bi_2Sr_{1.6}La_{0.4}CuO_{6+\delta}$ where the substitutions stretch the Cu-O bond-length. Thermo-electric power and magnetization measurements on $Bi_2Sr_{1.6-x}Ba_xLa_{0.4}CuO_{6+\delta}$ samples (where x = 0, 0.2, 0.4) enabled us to estimate the hole concentration and hence how T_c changes with increasing hole concentration. This in turn enabled us to estimate the maximum T_c, T_c^{max}, which should decrease in the disorder model or increase in the chemical pressure model with increasing barium concentration.

A piston-rotaxane as a molecular shock absorber[1]

E.M. Sevick and D.R.M. Williams

Research School of Chemistry & Research School of Physical Sciences & Engineering, The Australian National University, Canberra 0200,

Rotaxanes are molecules architecturally similar to some baby rattles: one or more ring-like molecules threaded onto a molecular axle which is capped on both ends with large stoppers to prevent the rings from sliding off. These molecules were first synthesized over 40 years ago and they are now routinely synthesized in large quantities. Rotaxanes also occur naturally as the structure has been recognised in some proteins. They can be small molecules or, using longer axles, larger polyrotaxanes - and there is an endless zoo of possible architectures.

Rotaxane molecules also lend themselves to exact analysis by equilibrium statistical mechanics. Previous descriptions have focussed predominantly upon “slip-link" behaviour, where the axle slips through a single threaded ring or link. However, here we study a rotaxane system which is intrinsically different to these slip-link systems.

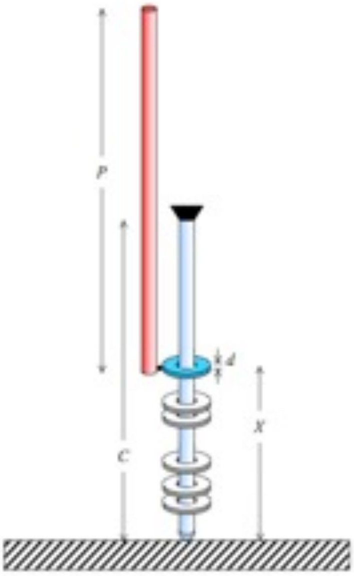

In our system there are numerous free rings whose translational entropy dominates the rotaxanes' behavior; we couple an external piston to one of the rings of a rotaxane molecule, Fig 1, and exploit the gas-like entropy of the other rings to determine the piston's elastic response. We refer to this molecular system, where the piston can compress the axle-bound rings, as a piston-rotaxane. It behaves as a molecular version of an automobile shock absorber and using statistical mechanics, we calculate the thermo-mechanical response of this system exactly. The resulting force laws are contrasted with those for a rigid rod and a polymer. In some cases the rotaxanes undergo a sudden transition to a tilted state when compressed. These piston-rotaxanes provide a potential motif for the design of new class of materials with novel thermo-mechanical response.

[1] E.M. Sevick & D.R.M. Williams, submitted to *Langmuir* Oct.2009.

Solid State Coulometric Investigations in the System Ir/Sn/O - Determination of the thermodynamical data of $Ir_{10}Sn_{45}O_{44}$, $IrSn_4O_{4-x}$, $Ir_3Sn_8O_4$, Ir_5Sn_7 and $IrSn_2$

T. Söhnel[a], W. Reichelt[b] and K.Teske[b]

[a] *Department of Chemistry, The University of Auckland, Auckland 1142, New Zealand.*

[b] *Institute of Inorganic Chemistry, Technical University Dresden, Germany.*

Based on systematic investigations in the ternary system Ir/Sn/O the phase relations in a temperature range between 973 K and 1173 K could be solved. It turns out that three ternary phases exist in this system: $Ir_{10}Sn_{45}O_{44}$, $IrSn_4O_{4-x}$, $Ir_3Sn_8O_4$. The determine the thermal stability of the intermetallic phases the phase diagram had to be investigated as well. The stable phases in this temperature range are Ir_5Sn_7 and $IrSn_2$.

Solid state coulometry is a dynamical technique which can be used to measure the oxygen partial pressure of a solid phase - gas phase equilibrium (OXYLYT-System [1]). It is possible to investigate the description of the decomposition equilibria in an oxid system with the measurement of the oxygen partial pressure in dependence of the temperature. In this temperature range the free reaction enthalpy, reaction entropy and enthalpy can be examined from the measured oxygen partial pressures. By choosing the appropriate decomposition equilibria the unknown thermodynamical data of one equilibrium phase can be obtained.

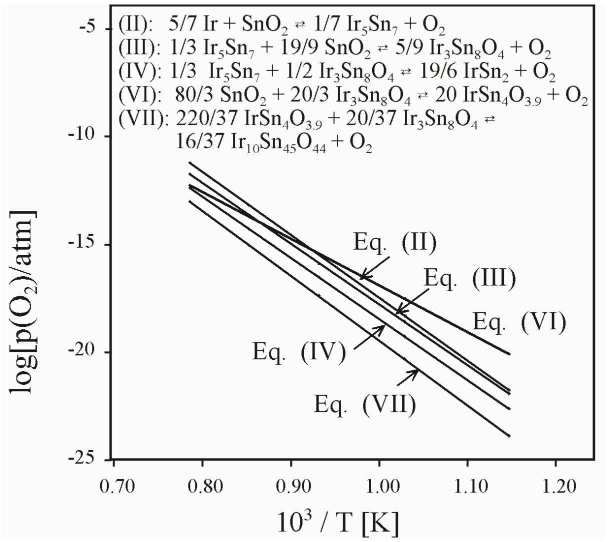

The pO_2 of five different coexistence areas have been measured (Fig. 1). The calculation of the thermodynamical data has been done in order of the equations (II) to (VII) by using the Hess' law. To ensure that the data obtained are consistent with the experimental phase relations, a testing of the compatibility has been done.

[1] K. Teske, H. Ullmann, N. Trofimenko, *J. Therm. Anal.* **49**, 1211 (1997).

Nano-composites with physical crosslinks introduced by core cross-linked star polymers into a like-polymer

S. Spoljaric[a], T. Köpplmayr[b], A. Genovese[a], T.K. Goh[c], A. Blencowe[c], G.G. Qiao[c]
and R.A. Shanks[a]

[a] *CRC for Polymers, RMIT University, GPO Box 2476V, Victoria 3001, Australia.*

[b] *Montanuniversität Leoben, Franz-Josef-Strasse 18, 8700 Leoben, Austria.*

[c] *Polymer Science Group, Chemical & Biomolecular Engineering, University of Melbourne, Victoria 3010, Australia.*

Core cross-linked star (CCS) polymers prepared from a glycol acrylate core with polystyrene (PS) or poly(methyl methacrylate) (PMMA) branches were added as filler to linear PS or PMMA, respectively. The matrix PS is a good solvent for the PS star branches so they will be mutually interspersed, while the cross-linked cores will constrain movement of the PS branches. The PMMA system will function the same. In contrast with a typical filled system, some of the PS, the star branches, will be bonded to the nano-scale cores. The cores restrain the polymer branches, they will not contribute to modulus and strength as do mineral fillers.

The materials were analysed using modulated temperature–thermomechanometry [1] (mT-TM) to examine the influence of hyperbranching on the structure, morphology and relaxation properties. mT-TM is a novel technique that involves application of an oscillating heating rate over a conventional heating program. The dimension changes are resolved into a reversing change that is in-phase with the temperature modulation, and non-reversing change (out-of-phase). This allows phenomena such as thermal relaxations, structural relaxation and morphological changes to be interpreted. This is useful for characterisation of materials utilised in fields such as packaging, drug delivery and electrical applications. The glass transition temperature (T_g) and coefficient of linear thermal expansion (CTE) were determined. Annealing was performed before the onset of T_g at logarithmically spaced intervals (1, 10, 100 h) to observe the contribution of physical ageing to structural relaxation.

Addition of CCS polymers caused an increase in T_g attributed to restrictions that these macromolecules impart on segmental motions within the linear matrix. This suggests that CCS polymers behave as physical crosslinks. CTE was shown to decrease with CCS content, due to the restraints hyperbranched molecules placed on vibrational modes underlying the expansion ability of a linear matrix. Annealing before the onset of T_g increased both the T_g and CTE, with materials annealed for 100 h yielding the highest T_g. Increased T_g is attributed to reduction in free volume and mobility within the nanocomposite during structural relaxation processes.

[1] D. Price, *J. Therm. Anal.* **51**, 231 (1998).

Long term structural integrity of high density polyethylene blends investigated by static force thermomechanometry

S. Spoljaric[a], A. Genovese[a], T. Köpplmayr[b] and R.A. Shanks[a]
[a] *CRC for Polymers, RMIT University, GPO Box 2476V, Victoria 3001, Australia.*
[b] *Montanuniversität Leoben, Franz-Josef-Strasse 18, 8700 Leoben, Austria.*

Polymer materials will undergo a progressive deformation at a constant stress, referred to as creep. The creep behaviour of polymers will control the suitability as a structural material and therefore is important to elucidate long-term performance under similar conditions to which would be its service life. To determine the creep performance, a specimen is maintained at a constant temperature and stress while the strain is monitored as a function of time. On application of a specific stress, an instantaneous purely elastic response occurs. Deformation then continues involving a viscoelastic response. At longer time, a steady state of linear deformation prevails indicating viscous flow. On extended time, the flow will continue until a specimen will undergo a rapid accelerated deformation and result in fracture. A typical creep response is shown in Figure 1. At 40 ºC the polymer exhibited the anticipated deformations and viscous creep, however, at elevated temperature molecular motions are thermally activated and creep occurs rapidly before rupture.

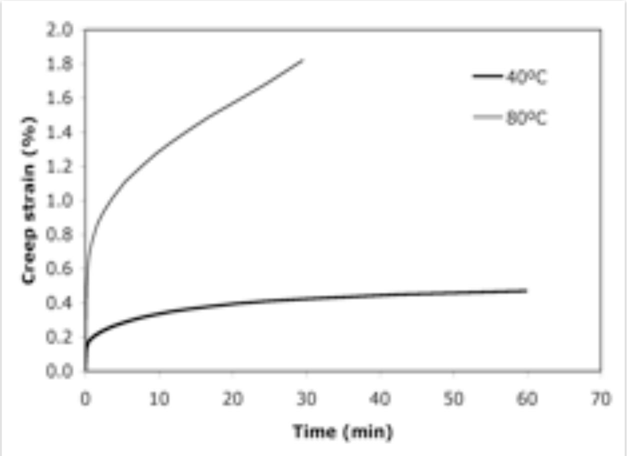

Figure 1: Representative creep strain response of HDPE-EVA blend at 40 and 80 ºC.

A series of HDPE-EVA blends will be investigated using time-temperature superposition to compare strain response and thermomechanical stability.

Magnetic and electronic study of the colossal magnetoresistance compound, Sr_2FeMoO_6

J. Stephen[a,b], G.V.M. Williams[a] and B. Ruck[b]

[a]*Industrial Research, P.O. Box 31310, Lower Hutt, New Zealand.*

[b]*The MacDiarmid Institute, Victoria University of Wellington, P.O. Box 600, Wellington, New Zealand.*

The discovery of high magnetoresistance in Sr_2FeMoO_6 has led to renewed interest in these materials. They exhibit close to 100% electronic spin polarisation at low temperatures and they are believed to have a high degree of electronic spin polarisation for temperatures up to room temperature. This makes them potential candidates for spintronics applications [1]. Even polycrystalline samples have been found to display a colossal magnetoresistance that can be attributed to intergrain tunnelling [2,3,4].

In this talk we report the results from magnetoresistance, magnetothermopower, Hall and magnetisation measurements on polycrystalline Sr_2FeMoO_6 samples at a range of temperatures and for magnetic fields of up to 8 T. We also report the results from similar measurements made on lanthanum doped Sr_2FeMoO_6 to investigate the effect of electron doping. The ordinary and anomalous Hall coefficients are found to be negative and positive respectively for pure as well as La doped Sr_2FeMoO_6. We also observe magnetothermopower for temperatures below the Curie temperature. The magnetothermopower can possibly be explained in terms of effects that include magnon drag and a reduction in carrier scattering length.

[1] K.-I. Kobayashi, T. Kimura, H. Sawada, K. Terakura, and Y. Tokura, *Nature* **395**, 677 (1998).
[2] D. Serrate, J.M. De Teresa, P.A. Algarabel, M.R. Ibarra, and J. Galibert, *Phys. Rev. B* **71**, 104409 (2005).
[3] E. K. Hemery, G. V. M. Williams, and H. J. Trodahl, *Physica B* **390**, 175 (2007).
[4] E. K. Hemery, G. V. M. Williams, and H. J. Trodahl, *J. Magn. Magn. Mater.* **310**, 1958 (2007).

Carbide Composition and Stress Measurement in Ethylene Pyrolysis Tubes

K.J. Stevens[a,b], B. Ingham[b,c], M. Ryan[c], J.A. Kimpton[d], K.S. Wallwork[d], V. Luzin[e]
and K. Cheong[f].
[a]*Quest Reliability Ltd, P.O. Box 38-096, Lower Hutt, New Zealand*
[b]*The MacDiarmid Institute for Advanced Materials and Nanotechnology,*
P.O. Box 600, Wellington, New Zealand
[c]*Industrial Research Ltd, P.O. Box 31-310, Lower Hutt, New Zealand*
[d]*Australian Synchrotron, 800 Blackburn Rd, Clayton, VIC 3168*
[e]*Bragg Institute, Australian Nuclear Science and Technology Organisation, Private Bag 1,*
Menai, NSW 2234.
[f]*British Energy Generation Ltd, Barnett Way, Gloucester, GL4 3RS, United Kingdom.*

Ethylene is important in the production of polyethylene, used in thin film packaging, piping and cable sheathing. It is produced by steam cracking of naptha, LPG or ethane at temperatures around 950°C at high flow velocities. Carburisation of ethylene pyrolysis tubes (typically of nominal composition 31%Fe, 37%Ni and 25%Cr) causes a loss in weldability, corrosion resistance and ductility, and provides a source of micro-cracking. Plant operators prefer to replace tubes at planned outages and are interested in remaining life assessments assisted by description and modelling of the progress of carburisation. The powder diffraction beamline at the Australian Synchrotron has been used to radially scan mounted and polished tube sections prepared from ex-service carburised tubes. Radial dependence of carbide phases in the tubes is being quantified using Bruker TOPAS software for whole pattern line fitting. Composition analysis and microscopy is being used to create a representative microstructure in Abaqus Finite Element Analysis (FEA) models and to interpret non-destructive eddy current measurements [1] of carburisation. The austenite diffracting planes give a peak shift response to stress that is anisotropic and is being interpreted with FEA based crystal plasticity models. Neutron diffraction at the Kowari beamline at OPAL (Open Pool Australian Lightwater reactor) was used to measure strain in unsectioned tubes at room temperature. This was compared to FEA models of the strain created by differential thermal expansion between carbide phases and austenite, assuming creep relaxation at normal tube operating temperature.

[1] K.J. Stevens and W.J. Trompetter, *J. Phys. D:Applied Physics* **37** 501 (2004).

The Crystal Field Schemes for Er^{3+} in $ErCr_2Si_2$ and $ErMn_2Si_2$

B. Saensunon[a], G. Stewart[a], P.C.M. Gubbens[b], M. Russina[c] and E. Kemner[c]
[a]*School of Physical, Environmental & Mathematical Sciences,*
University of New South Wales, ADFA, Canberra, ACT 2600, Australia.
[b]*Fundamental Aspects of Materials & Energy, Faculty of Applied Sciences,*
Delft University of Technology, Mekelweg 15, 2629 JB Delft, The Netherlands
[c]*Berlin Neutron Scatteringe Center, Helmholtz-Zentrum-Berlin,*
Glienicker Strasse 100 D-14109 Berlin Germany.

We present here inelastic neutron scattering spectra that were recorded at the Berlin Neutron Scattering Centre (BENSC) for both $ErMn_2Si_2$ and $ErCr_2Si_2$. These compounds distinguish themselves from the remainder of the RT_2Si_2 series (R = rare earth, T = Cu, Ni, Co and Fe) in that their T sub-lattices order at Néel temperatures of $T_N \approx 500$ K and 700 K, respectively, but their R sub-lattices still order close to liquid helium temperature [1, 2]. The suppression of the R magnetic order is partly linked to the fact that the R and T sub-lattices reside in separate layers with only a weak exchange interaction between them. However, it has also been proposed that the CF interaction at the R-site favours low-lying ground states that frustrate the R-R exchange process.

As an initial stage of the CF characterisation, the lowest temperature (11 K) INS spectra for both intermetallics have been fitted with pseudo-voigt line shapes where $\Gamma_{FWHM} = 2.2$ meV for $ErCr_2Si_2$. The larger value of $\Gamma_{FWHM} = 2.8$ meV required for $ErMn_2Si_2$ is consistent with the superposition of transition peaks starting from the lowest two CF levels with an energy separation of just 2.5 meV. Based on these observations, tentative CF schemes are proposed for the Er^{3+} sites in the two compounds and the schemes are compared with data recorded using other techniques such as specific heat, magnetic susceptibility and ^{169}Tm-Mössbauer spectroscopy.

[1] O. Moze *et al.*, *Eur. Phys. J. B* **36**, 511 (2003).
[2] M. Hofmann *et al.*, *J. Magn. Magn. Mater.* **176**, 279 (1997).

Parametric Rietveld refinement applied to *in-situ* diffraction studies

M.J. Styles[a], D.P. Riley[a] and I.C. Madsen[b]

[a] *Mechanical Engineering, University of Melbourne, Victoria 3010, Australia.*

[b] *CSIRO Minerals, Clayton, Victoria 3168, Australia.*

In-situ diffraction studies in which data is collected as a function of a particular external variable (for example time or temperature), are often conducted with the aim of developing models to predict the response of materials to certain operational or processing conditions. The traditional approach to analysing powder diffraction data collected in this manner is to refine a model of each pattern independently using the Rietveld method [1] and progress through the data sets sequentially. Obtaining accurate results via this method can be problematic, particularly in instances where the nature of the material system is such that data must be collected under less than ideal circumstances [2].

An alternative approach is to take advantage of known relationships between parameters to describe their evolution over the entire collection of diffraction data [3]. The total number of independent parameters is hence reduced, enabling a large number of data sets to be analysed simultaneously and models of material behaviour to be refined directly. This approach has recently been used to extract accurate measurements of sample temperature from neutron and synchrotron powder diffraction data of reacting carbide and oxide systems, and to stabilise the analysis of phase composition as a function of time for the purposes of kinetic modelling.

[1] H.M. Rietveld, *J. Appl. Cryst.* **2**, 65 (1969).
[2] D.P. Riley et al, *J. Am. Ceram. Soc.* **85**, 2417 (2002).
[3] G.W. Stinton and J.S.O. Evans, *J. Appl. Cryst.* **40**, 87 (2007).

In-field performance and microstructure of metal-organic deposited YBCO films doped with $BaZrO_3$

E.F. Talantsev[a], N.M. Strickland[a], J.A. Xia[a], N.J. Long[a], M.W. Rupich[b], X. Li[b] and
S. Sathyamurthy[b]

[a] *Industrial Research Limited, P.O. Box 31-310, Lower Hutt, 5040, New Zealand.*

[b] *American Superconductor Corporation, 64 Jackson Road, Devens, MA 01434, U.S.A.*

Second-generation high-temperature superconducting wires consist of a highly textured film of $YBa_2Cu_3O_7$ (YBCO) grown epitaxially on a flexible metal substrate. Essential to the in-field current-carrying performance of the films is the inclusion of a high density of nanoscale flux pinning centers. Critical current densities in these films can exceed 3 MA/cm^2 at 77K.

In the present work we continue our previous investigations into creating a high density of $BaZrO_3$ nanoparticles [1], while maintaining a high superconducting transition temperature and percolation path. This results in significant enhancements to the critical current densities in moderate to high magnetic fields. We have found that in growth by metal-organic deposition, $BaZrO_3$ forms 15-30 nm sized randomly oriented nanoparticles, rather than the extended correlated columnar structures observed in vapour deposition methods. This gives an isotropic contribution to flux pinning, and also delays the suppression in T_c. The microstructure and phase composition of YBCO+15at.%Zr films were studied with X-ray diffraction and transmission electron microscopy. The distribution of $BaZrO_3$ nanoparticle size and density are given. The pinning force and in-field critical currents are presented.

[1] N.M. Strickland, N.J. Long, E.F. Talantsev, P. Hoefakker, J. Xia, M.W. Rupich, T. Kodenkandath, W. Zhang, X. Li and Y. Huang, *Physica C* **468** 183 (2008).

^{100}Pd/Rh gamma-ray perturbed angular correlations in GaN and ZnO – Are these semiconductors suitable for spintronics?

P. Kessler[a], Th. Geruschke[a], H. Timmers[b], A.P. Byrne[c], R. Vianden[a]

[a] *Helmholtz - Institut für Strahlen- und Kernphysik der Universität Bonn, Germany*

[b] *School of Physical, Environmental and Mathematical Sciences, University of New South Wales at the Australian Defence Force Academy, Canberra,*

[c] *Department of Nuclear Physics and Department of Quantum Science, Research School of Physics and Engineering, Australian National University, Canberra,*

Theoretical work predicts that the GaN and ZnO binary semiconductors, with appropriate doping, may show dilute magnetism with Curie temperatures above room temperature [1]. This would make them suitable for spintronics applications. In particular, doping with Co, Mn or Fe transition metals has been suggested to introduce the dilute magnetism. However, no evidence of ferromagnetic order in these semiconductors caused by isolated transition metal impurities has yet been found. Since the perturbed angular correlation (PAC) probe ^{100}Pd/^{100}Rh is isoelectronic to Co, it is well suited to investigate the incorporation of transition metals into these compounds. Specifically, such measurements may shed light on the question if the Pd atoms are incorporated on lattices site and to what extend this may occur. Substitutional integration in the lattice is essential for spintronics, since otherwise the clustering of dopant atoms is likely.

Experiments have been carried out at the 14UD Pelletron accelerator of the Australian National University where ^{100}Pd was recoil-implanted into GaN, ZnO and reference samples, following the fusion evaporation reaction ^{92}Zr(^{12}C, 4n)^{100}Pd. The recovery of lattice damage due to the recoil-implantation was studied in an isochronal annealing programme, with annealing times of 10 min. Unlike for other PAC probes, namely ^{111}In, ^{181}Hf, ^{77}Br, and ^{117}Cd, a recovery of implantation-induced damage, i.e. a significant presence of the ^{100}Pd/Rh probe on lattice sites in GaN and ZnO, has not been observed. This suggests that Pd-doping of GaN or ZnO, even at the extremely diluted concentrations studied here, results most likely in Pd-clustering in the material. Iso-electronic atoms such as Co may behave similarly.

[1] T. Dietl, *Science*, **287** 1019 (2000).
[2] R. Dogra, A.P. Byrne, and M.C. Ridgway, *Optical Materials* **31** 1443 (2009).

Micro-scratching of UHMW polyethylene surfaces

Y. Liu[a], L.G. Gladkis[a], H. Timmers[a]

[a] *School of Physical, Environmental and Mathematical Sciences, University of New South Wales at the Australian Defence Force Academy, Canberra*

Polymers, such as polyethylene, are used for a variety of macroscopic applications in areas as diverse as food packaging, aerospace and automotive manufacturing, and biomedical engineering. More recently polymers have been applied extensively as one of the preferred materials towards the miniaturization of functionality in the form of micro-, and even nano-scale machines and devices. The tribological performance of polymers under such circumstances, where loads are small and where surface properties tend to be more important than bulk properties, is expected to be significantly different than in macroscopic applications [1]. Nevertheless, it has been suggested that the amount of wear debris generated by a small number (< 20) of micro-scratches correlates linearly with the macroscopic abrasive wear performance, as it may, for example, be measured in conventional pin-on-disk wear tests [2]. For some polymers, such as epoxy, where a single micro-scratch produces many debris particles, the existence of such a linear relationship is more readily acceptable than for others, such as ultra-high molecular weight polyethylene (UHMWPE). UHMWPE, because of its ductility, can be micro-scratched without any debris being generated, while macroscopic abrasive wear rates are comparatively low, however, still considerable. For example, the significant amount of UHMWPE wear particles produced in total knee- or hip-replacements is the limiting factor in the clinical performance of such prostheses. In the scratching of UHMWPE a threshold must thus exist beyond which UHMWPE shows abrasive wear. This threshold may be defined by the applied load, the dimensions or material properties of the micro-asperity, the frequency or the repetition of the actuation, the direction of scratching, the temperature of the polymer or a combination of those parameters.

Taking advantage of the fact, that silicon fractures along crystal planes with nano-scale definition, silicon micro-asperities have been made and characterized with electron microscopy. The micro-scratching of UHMWPE by these asperities is being studied in an effort to understand how debris production depends on actuation parameters. Individual micro-scratch grooves and abrasive debris generated by the scratch have been characterized and quantified using scanning electron and scanning probe microscopy. The three-dimensional spatial sensitivity of scanning probe microscopy allows for detailed volumetric measurements of scratch grooves and of debris particles previously not achieved with electron microscopy. Progress is reported and an outlook given on future work.

[1] J.S.S. Wong, H.-J. Sue, K.-Y. Zeng, R.K.Y. Li, Y.-W. Mai, *Acta Materialia* **52** 431 (2004).

[2] S.K. Sinha, W.L.M. Chong, S.-C. Lim, *Wear* **262** 1038 (2007).

Optical purification via sublimation – DFT results on lactic acid derivatives

R. Tonner[a], V.A. Soloshonok[b] and P. Schwerdtfeger[a]

[a] *Center for Theoretical Chemistry and Physics, Massey University Auckland, New Zealand*

[b] *Department of Chemistry and Biochemistry, University of Oklahoma, Norman, Oklahoma*

The purification of racemic mixtures of organic compounds is a formidable task for preparational chemistry due to the identical physical properties of enantiomers. One possible solution to this problem is the transfer of enantiopure and racemic compounds into the solid state. One can thereby take advantage of different crystallographic structures which enables the usage of established purification procedures in the lab. In a recent publication,[1] Soloshonok et al. described the separation of (*S*)-α-(trifluoromethyl)-lactic acid from the respective racemic crystal via sublimation, reaching an enantiopure (ee > 99.9 %) product. The authors suggested density differences and molecular arrangements to be responsible for the different sublimation rates (*k*(racemate) / *k*(enantiopure) ~ 1.5) and we believe that computations can shed further light on this intriguing observation. To this end, we employed calculations with periodic boundary conditions in a planewave code (VASP) to explore the structures and the energy differences between the two crystal structures. Very tight parameters had to be chosen to reach an accuracy necessary for the small energy differences assumed. From a more fundamental perspective, the stereoselective sublimation discussed here has implications on the origin of a homochiral environment on the prebiotic earth.[2]

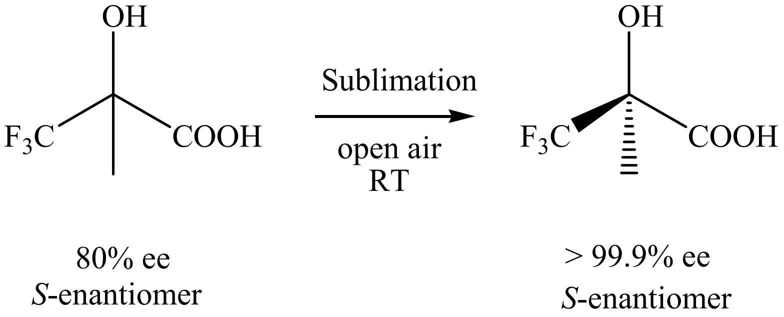

[1] V.A. Soloshonok, H. Ueki, M. Yasumoto, S. Mekala, J.S. Hirschi, D.A. Singleton, *J. Am. Chem. Soc.* **129**, 12112 (2007).

[2] P. Cintas, *Angew. Chem. Int. Edit.* **47**, 2918 (2008).

COMB-LIKE COPOLYMERS BASED ON POLYTHIOPHENE

C. Roux, D. Williams, J. Travas-Sejdic

Polymer Electronics Research Centre, University of Auckland

and MacDiarmid Institute for Advanced Materials and Nanotechnology

Surfaces whose properties could be tuned by external stimuli are of great interest, and possible applications range from micro and nanofluidics, self-cleaning surfaces, environmental clean-up or bioengineering purposes. Smart surfaces have been the subject of several reviews recently.[1] Conducting polymers, which can be switched between oxidised and neutral state by electrical stimulus, have already been employed to prepare such switchable surfaces.[2] With the aim to use them as electrically responsive layers for the preparation of smart surfaces, we prepared comb-like copolymers based on polythiophene. We thus envisaged a precursor that could potentially be used in a "graft from" strategy or in solution. Both strategies relied on a common terthiophene derivative, equipped with a bromoester to enable Atom Transfer Radical Polymerization (ATRP). This precursor was shown to be polymerizable both chemically and electrochemically (Figure 1).

In solution, the chemically polymerized macroinitiator was used as a platform to build comb-like copolymers, with sidechains composed of polystyrene and polyacrylate blocks. The ATRP process gave us good control over the growth of the side chains, thus keeping the chains short with low polydispersity. The final polymer showed a good electroactivity in organic solvents (Figure 1).

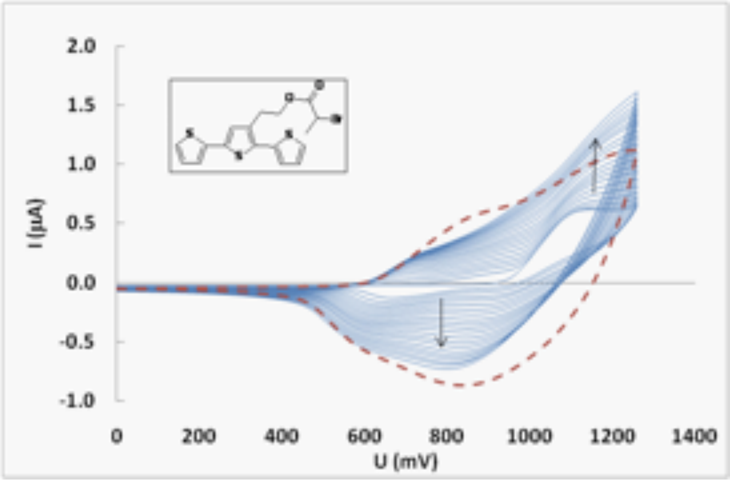

Figure 1. Solid lines: electrochemical growth of terthiophene derivative on a glassy carbon disc electrode using cyclic voltammetry (20 cycles in 0.05M $LiClO_4$, [tTh]= 0.005M). Dashed line: cyclic voltammograms of tTh film in 0.05M $LiClO_4$ in CH_3CN, scan rate=100mV/s

1. Liu, Y. et al. Controlled switchable surface. Chemistry - A European Journal 11, 2622-2631 (2005).
2. Xu, L. et al. Reversible conversion of conducting polymer films from superhydrophobic to superhydrophilic. Angewandte Chemie - International Edition 44, 6009-6012(2005).

X-ray phosphor properties of Eu^{2+} - doped lanthanum-stabilised cubic barium chloride

A. Edgar[a,b], J. Zimmermann[c], H. von Seggern[c] and C.R. Varoy[a]

[a]*School of Chemical and Physical Sciences, Victoria University, Wellington 6140, New Zealand*

[b]*MacDiarmid Institute, Victoria University, Wellington 6140, New Zealand*

[c] *Institute of Materials Science, Electronic Materials Division, Technische Universitaet Darmstadt, Germany 64287*

We report the photoluminescence and X-ray luminescence of lanthanum-stabilised cubic barium chloride with europium (Eu^{2+}) doping, of general composition $Ba_{1-x-y} Eu_y La_xCl_{2+x}$. X-ray diffraction patterns confirm that the material adopts a cubic fluorite structure for $x = 0.125$ and $0 < y < 0.1$. The photoluminescence shows an intense band comprising two components with maxima at 420 and 394 nm. The 394 nm band is assigned to Eu^{2+} substituting for Ba^{2+} giving a site of cubic symmetry, based on the excitation spectra which show a T_{2g} band and E_g bands similar to those in cubic $SrCl_2$:Eu. The 420 nm band has a very different excitation spectrum and is assigned to Eu^{2+} ions which have an adjacent chlorine interstitial ion, giving a site of C_{4v} symmetry. The two bands are also found in the X-ray luminescence spectra. For both bands, and an additional minor emission at 520 nm found only at low temperatures and for high Eu concentrations, there is a common excitation in the uv from 150-200 nm which we attribute to excitons associated with the high concentration of chlorine interstitials in these materials. The materials show strong X-ray luminescence at room temperature, visible to the eye in room lighting. A measurement of the X-ray luminescence intensity compared to a standard commercial Gd_2O_2S:Tb phosphor sheet shows a comparable efficiency for a doping level of $y = 0.02$.

Magnetic Phase Transitions in Layered $NdMn_2Ge_{2-x}Si_x$

J.L. Wang[a,b], S.J. Campbell[a], J.M. Cadogan[c], A.J. Studer[b], R. Zeng[d] and S.X. Dou[d]

[a] *School of Physical, Environmental and Mathematical Sciences, University of New South Wales, Australian Defence Force Academy, Canberra ACT 2600*

[b] *Bragg Institute, ANSTO, Lucas Heights, NSW 2234*

[c] *Department of Physics and Astronomy, University of Manitoba, Canada*

[d] *ISEM, University of Wollongong, NSW 2522*

The discovery of a giant magnetocaloric effect (GMCE) near room temperature in $Gd_5Si_2Ge_2$ has led to much attention being paid to layered structures in order to understand the MCE behaviour of such materials [1]. $NdMn_2Ge_{2-x}Si_x$ offers interesting prospects for enhanced magnetocaloric behaviour as the tetragonal, layered structure allows the structural and magnetic states to be controlled *via* inter- and intra-planar separations of the Mn atoms.

We have investigated the structural and magnetic behaviour of $NdMn_2Ge_{2-x}Si_x$ (x=0-2.0) by magnetic measurements, X-ray and neutron diffraction (Wombat, OPAL) over the temperature range 6-465 K. Replacement of Ge by Si leads to contraction of the unit cell with lattice constant *a* of $NdMn_2Ge_{2-x}Si_x$ passing through two critical values a^{crit1} and a^{crit2} in RMn_2X_2 [2]: a^{crit1}=4.06 Å at x~1.0 and a^{crit2}=4.02 Å at x~1.8. This leads to significant modifications of the magnetic states of $NdMn_2Ge_{2-x}Si_x$. For example, at room temperature both $NdMn_2Ge_{1.6}Si_{0.4}$ and $NdMn_2Ge_{1.2}Si_{0.8}$ are found to exhibit canted ferromagnetism (Fmc) while $NdMn_2Ge_{0.8}Si_{1.2}$ and $NdMn_2Ge_{0.4}Si_{1.6}$ show canted antiferromagnetism (AFmc). By comparison, $NdMn_2Si_{2.0}$ exhibits interlayer antiferromagnetism (AFil) at 300 K [3]. We have established that Fmc and AFmc co-exist for $NdMn_2Ge_{1.2}Si_{0.8}$ between T_C^{Nd} (~90 K) and T_N^{inter} (~180K) while $NdMn_2Ge_{0.4}Si_{1.6}$ has a GMCE value of $-\Delta S_M^{max}=18.4$ J kg^{-1} K^{-1} around $T_C^{Nd}=36$ K for a field change $\Delta B = 5$ T. The overall magnetic behaviours of $NdMn_2Ge_{2-x}Si_x$ compounds are governed by the strong dependence of the magnetic couplings on the Mn-Mn spacing within the ab-plane. A detailed magnetic phase diagram for the $NdMn_2Ge_{2-x}Si_x$ system has been constructed over the entire temperature and composition ranges.

[1] V.K. Pecharsky and K.A. Gschneidner Jr, *Phys Rev Lett* **78,** 4494 (1997).
[2] I. Dincer et al., *J. Magn. Magn. Mater*. **313**, 342 (2007).
[3] R. Welter, G. Venturini, D. Fruchart and B. Malaman, *J. Alloy. Comp*. **191**, 263 (1993).

The Angled Crack Problems in Compression and Tension

M. Watanabe

School of Engineering, Kinki University, Higashi-Hiroshima 739-2116, Japan.

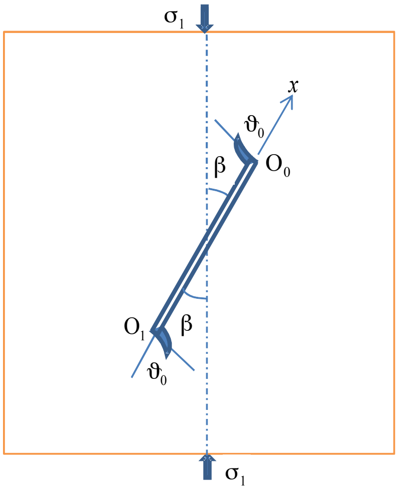

Fig. 1 Angled crack problem in compressive stress

The Griffith-model of brittle fracture of elastic solids is based on the hypothesis that fracture occurs when the potential energy released by a crack exceeds the work required for the formation of the new surfaces, which has played dominant role in fracture mechanics. However, how to determine the direction and the critical stress of crack extension under general plane loading has been an important subject of fracture mechanics. Erdogan and Sih [1] performed the experiment, in which the tensile loading axis is oblique to the crack in the elastic plate. Williams and Ewing [2] performed the detailed experiment and named this problem as "an angled crack problem". They showed disagreement between the theory [1] and the experiment for some parameter regime of the tensile angled crack problem. Cotterell [3] performed the experiment of compressive angled crack problem using the elliptic crack made in the plate of fused glass, while Kobayashi [4] performed the experiment using PMMA and thin cement plate for both of the uni-axial and biaxial compression. It is well known (Bobet and Einstein[5]) that the tensile angled crack problem shows unstable crack propagation, while the wing crack in compressive angled crack problem, shown in Fig. 1, shows stable fracture although both of the new cracks generated are driven by the tensile stress at the tip of the crack. Although numerous theories have been proposed, the fracture criterion associated with the stress at the tip of the crack is used for fracture in compression, while the fracture criterion associated with the energy release rate is used for tensile fracture, and we still do not have unified fracture criterion. Theoretically the difference between tensile and compressive stress is simply the sign of the stress and it is natural to expect to have unified fracture criterion for angled crack problems. We propose such unified fracture criterion, which predict the direction of crack propagation consistent with the experimental observations for both of the tensile and compressive case, while the critical stress of the crack propagation is consistent with the experimental observations only for the tensile angled crack problem. The criterion predicts the critical stress by two or three factors below the experiment for the compressive angled crack problem.

[1] F. Erdogan and G. E. Sih, *J. Basic Engng*. **85**, 519 (1963).
[2] J. G. Williams, and P. D. Ewing, *Int. J. of Fracture Mech*. **8**, 441 (1972).
[3] B. Cotterel, *Int. J. Fract. Mech*. **8**,195 (1972).
[4] S. Kobayashi, *Zairyo* **20**, 164 (1971).
[5] A. Bobet and H. H. Einstein, *Int. J. Rock Mech. Min. Sci*. **35**, 863 (1998) and references cited therein.

A Variable Energy Positron Beamline for PALS experiments

M. Went, J. Roberts, R. Weed, S. Buckman and J. Sullivan

Centre for Antimatter-Matter Studies, Atomic and Molecular Physics Laboratories
Research School of Physics and Engineering, Australian National University, ACT Australia

A new materials analysis capability has recently come online, making use of positrons for analysis of nano-vacancy structure in materials of interest. The experiment implants a pulsed, variable energy positron beam into the sample and measures the decay lifetime of the positrons within it. These lifetimes can be related to the size and distribution of voids and open volume inside the material.

Positrons are emitted from a 22-Na radioactive source. They are initially moderated using solid neon, which reduces the energy spread of the positrons to ~1.5 eV with an efficiency of around 1%. These positrons are then guided magnetically and electrostatically to a Surko trap, where they are confined and further cooled to room temperature. They are released as a variable energy pulse, which can be temporally compressed to 800 ps. Upon injection into the sample, the positrons quickly thermalise and annihilate, and the annihilation lifetime is measured. The variable energy of the beam allows for different implantation depths into the sample, and analysis can thus be performed as a function of depth, typically up to a few microns depending on the sample density.

Positron Annihilation Lifetime Spectroscopy (PALS) has long been established as a useful tool for investigating nano-sized voids in material structures and is the basis of the instrument described in this paper. A description of the operation of the apparatus will be presented, along with detail on the analysis techniques that enable the investigation of nanovoids. Examples of some of the initial measurements made using this facility will be presented. Future expansion plans to incorporate new analysis techniques will also be outlined.

CsBr:Eu^{2+} X-Ray Storage Phosphor Imaging Plates

N.M. Winch[a] and A. Edgar[a,b]

[a] *School of Chemical and Physical Sciences, Victoria University of Wellington, Wellington, New Zealand.*

[b] *MacDiarmid Institute for Advanced Materials and Nanotechnology, Victoria University of Wellington, Wellington, New Zealand.*

Caesium bromide doped with europium (CsBr:Eu^{2+}) is a new commercially available x-ray storage phosphor imaging plate [1]. Storage phosphor imaging plates store the x-ray image as a varying concentration of electron hole pairs. The image is read out by raster scanning a focused laser beam across the plate. The CsBr imaging plates are made by vacuum depositing CsBr:Eu^{2+} onto a substrate. The crystals grow in needle-like structures which act like light guides for the readout light avoiding the scattering problems and low resolution (4 lp/mm at MTF=0.2 [2]) of the usual BaFBr:Eu^{2+} imaging plates. This leads to a higher resolution imaging plate (6 lp/mm at MTF=0.2 [3]) which can be used for mammography.

However, the spatial resolution is still not as high as what can be achieved by transparent materials such as glass ceramics [2][4] as the CsBr needle imaging plates are limited in resolution by light guiding properties of the needle-like structures.

To overcome this we are investigating ways in which to make transparent CsBr:Eu^{2+} imaging plates which show minimal scattering effects. We have investigated the effects of moisture content, concentration and annealing temperatures on the transparency and PSL intensity, and show representative images.

[1] S. Schweizer, U. Rogulis, S. Assmann and J.-M. Spaeth, *Rad. Meas.* **33**, 483 (2001).

[2] N. Winch and A. Edgar, *J. Appl. Phys.* **105**, 023506 (2009).

[3] H. Bosmans, K. Lemmens, J. Jacobs, B. Verbrugge, K. Michielsen, F. Zanca, J. Nens, C. Van Ongeval and G. Marchal, *Lecture Notes in Computer Science* **5116**, 724 (2008).

[4] A. Edgar, G.V.M. Williams, S. Schweizer and J.-M. Spaeth, *Cur. Appl. Phys.* **6**, 399 (2006).